Copyright Warning & Restrictions

The copyright law of the United States (Title 17, United States Code) governs the making of photocopies or other reproductions of copyrighted material.

Under certain conditions specified in the law, libraries and archives are authorized to furnish a photocopy or other reproduction. One of these specified conditions is that the photocopy or reproduction is not to be "used for any purpose other than private study, scholarship, or research." If a, user makes a request for, or later uses, a photocopy or reproduction for purposes in excess of "fair use" that user may be liable for copyright infringement,

This institution reserves the right to refuse to accept a copying order if, in its judgment, fulfillment of the order would involve violation of copyright law.

Please Note: The author retains the copyright while the New Jersey Institute of Technology reserves the right to distribute this thesis or dissertation

Printing note: If you do not wish to print this page, then select "Pages from: first page # to: last page #" on the print dialog screen

ABSTRACT

THE RELATIONSHIP BETWEEN THERMOREGULATORY AND HAEMODYNAMIC RESPONSES OF THE SKIN TO RELAXATION AND STRESS

by
Paul O. Nketia

The present study investigated the effects of stress and relaxation on (1) EEG coherence and (2) peripheral blood flow.

EEG coherence of two meditators in two different but adjacent rooms was measured during eyes opened, eyes closed, single meditation and group meditation. The skin temperatures of the subjects together with their room temperatures were also recorded. EEG coherence plots (Cospar) showed a spread out of the alpha band to the beta, theta and occasionally to the delta wave bands during group meditation. The area above the 0.98 coherence threshold in the alpha band was greater during group meditation than during single meditation and eyes closed.

The peripheral blood flow study included measurement of arterial and venous blood volume, and temperature of the fingertips. Finger blood flow and temperature were measured by photoplethysmography and thermistor, respectively. The mean of the peak cross correlation between the blood volume and the temperature of the fingertips of the nine cases studied was 0.9236 ± 0.0408. The finger temperature closely followed that of the finger blood flow but at a slower rate. It was also observed that the finger blood flow and the temperature increased during eyes closed relaxation, but decreased during stressful state. Changes in venous blood volume (temperature), corresponded to changes in the amplitude of the arterial blood volume. Thus, during relaxation the finger arterioles are vasodilated, and during stress they are vasoconstricted.

THE RELATIONSHIP BETWEEN THERMOREGULATORY AND HAEMODYNAMIC RESPONSES OF THE SKIN TO RELAXATION AND STRESS

by
Paul O. Nketia

A Thesis
Submitted to the Faculty of
New Jersey Institute of Technology
in Partial Fulfillment of the Requirements for the Degree of
Master of Science in Biomedical Engineering

Biomedical Engineering Committee

May 1997

APPROVAL PAGE

THE RELATIONSHIP BETWEEN THERMOREGULATORY AND HAEMODYNAMIC RESPONSES OF THE SKIN TO RELAXATION AND STRESS

Paul O. Nketia

Dr. Stanley S. Reisman, Thesis Advisor — Date
Professor of Electrical and Computer
Engineering, NJIT

Dr. David Kristol, Committee Member — Date
Professor of Chemistry and Director of Biomedical
Engineering Program, NJIT

Dr. Edip Niver, Committee Member — Date
Associate Professor of Electrical and Computer
Engineering, NJIT

BIOGRAPHICAL SKETCH

Author: Paul O. Nketia

Degree: Master of Science

Undergraduate and Graduate Education:

- Master of Science in Biomedical Engineering
  New Jersey Institute of Technology, Newark, NJ, 1997

- Master of Science in Electrical Engineering
  Leningrad Polytechnic Institute, Leningrad, Russia, 1990

Major: Biomedical Engineering

To my beloved parents who did not live to share this achievement

ACKNOWLEDGMENT

The author would like to express his sincere gratitude and deepest appreciation to his advisor, Dr. Stanley S. Reisman, for his patience, guidance, friendship, and moral support throughout this research.

Special thanks are extended to Dr. David Kristol for not only serving as a member of the committee but also for enabling me to participate in an internship training program at UMDNJ. Special thanks are also given to Dr. Edip Niver for serving as a member of the committee, and for the invaluable technical assitance offered for this research.

The author also wishes to thank the following NJIT students: Xiaori Tang, Melissa Leifer, Vincent Ralph, Robert Okojie, Robert Ongosi, Haritha, K. Teddy, Jose Torrealba and the others for volunteering their time being the subjects for this research.

TABLE OF CONTENTS

TABLE OF CONTENTS
(Continued)

TABLE OF CONTENTS
(Continued)

Chapter Page

LIST OF TABLES

LIST OF FIGURES

Figures **Page**

LIST OF FIGURES
(Continued)

Figures **Page**

LIST OF FIGURES
(Continued)

Figures **Page**

LIST OF FIGURES
(Continued)

Figures Page

CHAPTER 1

INTRODUCTION

1.1 Scope of the Research

This research explores the effect of stress and relaxation on (1) EEG coherence, and (2) peripheral blood flow. A brief discussion on EEG, meditation, skin temperature and skin blood flow will be presented in this chapter.

For thousands of years men have speculated about the nature of human consciousness. Only within the last 70 years, after the discovery of the electroencephalogram (EEG), have scientists gained the technical ability to describe the physiological and biochemical correlates of states related to consciousness.

Following the discovery of EEG, and the subsequent discovery of evoked potentials (EP), there has been various findings about the magnetic field evoked by visual, somatic, and auditory stimuli which have been analyzed as arising from current dipole sources lying within the primary projection areas of the cortical activities for the respective stimulus modality (intensive studies have also been carried out for the past 20 years to investigate if consciousness is a field?)

Recent studies have shown that the practice of meditation has a significant physiological and psychological effect on the human body. Other studies have also revealed that the practice of meditation has sociological effects and that a mass meditation may influence population of a big city resulting in a decline in the city's crime rate [18]. Baker [17], Schmidt-Koening & Keeton [18] have shown that many species are

sensitive to stimuli which were not previously known to be within the receptive domain. Humans for example have been shown to be responsive to weak electromagnetic fields on the order of 10 Hz with brain tissue gradient of 10^{-5} to 10^{-7} V/cm which are many orders of magnitude less than the gradient needed to fire neuronal action potentials [18]. In other series of studies to support Frohlich's mechanism, reseachers have shown profound and highly resonant effects on the growth and functions of cells when they are irradiated with 6-8 millimeter-band electromagnetic waves at low intensities in the range of 0.01 milliwatt per square centimeter [17]. The fact that the human eye can respond to one or two photons of green light or that the olfactory sense is sensitive to a single molecule stimulant indicates that "sensory awareness regularly functions at the ultimate limit of a single quantum sensitivity" [17].

For the last twenty one years, Orme-Johnson, Dillbeck, Wallace, et al have been studying the effects of the Transcendental Meditation (TM) program on EEG spectra and coherence in the individual. Their results are interpreted as supporting a field theory of consciousness. The originator of the technique, Maharishi Mahesh Yogi, proposed that the larger the group practicing the TM technique together, the greater effect it will have on this field. Since the EEG is sensitive to changes in consciousness, it is hypothesized that field fluctuations might be detected by analyzing the EEG coherence between subjects - their EEGs might be expected to rise and fall in synchrony. This thesis measured the EEGs of two meditators in two different adjacent rooms and computed the frontal EEG coherence of each subject. Data analysis methods in terms of time-frequency

and spectral methods were based on Levine [22] and Hebert coherence. A detailed description of coherence will be given.

The second part of the present study was concerned with the effects of stress and relaxation on cutaneous blood volume and temperature. Reflex regulation of human skin blood flow is complex. Body cooling causes cutaneous vasoconstriction via a generalized increase of adrenergic vasoconstrictor activity [7]. Body warming, on the other hand, increases skin blood flow partly because of inhibition of vasoconstrictor activity and partly via an active vasodilator mechanisms. However, the exact nature is unknown. Maneuvers such as deep inspirations, arousal and emotional stress are generally believed to cause reflex vasoconstriction.

Recent studies have shown that painful intraneural electrical stimulation in the superficial peroneal nerve caused bilateral vasodilation of reflex origin in the skin on the dorsal side of the foot; the vasodilation was augmented by body cooling. In another study Elam and Wallin showed that mental stress caused vasoconstriction in warm subjects and vasodilation in cold subjects [8]. These findings suggest that thermoregulatory mechanisms may exert powerful modulatory effects on different cutaneous vasomotor reactions. Because stress and relaxation are the primary focuses in this thesis, we shall briefly introduce them in the remaining of this section.

Stress has become a predominant cause of many diseases in our society today. By definition, stress is the body's reaction to a perceived mental, emotional, or physical distress. This triggers a mass discharge of the sympathetic portion of the autonomic nervous system which may cause faster heartbeat, increased blood pressure, increased

blood flow to vital organs such as the brain and skeletal muscles with a corrresponding decrease in blood flow to "non-essential" organs such as the skin, kidneys, gastrointestinal tract, and a mobilization of fat reserves.. Chronic stress reactions of this nature can therefore lead to physical and mental disorders such as peptic ulcers, heart attacks, nervous breakdowns, Raynaud's and Chronic Venous Insufficiency (CVI) diseases.

Recent studies have demonstrated that relaxation has a measurable effect on the body's reaction to stress, and suggests that persons may be deriving both physical and psychological benefits from the practice of relaxation. Relaxation response is defined by a set of integrated physiological changes that are elicited when a subject assumes a relaxed position in a quiet environment, closes his or her eyes, engages in a repetitive mental action, and passively ignores distracting thoughts. These behaviors are associated with physiological changes that include decreased changes in heart rate, respiratory, arterial blood pressure, autonomic function, and changes in peripheral circulation, and skin conductance and temperature, among others [2]. The second part of this thesis investigated how stress and relaxation affect skin temperature and peripheral blood flow such as the fingertip.

1.2 Meditation

1.2.1 What is Meditation?

Meditation is a stylized mental technique repetively practiced for the purpose of attaining a subjective experience that is frequently described as very restful, silent, and of

heightened alertness, often characterized as blissful [15]. The practice of meditation as a method of quiescent, tranquil restfulness has been used for centuries in Vedic, Bhuddist, and Taoist traditions in southern and east Asia. Practitioners report experiencing a wakeful state of "samadhi," or "pure consciousness," that is very pleasant and relaxing [15].

There are three principal types of meditation techniques: contemplation, concentration and transcendental. The term contemplation describes all practices of thinking about meaning. The technique involves allowing the attention to dwell upon internal or external objects of experience. A person may contemplate a physical object, a devotional prayer, a philosophical concept, or a generalized issue like "Who am I?", "Who is God?", etc. [15]. Techniques of concentration involve holding or focusing attention on an object of experience which in most cases involve voluntary focusing on a particular object of experience, such as a physical object like a candle flame, a sensation-emotion like a feeling of bliss, an insoluble philosophical paradox like a Zen koan, or a more generalized state like the absence of all thought. In this case an individual attempts to transform the quallity of his experience by direct mental control [15]. Transcendental meditation (originating in the Vedas–the oldest Indian teachings [15]), the last category of meditation technique was introduced by Maharishi Mahesh Yogi in the late 1950's. The novelty of the technique is that it is very easy and effortless, and it requires no special circumstances for practice, no holistic philosophy, nor any special diet or lifestyle changes. These qualities make TM technique more easily adaptable to studies on consciousness than the concentration and contemplation techniques described above. The

TM technique is defined as "turning the attention inwards towards levels of a thought until the mind transcends the experience of the subtlest state of the thought and arrives at the source of thought" [17]. The TM technique attributes the same qualities of quiescence, orderliness, and stability, and "pure potentiality" to transcendental consciousness, analogous to the quantum mechanical ground state, the state of least excitation of a physical system, which is characterized by zero activity, zero entropy, maximum stability, perfect orderliness, and by being the basis for the many states of higher excitation of the system [17].

Through the practice of the TM technique, the human nervous system can attain what is called the transcendental state–it is a state of profound rest coupled with heightened alertness which goes beyond the familiar level of wakeful experience. Studies on practitioners of TM technique have revealed the following physiological and psychological changes:

- decrease of plasma cortisol, a biochemical indication of stress
- reduction of the metabolic rate by up to 25-30%
- reduction of the total oxygen consumption by up to 20%
- reduction of the breathing rate to 4-6 breaths per minute from 12-14 per minute
- increase autonomic stability
- increase orderliness of brain function
- increase in in-phase interhemispheric correlation in the alpha band
- reduction of the blood pressure by an average of 20% in hypertensive patients
- more than five times increase of the skin resistance

- changes in the pH and sodium bicarbonate concentration of blood

- decrease of the cardiac output by about 25%, and so on

Maharishi, the proponent of the TM technique describes a fourth state of consciousness after waking, dreaming and sleep as pure consciousness or the transcendental state. There is claimed to be a systematic process of stabilization of the fourth state by habituation due to repeated experience through continued practice of the TM technique. The result of this habituation is the progressive rise of an ability in the nervous system to maintain the pure consciousness state superposed on the usual thinking and perceptual activity of waking, dreaming, or sleep [15]. When this state is permanent, it gives rise to a distinct fifth style of functioning of the nervous system, whose associated state of consciousness has variously been called "cosmic consciousness," "enlightenment," or "nirvikalpa samadhi." It is predicted that the inner wakefulness is maintained uninterrupted even during sleep in those individuals established in the fifth state. The time we spent in sleep is apparently used to rejuvenate the body by the release of certain growth hormones, and to remove body fatigue so we can function physically during wakefulness. The time we spend during dreaming is apparently used to remove psychological strains and stress from our minds so that we can function better mentally and physically during wakefulness. Many well known sleep and dreaming deprivation experiments on humans and animals support this view [21].

Similarly, the time spent during meditation is used to rejuvenate both the body and the mind at deeper and finer levels; this is the way of rejuvenating the machinery of experiencing the central nervous system itself. If an individual is deprived of a daily

meditation, then the individual feels not as sharp, not as clear, not as fulfilled. Furthermore, the individual is not energetic and strains more in whatever he does. TM, which takes the practitioner to the fourth state of consciousness comes to fill this vital need of our time.

1.2.2 Meditation Research

Although the concept of "higher" states of consciousness, which might occur during techniques of meditation has been postulated for centuries, scientific study of meditation began as early as 1935 when a French cardiologist went to India and made physiological measurements on various practitioners of yoga exercises. Brosse reported that one of her subjects was able to stop his heart. In 1957 two American physiologists conducted a more extensive investigation in collaboration of the All-India Institute of Medical Sciences as a follow up of Brosse's study. They found a decreased respiratory frequency, an increased skin resistance, and no consistent change of heart rate, blood pressure, and EEG during physical and mental yoga exercises [17].

Anand et al. [17] studied the EEG of four yogis and reported increased alpha-wave amplitude during the practice of meditation. Other studies on Zen meditators showed such changes as significant decreases of respiration rate, oxygen consumption, and slight increase of pulse rate and blood pH during meditation [17]. Initial EEG studies of TM meditators reported [17]:

1. alpha wave (8–12 Hz) increased in amplitude, slowed down in frequency, and extended to anterior channels at the beginning of meditation;

2. theta frequencies (5-7 Hz) different from those of sleep diffused from frontal to posterior channels which took the form of short theta periods or longer rhythmic trains;
3. rhythmic amplitude-modulated beta waves (13–30 Hz) were present over the whole scalp in a third stage of deep meditation by advanced meditators;
4. synchronization of anterior and posterior channels.

Levine et al. have shown that during the TM technique there is an increase in frontal and central alpha coherence and a spreading of coherence to other frequencies, particularly theta. The most common feature was the onset of strong alpha coherence (above 0.95) during the TM technique relative to the eyes-closed control period [17]. In addition, intrahemispheric TM-specific effects were observed as frequently in the left hemisphere as in the right hemisphere with interhemispheric coherence appearing more frequently and more dominantly in the frontal derivations than in the central.

There is enough experimental evidence which shows that when a relatively small number of individuals participated in the TM and TM-Sidhi program, there was a reduction in social disorder in the surrounding population [18]. In a study about the social behavior of 160 U.S. cities for a period of over 15 years, a significant correlation between decreasing crime and percentage of TM participants in a city was observed [18]. In addition , Dillbeck [18] conducted studies which consistently supported the interpretation of a casual influence of the TM program on crime rate reduction. In an effort to extend Dillbeck's studies, Aron and Aron [18] conducted three separate replications and found that when they moved 28–40 individuals participating in the TM-

Sidhi program from their usual low crime area of residence in Atlanta to do their evening TM-Sidhi program in the high crime area for one-week periods, the crime rate decreased during that period in the high crime area and increased in the low crime area they had left. The effect reversed when they moved back to their original site [18]. Orme-Johnson found that extreme social violence decreased in five trouble-spot countries (in Central America, Southern Africa, South and East Asia, and the Middle East) during the approximately one-month period in which groups of hundreds or more participated collectively in the TM-Sidhi program. In both of the above instances, the TM participants did not directly interact with the local population [18]. In still other studies, researchers measured EEG coherence between pairs of three different subjects during a one-hour practice of the TM program. Coherence between subjects was evaluated for two sequential fifteen minute periods. On six experimental days, these periods preceded and then coincided with a fifteen minute period during which 2500 students participated in the TM-Sidhi program at a course over 1000 miles away. After the course had ended coherence was evaluated on six control days. It was found that intersubject coherence was generally low, between 0.35 and 0.4, with coherence in the alpha (8–12 Hz) and beta (16–20 Hz) frequencies significantly higher than at other frequencies . On the experimental days, intersubject EEG coherence increased during the experimental period relative to the fifteen minute baseline period immediately preceding the experimental period. Coherence increased significantly from baseline to experimental periods on experimental days compared with control days. These results reinforce the above sociological studies showing decreased social disorder in the vicinity of TM and TM-

Sidhi participants and are discussed in terms of a field theoretic view of consciousness [18].

1.3 Skin Blood Flow

The responses of the peripheral blood vessels to mental stress display complex regional variations. While dilatation occurs in the forearm musculature, the vessels of the forearm skin generally constrict when initial cutaneous flow is large. The proportion of skin to muscle is higher in the hands and feet than in the arms and leg; the fall in the hand blood flow during mental stress in warm surroundings, therefore, parallels the change in forearm skin [1].

1.3.1 Skin Blood Volume and Skin Temperature Research

Halperin et al. indicated that when a stress was caused, there was a definite sympathetic response, which is represented by a drop in skin temperature caused by a constricting of the cutaneous blood vessels. During relaxation, however, the cutaneous blood vessels are vasodilated allowing more blood to flow to the cutaneous vessels and hence increasing the skin temperature. Since the cutaneous blood vessels are controlled by the sympathetic nervous system only, changes in skin temperature or skin blood volume corresponds to changes in sympathetic tone [2] and [1]. Halperin et al also found out that mental arithmetic stress increases fingertip blood flow and decreases vascular resistance in patients with Raynaud's disease, and that this differs from the digital vascular reaction in either dilated or constricted normal subjects [1].

In another study conducted by Oberle, Elam, et al. about the putative influence of the thermoregulatory state on skin blood-flow responses to various stimuli, the authors reported that intraneural electrical stimulation and mental stress were accompanied by virtually identical changes in skin blood flow, warm subjects responding with cutaneous vasoconstriction whereas cold subjects responded with vasodilation. Similar but less pronounced responses were obtained with arousal stimuli and single deep breaths. Their report indicate that the thermoregulatory state profoundly influences the extent and direction of various cutaneous vasomotor reflex responses. Furthermore, there were differences between responses in hands and feet, suggesting a spatial organization of vasomotor control [3].

Studies by Cooke, Creager, et al. to determine whether there are gender differences in local or central control of cutaneous blood flow to account for the increased incidence of Raynaud's disease in women, reported that: 1) cutaneous blood flow in women is less than in men, 2) this gender difference is due to differences in central, rather than local, control mechanisms, 3) maneuvers generally believed to increase sympathetic outflow to the extremities induce cutaneous vasoconstriction in men but a paradoxical vasodilation in women, and 4) this paradoxical vasodilation is unmasked in men under conditions in which sympathetic tone is elevated [4].

Blumberg and Wallin conducted intraneural stimulation in the superficial peroneal nerve at the ankle. Their findings showed that vasodilation was due to activation of a reflex pathway. The reflex vasodilation was bigger in the stimulated area than in the opposite foot. At the same time there were signs of skin vasoconstriction in the fingers.

The authors further suggested that reflex vasodilation is of sympathetic nature and is induced by stimulation of thin afferent fibers, and the local vasodilation is due to centrifugally conducted impulses in non-myelinated fibers [5].

CHAPTER 2

PHYSIOLOGICAL BACKGROUND

2.1 Introduction

This chapter will provide an overview of the physiological systems that pertains to this thesis. The understanding of these physiological systems is essential to the interpretation of the experimental results and to further expand upon this research.

2.2 The Cerebral Electrical Activity

Before we examine the cerebral electrical activity and the electroencephalogram (EEG), it will be appropriate to give a brief background of the structure or the anatomy and the physiology of the brain.

The brain is the main structure of the central nervous system, and is the seat of all conscious and most subconscious control of the body. The brain lies within the skull, and the spinal cord within the vertebral column. Between the soft neural tissues and the protective bones that house them are three protective membranous coverings called meninges [24]. The brain is composed of six subdivisions: cerebrum, diencephalon, pons, medulla oblongata, and cerebellum (figure 2.1).

2.2.1 The Subdivisions of the Brain

The division of the brain into three main parts - brainstem, cerebellum, and forebrain provides a useful basis for the study of brain localization and function.

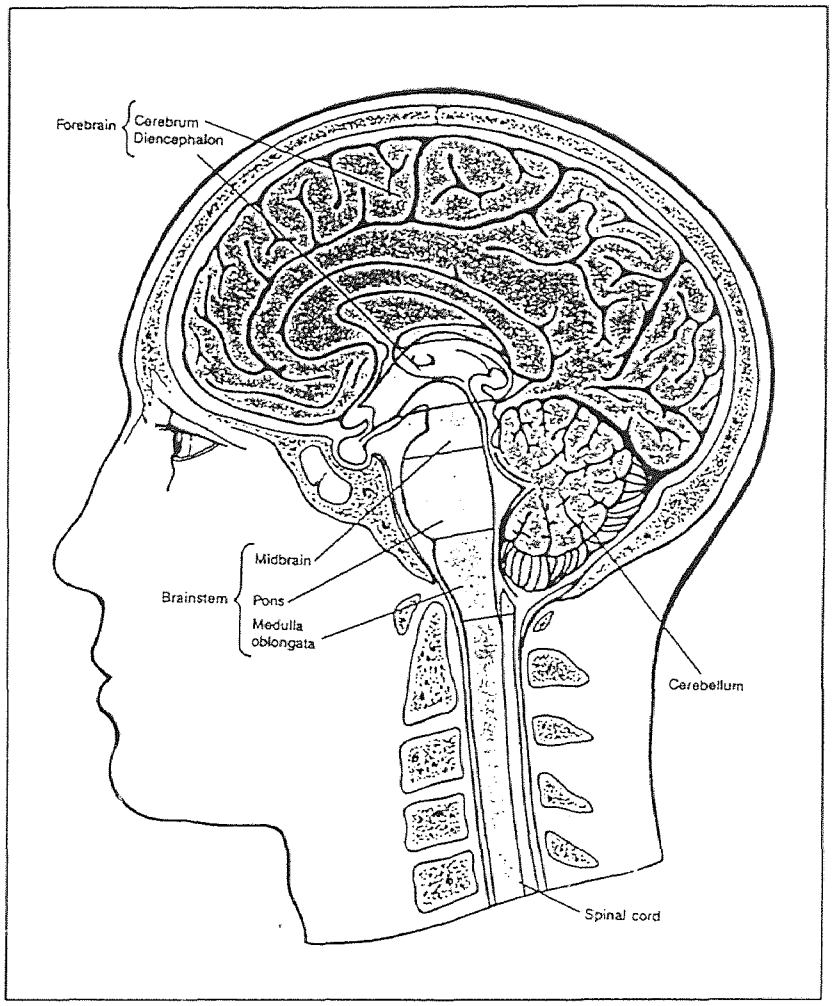

Figure 2.1 The Spinal Cord and Six Divisions of the Brain
(from Vander A. J. et al. *Human Physiology,* 1994)

2.2.1.1 The Brainstem: The brainstem is literally the stalk of the brain. Through it pass all the nerve fibers that relay signals between the spinal cord and the forebrain or cerebellum. Information is transmitted between the brainstem and cerebellum by three large bundles of nerve fibers, the cerebullar peduncles. The Reticular formation runs through the core of the brainstem. It receives and integrates input from all regions of the central nervous system, and outputs a great deal of neural information. The reticular formation divide into thalamus (a large sensory way station in the forebrain), and the

hypothalamus (a center critical for regulation of the internal environment). The reticular formation connects the cerebellum and the spinal cord. The reticular formation has nuclei for controlling the cardiovascular, respiration, swallowing, vomiting, eye movement and the reflex orientation in space [12].

2.2.1.2 The Cerebellum: The cerebellum is involved with the control of skeletal muscle functions. It is connected to the brainstem by cerebllar peduncles [12]. Although the cerebellum does not initiate voluntary movements, it is an important center for coordinating and learning movements and for controlling posture and balance. In order to carry out these functions, the cerebellum receives information from the muscles and joints, skin, eyes and ears, viscera, and the parts of the brain involved in control of movements.

2.2.1.3 The Forebrain: The central core of the forebrain is formed by the diencephalon. It is covered by the cerebrum, which consists of the right and left cerebral hemispheres. The cerebral hemispheres consists of the cerebral cortex and the many nerve fibers that bring information into the cerebrum, carry information out, and interconnect the neurons in the cerebrum [12]. The hemispheres, although largely separated by a longitudinal division, are connected to each other by bundles of nerve fibers known as commissures.

The cortex of each hemisphere is divided into four lobes: the frontal, parietal, occipital, and temporal. The cortex is highly folded, which increases the area available for

cortical neurons without increasing the volume of the brain. Its cells are arranged in six layers. There are two types of the cortical neurons: pyramidal and nonpyramidal cells.

The cerebral cortex is necessary for bringing together basic afferent information into meaningful perceptual images and for the ultimate refinement of controlling the systems that govern the movement of the skeletal muscles.

The diencephalon, the second component of the forebrain contains the thalamus and the hypothalamus. The thalamus is a synaptic relay station for sensory pathways on their way to the cortex. The hypothalamus accounts for less than 1 percent of the brain's weight, yet it is crucial for homeostatic regulation and is the principal site for regulating the behavior essential to the survival of the individual species [12].

An area of the forebrain that includes both gray and white matter is the limbic system. It is associated with learning, emotional experience and behavior, and a wide variety of visceral and endocrine functions.

2.3 The Cardiovascular System

The purpose of the cardiovascular system is to provide the body's tissues with necessary nutrients such as oxygen as well as to carry away waste products such as carbon dioxide to be expelled from the body. The primary components of the cardiovascular system are the blood, the blood vessels, and the heart. The heart is responsible for pumping blood through the vasculature. The lungs and kidneys also play an important role in the cardiovascular system. The lungs are the site of the blood's gas exchange and the kidneys

are responsible for the filtration of substances in the blood that are not utilized by the body.

2.3.1 The Heart and the Cardiac Cycle

The heart, as shown in figure 2.2, is actually two separate pumps: a right heart that pumps the blood through the lungs and a left heart that pumps the blood through the peripheral organs. Each of these two separate hearts is a pulsatile two-chamber pump composed of an atrium and a ventricle. The atrium functions as a blood reservoir and as entryway to the ventricle, but it also pumps weakly to help move blood into the ventricle. The ventricle in turn supplies the main force that propels the blood through either the pulmonary system or the peripheral circulation [6].

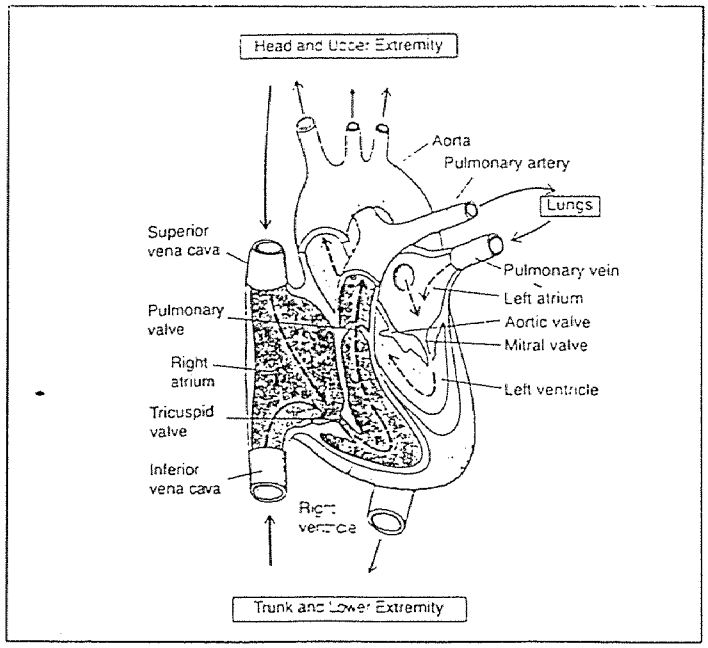

Figure 2.2 Structure of the heart and course of blood flow through the heart chambers. (from Guyton, A. C. *Human Physiology and Mechanisms of Disease*,1992)

The period from the beginning of one heartbeat to the beginning of the next is called the cardiac cycle. Each cycle is initiated by spontaneous generation of an action potential in the sinus node. This node is located in the superior lateral wall of the right atrium near the opening of the superior vena cava, and the action potential travels rapidly through both atria and thence through the A-V node into the ventricles with 0.1 sec. delay to allow the atria to contract ahead of the ventricles [6].

The pumping effectiveness of the heart is highly controlled by the sympathetic and parasympathetic nerves, which abundantly supply the heart. Sympathetic stimulation of the heart can increase the heart rate and the force with which the heart muscle contracts, also increasing the volume of blood pumped as well as increasing the ejection pressure.

Parasympathetic (vagal) stimulation of the heart decreases the heart rate and the strength of contraction by as much as 20 to 30% [6].

2.3.2 The Functional Parts of the Circulation

The function of the arteries is to transport blood under high pressure to the tissues. For this reason, the arteries have strong vascular walls, and blood flows rapidly in the arteries.

The arterioles are the last small branches of the arterial system, and they act as control valves through which blood is released into the capillaries. The arteriole has a strong muscular wall that is capable of closing the arteriole completely or of allowing it to be dilated severalfold, thus having the capability of vastly altering blood flow to the capillaries in response to the needs of the tissues.

The function of the capillaries is to exchange fluid, nutrients, electrolytes, hormones, and other substances between the blood and the interstitial fluid. For this role, the capillary walls are very thin and are permeable to small molecular substances.

The venules collect blood from the capillaries; they gradually coalesce into progressivelly larger veins.

The veins function as conduits for transport of blood from tissues back to the heart. They serve as a major reservoir of blood. Because the pressure in the venous system is very low, the venous walls are very thin. They are muscular, and this allows them to contract or expand and thereby act as a reservoir for extra blood.

2.3.3 Blood Pressure

In order to describe blood pressure, certain concepts regarding hydrostatic pressure (the pressure exerted by a fluid) must first be explained. A difference in pressure between two points will cause fluid to flow from the region of higher pressure to the region of lower pressure [12]. A factor in the determination of flow is the amount of resistance in the path of the fluid. A linear approximation of fluid flow is as follows:

$$Q = \frac{\Delta P}{R} \tag{2.1}$$

where ΔP is the difference in pressure between two points in the fluid, R is the resistance, and Q is the flow rate.

The resistance in blood vessels is varied by altering the radius of the blood vessels. The following equation relates the radius of the blood vessel to its resistance to flow:

$$R = \frac{8\eta L}{\pi r^4} \tag{2.2}$$

where η is the blood viscosity, L is the length of the blood vessel, and r is the radius of the blood vessel [12]. From equation (2.2), it can be seen that the resistance from the blood vessels is highly dependent on its radius. For example, only doubling the radius of the blood vessel corresponds to a decrease of resistance by a factor of 16. This demonstrates the effectiveness of varying blood vessel diameter in the regulation of blood pressure.

From equation (2.1), the relationship between flow, pressure, and resistance can be used to determine the mean systemic arterial pressure (MAP) [12].

$$MAP = CO \times TPR \tag{2.3}$$

where CO is the cardiac output (the volume of blood pumped by the heart per unit time) and TPR is the total peripheral resistance, which is defined as the sum of the resistance to flow offered by all the systemic blood vessels.

The total quantity of blood that can be stored in a given portion of the circulation for each change in pressure is called the vascular compliance or capacitance of that vascular bed [6].

$$VC = \frac{\Delta V}{\Delta P} \tag{2.4}$$

where ΔV is the change in volume, ΔP is the change in pressure. Compliance and distensibility are quite different. A highly distensible vessel that has a very slight volume may have far less compliance than a much less distensible vessel that has a very large volume;

$$VC = D \times V \qquad (2.5)$$

where D is the distensibility of the blood vessel, and V is the volume of the blood vessel. The compliance of a vein is about 24 times that of its corresponding artery because it is about 8 times as distensible and it has a volume about three times as great [6].

The very large compliance of the venous system allows most of the extra blood of the circulation to be stored in the veins. By constricting the veins even a slight amount, this forces extra blood into the heart and thereby causes the heart to pump greatly increased volumes of blood throughout the circulation. Thus, sympathetic stimulation of the veins can translocate large amounts of extra blood into the heart within seconds thereby increasing the cardiac output severalfold almost immediately [6].

2.3.4 Local Control of Blood Flow

The circulatory system is provided with a complex system for control of blood flow to the different parts of the body. There are three main types of controls:

(1) Local Control-the ability of each tissue to control its own local blood flow in proportion to its need. The specific needs of the tissues for blood flow include delivery of oxygen to the tissues, delivery of other nutrients (like glucose, amino acids, fatty acids,

and so forth), removal of carbon dioxide from the tissues, and removal of hydrogen ions from the tissues.

(2) Nervous Control-this often affects blood flow in large segments of the systemic circulation, such as shifting blood flow from the nonmuscular vascular beds to the muscles during exercise, stress, relaxation or changing the blood flow in the skin to control body temperature. Since the nervous control is the major focus of this thesis, we shall talk about it in more detail later.

(3) Humoral Control-various substances dissolve in the blood such as hormones, ions, or other chemicals that can cause either local increase or decrease in tissue blood flow [6]. The humoral factors that affect circulatory function are categorized as vasoconstrictor agents (norepinephrine, epinephrine, angiotensin, and vasopressin) and vasodilator agents (bradykinin, histamine, and prostaglandins) [6].

Norepinephrine is directly released when the sympathetic nervous system is stimulated during stress or exercise and this excites the heart, the veins, and the arterioles. Angiotensin acts simultaneously on all the arterioles of the body to increase the total peripheral resistance, thereby greatly increasing the arterial pressure. Vasopressin is the body's most potent constrictor substance.

Bradykinin causes very powerful arterial dilatation and also increased capillary permeability. Histamine is released when the tissue is damaged. It has a powerful vasodilator effect on the arterioles and, like bradykinin, also increases capillary porosity.

2.3.5 Autonomic Nervous System Regulation of Circulation

The autonomic nervous system is part of the nervous system that controls the visceral functions of the body. Regulation of internal activities such as blood pressure, heart rate, venous blood volume, body temperature, and gastrointestinal motility, among many others, is performed by the autonomic nervous system. Autonomic activity is controlled mainly by centers in the spinal cord, brain stem, and hypothalamus. Table 2.1 below summarizes the effects of the autonomic nervous system on organs [6]. The autonomic nervous system is divided into two anatomical and functional units with opposite properties: sympathetic and parasympathetic.

The sympathetic nervous system is responsible for creating an increased level of activity in an organism. Anatomically, sympathetic nerves are composed of two neurons:

Table 2.1 Autonomic effects on selected organs of the body. (from A. C. Guyton, *Human Physiology and Mechanisms of Disease,* 1992)

Organ	Effect of Sympathetic Stimulation	Effect of Parasympathetic Stimulation
Heart		
Muscle	Increased rate Increased force of contraction	Slowed rate Decreased force of contraction (especially atria)
Coronaries	Dilated (β_2); constricted (α)	Dilated
Lungs		
Bronchi	Dilated	Constricted
Blood Vessels	Mildly constricted	? Dilated
Systemic Arterioles		
Abdominal Viscera	Constricted	None
Muscle	Constricted (adrenergic α) Dilated (adrenergic β_2) Dilated (cholinergic)	None
Skin	Constricted	None

a preganglionic neuron and a postganglionic neuron. These neurons pass from the spinal cord through the white ramus into one of the sympathetic ganglia before reaching their destination as shown in figure 2.3. Most postganglionic sympathetic nerve endings secrete norepinephrine, a neurotransmitter that activates excitatory receptors, but in some cases can inhibit certain organs. The sympathetic nervous system is also responsible for the alarm or fight-or-flight response. This is caused by a mass discharge of all sympathetic nerve endings [6].

The parasympathetic nervous system, by contrast, generally lowers the activity of an organism, and is associated with a relaxed state. Anatomically, parasympathetic fibre

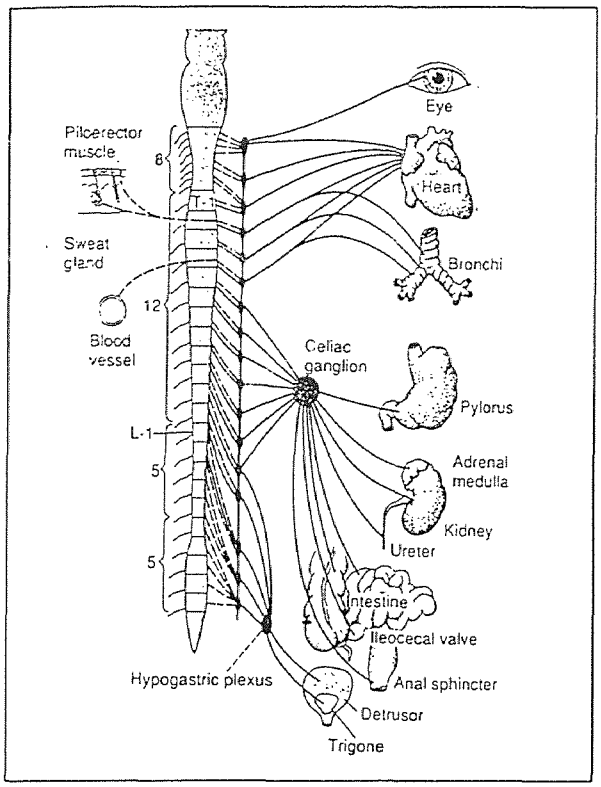

Figure 2.3 The sympathetic nervous system (from Guyton, A. C.*Human Physiology and Mechanisms of Disease*,1992)

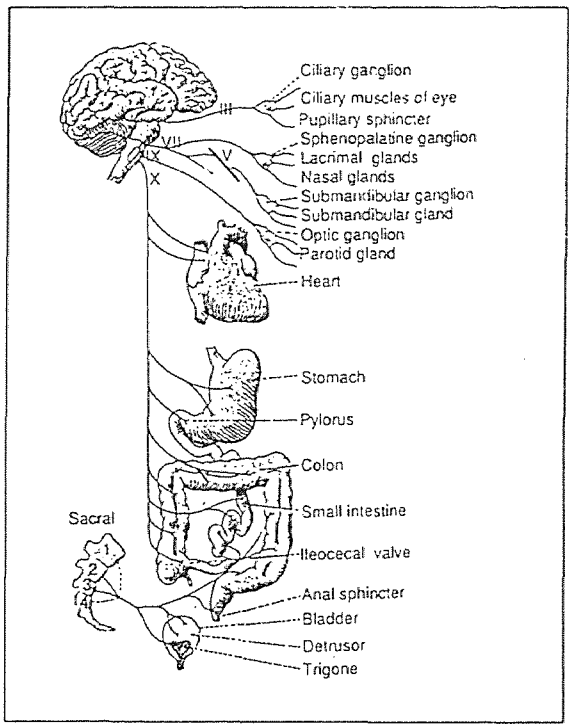

Figure 2.4 The parasympathetic nervous system (from Guyton, A. C.*Human Physiology and Mechanisms of Disease*,1992)

leave the brain through cranial nerves III, V, VII, IX, and X, and the second and third sacral spinal nerves (see figure 2.4).

Cranial nerve X is also called the vagus nerve, and since the vagus innervates much of the thorax and abdomen, especially the heart, the parasympathetic activity is often called vagal activity. All parasympathetic nerve endings secrete acetylcholine. Although acetylcholine generally has an excitatory effect, it is also known to have inhibitory effects as well, such as the slowing of the heart by the vagus nerve [6].

Both the sympathetic and parasympathetic nervous systems are continually active. These basal rates of activity are known as sympathetic and parasympathetic tone. The advantage of the tone is that it allows a single nervous system to increase or decrease activity in an organ. For instance, by changing the degree of sympathetic tone, the diameter of the arterioles can be increased or decreased. Without tone, the sympathetic nervous system can only cause vasoconstriction, and never vasodilation [6].

2.3.6 Venous Resistance and Peripheral Venous Pressure

Some exchange of materials occurs between the interstitial fluid and the venules. Indeed, permeability to macromolecules is often greater for venules than for capillaries [12]. The veins outside the chest, the peripheral veins, contain valves that permit flow only toward the heart.

The veins are the last set of tubes through which blood flows on its way back to the heart. In the systemic circulation the force driving this venous return is the pressure difference between the peripheral veins and the right atrium [12]. Most of the pressure

imparted to the blood by the heart is dissipated by resistance as blood flows through the arterioles, capillaries, and venules so that pressure in the first portion of the peripheral veins is only 5 to 10 mmHg. The right atrial pressure is close to 0 mmHg , so that the total driving pressure for flow from the peripheral veins to the right atrium is only 5 to 10 mmHg. This driving pressure is adequate because the veins have large diameters ,and therefore, they offer low resistance to blood flow, acting as low-resistance conduits to blood flow [12].

In addition to their function as low-resistance condiuts, the veins have diameters which are reflexly altered in response to changes in blood volume, thereby maintaining peripheral venous pressure and venous return to the heart [12]. In effect, the peripheral

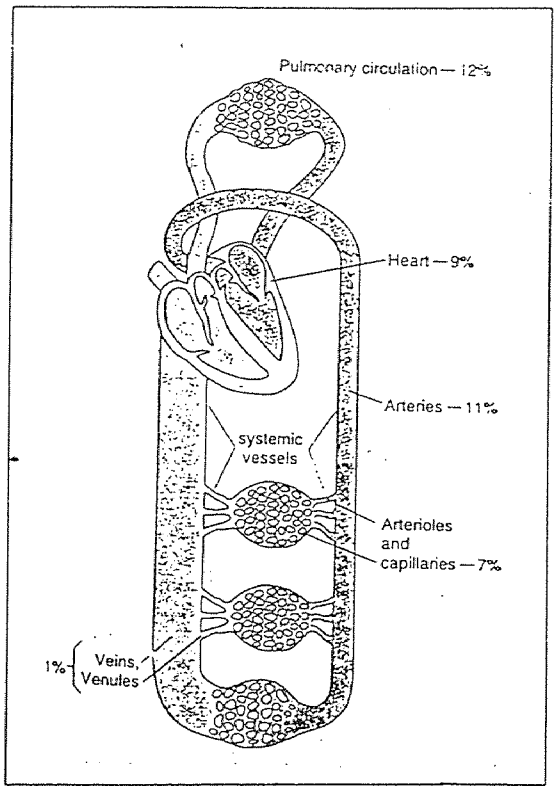

Figure 2.5 Distribution of the total blood volume in different parts of the cardiovascular system (from A. J. Vander, and J. H. Sherman. *Human Physiology*, 1994)

venous pressure is an important determinant of stroke volume. Because the walls of the veins are thinner and much more compliant than those of arteries, 60% of the total blood volume is present in the systemic veins at any given moment (figure 2.5) with an average pressure less than 10 mmHg.

Thus, veins can accommodate large volumes of blood with a relatively small increase in internal pressure [12].

The walls of the veins contain smooth muscle innervated by sympathetic neurons. Stimulation of these neurons releases norepinephrine, which causes contraction of the venous smooth muscle, decreasing the diameter and compliance of the vessels and raising the pressure within them [12].

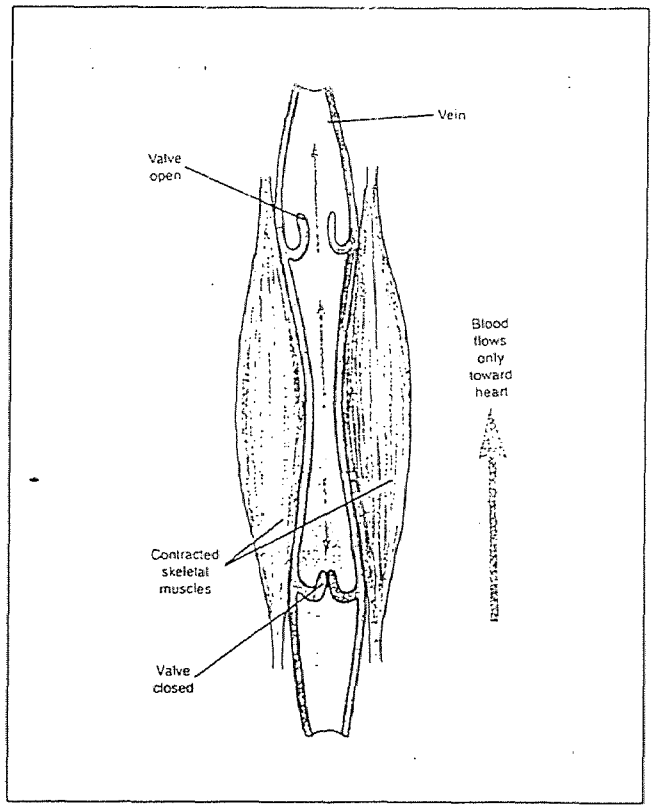

Figure 2.6 Skeletal muscle pump (from A. J. Vander, and J. H. Sherman. *Human Physiology*, 1994)

Two other mechanisms, skeletal-muscle pump and respiratory pump also increase venous pressure and facilitate venous return. During skeletal-muscle contraction, the veins running through the muscle are partially compressed, which reduces their diameter and forces more blood back to the heart. When the skeletal-muscle pump raises venous pressure locally, the valves permit blood flow only toward the heart and prevent flow back toward the tissues (figure 2.6). During inspiration, abdominal pressure increases and the thoracic pressure decreases. The net effect of these pressure changes in the abdomen and the thorax increase the pressure difference between the peripheral veins and the heart, and thus, venous return is enhanced [12].

2.4 Skin Temperature

The temperature of the inside of the body or in the "core" of the body remains almost exactly constant, within ±0.6 °C [6]. Heat is constantly being produced in the body as a byproduct of metabolism, and body heat is also continuously being lost to the

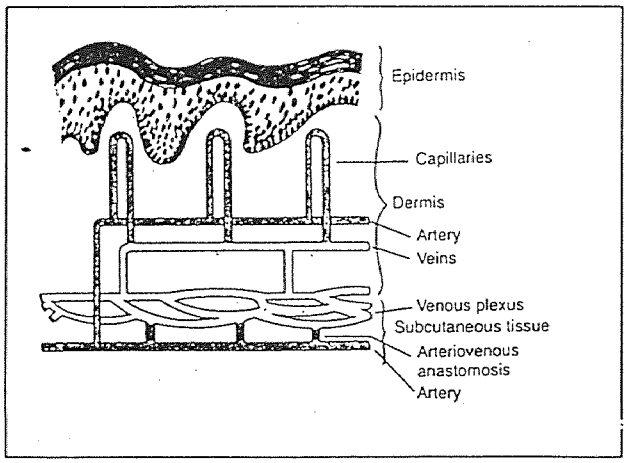

Figure 2.7 The skin circulation. (from Guyton, A. C. *Human Physiology and Mechanisms of Disease*,1992)

surroundings by radiation, conduction and evaporation. The amount of heat loss by each of these mechanisms depends on atmospheric conditions.

The skin, the subcutaneous tissues, and the fat of the subcutaneous tissues are heat insulators for the internal tissues of the body. The fat is especially important because it conducts heat only one third as readily as other tissues [6]. The insulation beneath the skin is an effective means of maintaining normal internal core temperature, even though it allows the temperature of the skin to approach the temperature of the surroundings [6].

Blood vessels penetrate the fatty subcutaneous insulator tissues and are distributed profusely immediately beneath the skin. Blood is also supplied to the plexus directly from the small arteries through highly muscular venous arteriovenous anastomoses, as illustrted in figure 2.7. The rate of blood flow into the venous plexus can vary from barely above zero to as great as 30 per cent of the total cardiac output. This high rate of blood flow causes heat to be conducted from the core of the body to the skin.

The temperature of the skin, as described above, is therefore, directly proportional to the amount of blood flowing through the cutaneous tissues, and its variation depends on three factors:

1. Changes in the core temperature of the body, which is regulated by the hypothalamus.
2. Changes in the environmental temperature, which cause local vasodilation or vasoconstriction. Widespread changes in skin temperature will cause temperature regulatory reactions from the hypothalamus.

For instance, when the body temperature rises too high, the hypothalamic thermostat will stimulate the sweat glands to cause evaporative heat loss from the body, and also will inhibit sympathetic centers that normally constrict the skin vessels, and thereby allowing vasodilation of the vessels [6]. On the other hand, the hypothalamic thermostat also possess heat conservation mechanisms that increase heat production when the body becomes cooled through intense vasoconstriction of skin vessel, piloerection (hairs stand on end), abolition of sweating, increased production of heat, and hypothalamic stimulation of shivering [6].

3. Changes in sympathetic tone, which vary the extent to which the peripheral arterioles are constricted or dilated [6].

Studies have shown that vasomotor reflexes are controlled almost entirely by the sympathetic nervous system [1]. Halperin et. al. demonstrated decreased fingertip blood flow in subjects under mental stress using venous occlusion plethysmography. Elam and Wallin also had reported that skin blood flow responses to mental stress depends on body temperature [8].

One aspect of this present study is to use measures of skin temperature and skin blood volume to indicate the reaction of the body to relaxation and stress.

CHAPTER 3

THE ELECTROENCENPHALOGRAM (EEG)

3.1 The History of EEG

The recording of brain potentials of man lagged for many years behind their demonstrations in animals, partly because in recording through the skull both electrodes lie at a distance from active brain tissue and the potentials are consequently attenuated. The realization that electrical activity of living tissue could be used as a sign of its function came in the mid 19th century after Du Boi-Raymond demonstrated that an electrical signal occurred concomitantly with the passage of nerve impulses. As a follow up of Raymond's research, Richard Caton demonstrated the existence of feeble electric currents in the brain of animals in 1875. The emergence of string galvanometer in 1906 introduced a new era in electrical recordings and more confirmations of Caton's original findings were made, including Neminski's demonstration in 1925 that recordings could be made through the intact skull. The first recordings from the human brain were made by Hans Berger in Jena in 1924 and published by him in 1929. Berger's observations were met with disbelief and mistrust, and it was not until 1934, when Adrian and Mathews in England repeated Berger's experiments and confirmed his observations, that his work became accepted by the scientific community. In his large number of observations, Berger demonstrated that the brain electrical activity consists more or less of a mixture of rhythmic, sinusoidal-like fluctuations in voltage having a frequency of about 1 to 60 Hz [32].

3.2 Types of Recordings

The recording of gross electrical activity from the brain through the intact skull constitutes an electroencephalogram (EEG). When the skull is trephined (opened with a circular saw) and the electrodes are placed either on the meninges covering the brain or within the cortex itself, the recordings constitute an electrocorticogram (ECoG). In a third recording procedure, the electrodes penetrate deep within the brain, and the recordings obtained are called depth recordings [31].

3.3 Electrode Connections

To record the voltage changes either through the skin covering the skull or from the surface of the cortex or from deep within the brain, the electrodes have to be arranged for either monopolar (also called referential or unipolar) or bipolar connections [32].

The principle of referential connection involves measuring the electrical activity at different electrodes simultaneously, in comparison with a common reference electrode. One of the electrode pair is over active cortical or subcortical tissue and the other on a far distant inactive point, such as the ear. Although the common reference in the monopolar recording allows valid comparisons to be made between amplitude measurements in different electrodes, there is no ideal reference electrode. There is no location on the head which is indifferent to the electrical activity inside it and no placement will give a truly indifferent reference. For example, the earlobes, commonly used sites of reference are close to the temporal lobes and hence pick up a considerable amount of cerebral electrical

activity from those areas. Another disadvantage of using the earlobes as a reference is that problems with ECG artifacts are more common.

In bipolar recording, the potential difference between two electrodes placed on the scalp is displayed. Unlike the case of referential recording, both electrodes are considered to be active, and the varying difference in voltage between the two is recorded. In this way, bipolar recordings do not provide an accurate measure of the amplitude of the waveform of a particular electrode. Depending on the magnitude and phase of the voltages, the signals are subject to cancellation or summation in the amplifier. For this reason, bipolar recording merely provides a comparison of the voltage at one electrode of a pair with respect to the voltage at the other.

3.4 The EEG Frequency Spectrum

Electric recordings from the exposed surface of the brain or from the outer surface of the head demonstrate continuous oscillating electric activity within the brain. Both the intensity and the patterns of this electric activity are determined by the overall excitation of the brain resulting from functions in the reticular activating system. The undulations in the recorded electric potentials are called an electroencephalogram (EEG).

The amplitude of the brain waves when measured through the scalp is about 10–100 μV, and their frequency can vary from 0.5 up to 100 Hz. The character of the brain waves is highly dependent on the degree of activity in the cortex [36]. Much of the time, especially during alert activity, the brain waves are small in amplitude and quite asynchronous. However, at other times the brain will exhibit very rhythmic activity that is

almost sinusoidal in nature. While the behavioral state of the subject remains so far as possible constant, the EEG changes continuously throughout life, rapidly during childhood and adolescence, and more gradually thereafter. Not only does the EEG of any individual changes continuously, but there are also considerable differences between one subject and another. However, the EEG that is best described statistically (in terms of its amplitude, spectral properties, etc.), retains some constant features and may, for most purposes, be regarded as a stationary random process [36].

The frequency spectrum in the EEG is broken down into alpha, beta, theta, and delta bands (or as commonly referred to; waves) . (see figure 3.1) [36].

Alpha waves consist of high-amplitude, well-synchronized sinusoidal waves having frequency of between 8 and 12 Hz. They occur in almost all adults, particularly in the back of the head, when they are awake but in a quiet, resting state with eyes closed. Alpha waves will disappear during sleep and when an awake person focuses attention on a specific mental activity [36]. Alpha waves are also prominent during meditation, and tend to decrease in frequency as meditation progresses. In experienced meditators, lower frequency alpha waves sometimes persist even after the person stops meditating. Alpha waves will not occur in the cortex without connections in the thalamus, so it is likely that a general thalamocortical origin of alpha exists, producing the periodicity and the ability to activate millions of neurons in the cortex.

Beta waves are desynchronized, lower-amplitude than alpha waves. Desynchronization is not only characteristic of the transition between the closing and the opening of the eyes, but also of the most alert, attentive, or excited states. Beta waves

normally occur at frequencies above 13 Hz, sometimes as high as 50 Hz, and they mostly appear in the parietal and frontal lobes during intense mental activity.

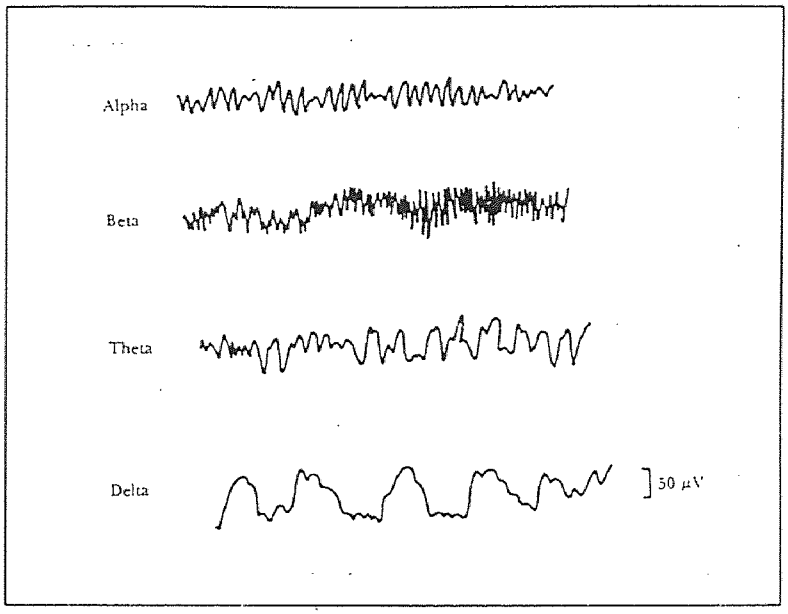

Figure 3.1 Examples of EEG (from Webster, J. G., *Medical Instrumentation: Application and Design*)

Theta waves oscillate at frequencies between 4 and 7 Hz. These waves occur mainly in the parietal and temporal lobes of children, but they can also appear during emotional stress in adults, especially during disappointment and frustration [36]. Theta waves also appear during deep meditation, especially in experienced meditators.

Delta waves include all frequencies below 4 Hz. They occur in very deep sleep, in infants, and in serious organic brain disease. They also have occurred in animals whose cerebral cortex has been transected from the thalamus, indicating the waves can occur in the cortex independent of other brain areas [36].

The EEG is still a very crude measurement of the brain functioning. All that is being detected is the overall pattern of the activity of millions of neurons. Like electricity, one can use the EEG as an index or measure of something without knowing precisely what it is or how it works. However, at more prosaic levels of consideration, the background spontaneous EEG has been a useful index of the psychological state of man, and that it is the most convenient technique available for assessing the general activity of the brain and relating it to different states of consciousness. In addition, the degree of synchronization or desynchronization or activation response of the EEG can be useful to warn when a change has taken place in the state of the brain's condition.

3.5 The 10–20 International System of Electrode Placement

As the EEG recording machines became more sophisticated with a corresponding emergence of multichannel machines, the question of where to place the many electrodes that it was possible to use, and how to hook them up, became a major issue. To bring a harmony into the resulting chaos, the First International Congress of EEG held in London in 1947 recommended that an attempt be made to standardize the electrode system used. Herbet Jasper studied the different systems used at the time and, in 1958, suggested adopting what is called the 10–20 International electrode placement [32].

The placement of electrodes in this system depends upon measurements made from standard landmarks on the skull. The system affords adequate coverage of all parts of the head, with electrode positions designated in terms of the underlying brain areas (i.e., frontal pole, frontal, central, parietal, occipital, and temporal) to which they

correspond. These are abbreviated using capital letters, with F corresponding to frontal, C corresponding to central, P corresponding to parietal, O corresponding to occipital, T corresponding to temporal and Fp corresponding to frontal pole. A single-digit number goes along with the letter. Odd numbers designate left-sided and even numbers right-sided locations.

The term "10–20" is used because the electrodes are placed either 10% or 20% of the total distance between a given pair of landmarks which makes it appropriate for use with infants as well as adults having very large heads.

For anteroposterior measurements, the distance between the nasion and inion over the vertex in the midline is taken. Five points are located along this line and designated front pole (Fp), frontal (F), central (C), parietal (P), and occipital (O). The point Fp is 10% of the nasion-to-inion distance; C is behind F at a distance of 20% , and so on. These points are marked off directly on the scalp [32].

The lateral measurements are made in the central coronal plane on the basis of the distance between the left and right preauricular points. Ten percent of the distance above the preauricular points marks the location of the T3 and T4 electrodes, C3 is at a distance of 20% above T3, and C4 20% above T4 (see figure 3.2). Using these directions, a total of 19 electrode placements are marked off on the scalp. Together with the earlobe placements (designated as A1 and A2), this comprises the 21 standard electrodes in the 10-20 International System.

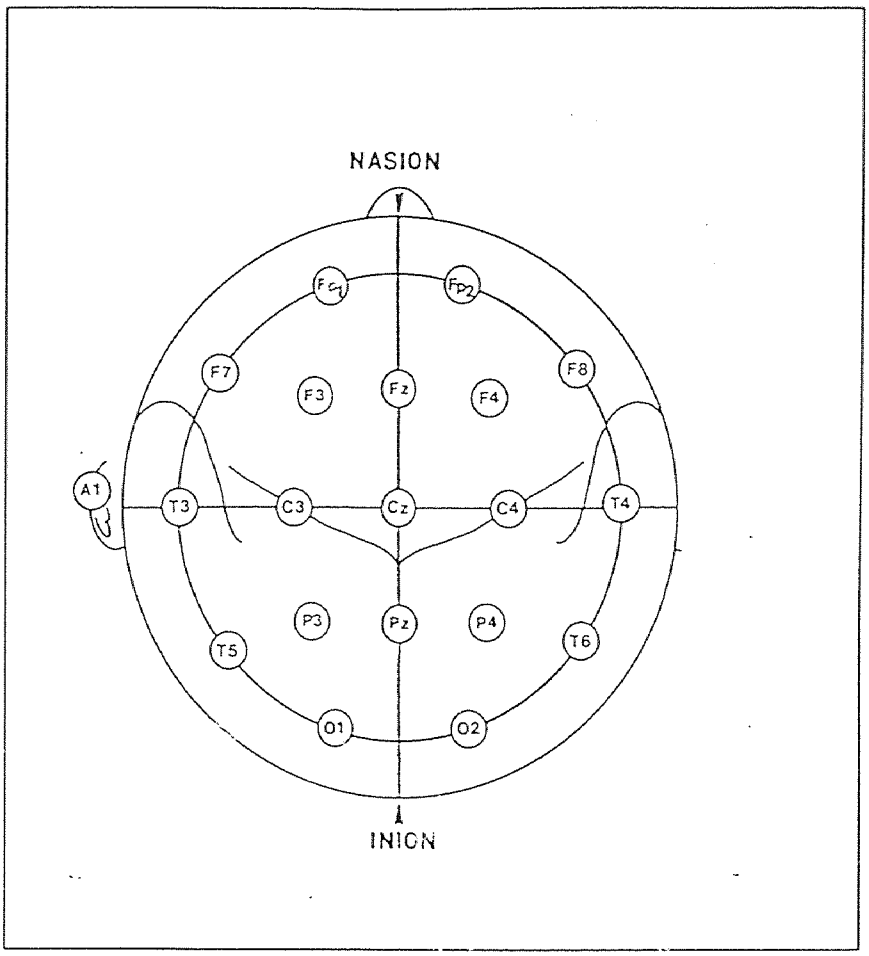

Figure 3.2 The 10-20 International System of Electrode Placement (from Duffy F.H., et. al *Clinical Electroencephalogram and Topographical Brain Mapping*)

CHAPTER 4

SIGNAL PROCESSING

This chapter summarizes the mathematical tools used in this thesis project to process and analyze the data collected on EEG activity of human subjects as well as blood flow and temperature of the fingertip. The signal processing techniques include Fast Fourier Transform (FFT), Power Spectral Density, Coherence, and Cross Correlation Function.

4.1 Signal Processing for Blood Flow

The second part of this thesis project concerned investigating the relationship between blood flow and skin temperature, and how these physiological parameters are affected by stress and relaxation. The sampling rate for this part of the thesis project was set at 100 Hz. The temperature and the venous blood volume of the fingertip change very slowly, therefore, choosing 100 Hz as sampling rate satisfies Nyquist's sampling rate theorem.

The autocorrelation function of a continuous function *X(t),* defined in this thesis as the signal from the venous blood volume of the fingertip, can be defined as [37]

$$R_X(\tau) = \frac{1}{T}\int_0^T X(t+\tau)X(t)dt \qquad (4.1)$$

and the corresponding power spectrum can then be defined as

$$S_X(j\omega) = \mathcal{F}[R_X(t)] = \frac{1}{T_0}\int^{T} R_X(t)e^{-j\omega t}\,dt \qquad (4.2)$$

Similar expressions can be written for the autocorrelation and power spectral density of a second function $Y(t)$. $Y(t)$ corresponds to the signal from the temperature of the fingertip. The cross correlation of the two signals $X(t)$ and $Y(t)$ can further be defined as

$$R_{XY}(\tau) = \frac{1}{T}\int_{0}^{T} X(t+\tau)Y(t)\,dt \qquad (4.3)$$

with the corresponding cross spectral density:

$$S_{XY}(j\omega) = \mathcal{F}[R_{XY}(\tau)] = \frac{1}{T}\int_{0}^{T} R_{XY}(\tau)e^{-j\omega\tau}\,d\tau \qquad (4.4)$$

Equation (4.4) is the basic mathematical tool for the signal processing techniques implemented in this thesis project, and it is often called the Wiener-Khinchine relation [37]. It shows the relationship between the Fourier Transform, the Cross Correlation, and the Power Spectral Density functions.

It is evident from equations (4.3) and (4.4) that the cross correlation function can be calculated in two ways. The direct method using equation (4.3), which involves the computation of average products among the sample data values. The second method (from equation (4.4)), the one used in this study, is the indirect approach of first computing the spectral density estimate using FFT procedures, and then computing the

inverse transform of the power spectrum. Although the direct approach is easier to program and represents a more logical approach, the second approach has more computational efficiency of FFT algorithms and much less expensive to execute [37].

Thus, the cross correlation between the finger blood volume and the finger temperature is computed by taking the inverse Fourier Transform of the cross spectral density from equation (4.4) as

$$R_{XY}(\tau) = \mathcal{F}^{-1}\left[S_{XY}(j\omega)\right] \tag{4.5}$$

Matlab estimates the cross spectral density $S_{XY}(j\omega)$ of signal vectors X and Y using Welch's [24] averaged periodogram method. X and Y are divided into overlapping sections (see section 5.1.4.2) each of which is detrended, then windowed by the window function, and then zero-padded to length nfft (see appendix A for the code). The Fourier transform of X is defined as:

$$X(\omega) = \frac{1}{T}\int_0^T X(t)\cdot e^{-i\omega t}\cdot dt \tag{4.6}$$

Similarly, Fourier transform of Y is given as:

$$Y(\omega) = \frac{1}{T}\int_0^T Y(t)\cdot e^{-i\omega t}\cdot dt \tag{4.7}$$

Now, Welch's method is as follows [24]:

Suppose $X(j), j = 0, \ldots, N-1$ are samples of a sequence X, and $Y(j), j = 0, \ldots, N-1$ are samples of a sequence Y. Suppose we have K segments; $X_1(j), \ldots, X_k(j)$, and $Y_1(j), \ldots, Y_k(j)$, and they cover the entire record. For each segment of length L we calculate a modified periodogram. That is, we select a data window $W(j), j=0, \ldots, L-1$, and form the

sequences $X_1(j)W(j), \ldots, X_k(j)W(j)$. Similarly, for Y we have $Y_1(j)W(j), \ldots, Y_k(j)W(j)$.

We then take the FFT of the two sequences as:

$$A_k(n) = \frac{1}{L}\sum_{j=0}^{L-1} X_k(j)\overline{Y}(j)W(j)e^{-2kijn/L} \qquad (4.8)$$

where $\overline{Y}$ is the conjugate of Y. Finally, we obtain the K modified periodograms

$$I_k(f_n) = \frac{L}{U}\left|A_k(n)\right|^2 \qquad k = 1, 2, \ldots, K, \qquad (4.9)$$

where

$$f_n = \frac{n}{L} \qquad n = 0, \ldots, L/2 \qquad (4.10)$$

and

$$U = \frac{1}{L}\sum_{j=0}^{L-1} W^2(j) \qquad (4.11)$$

The cross spectal estimate is the average of these periodograms, i.e.,

$$S_{XY} = \frac{1}{K}\sum_{k=1}^{K} I_k(f_n) \qquad (4.12)$$

A program called cor.m was written in Matlab to calculate the cross correlation between the two signals (see Appendix A for the code).

4.2 EEG Signal Processing

4.2.1 Coherence Spectral Array (COSPAR)

Application of the FFT to process a continuous analog signal such as EEG requires that

the analog EEG signal be digitized at above the Nyquist sampling rate. The sampling rate for the EEG was 200 samples per second. The highest frequency in the EEG spectrum is less than 100 Hz; therefore, sampling at 200 Hz satisfies Nyquist's sampling rate.

The relationship between the F3 and F4 signals coming from the left and right locations of the scalp of each subject, respectively, was evaluated using the coherence function. The coherence spectrum may be interpreted as a measure of the consistency of the relationship between matching frequency components of two signals over a length of time determined by the analysis epochs employed in the ensemble averaging to form the smoothed cross-spectra [22].

Coherence is a mathematical quantity which provides a measure of the constancy of the relationship between the phases of the EEG at a specified frequency when measured at two spatially separated points of the scalp. It is a sensitive indicator of the degree of long-range order in cortical activity-at least to the extent that such orderliness is mirrored in the EEG [18].

The coherence spectral array, or cospar, is a graphical representation of coherence. For the EEG signal, a high coherence (near 1) over time indicates a long range spatial ordering. Thus, coherence is unity if the two signals have the exact same frequency content, in other words, if one signal is completely linearly dependent on the other. This type of ordering increases in physical systems as they relax to lower states of excitation. Therefore, increased spatial ordering in the EEG indicates a lowering of the excitation

level of the brain, which is the response obtained from relaxation. The cospar graph makes this order in the EEG much easier to visualize [22].

The coherence function is then defined as the ratio between the cross spectral density of $X(t)$ and $Y(t)$ to the product of individual power spectral densities

$$\gamma^2_{XY} = \frac{|S_{XY}(j\omega)|^2}{S_X(j\omega)S_Y(j\omega)} \tag{4.13}$$

Levine developed a method for calculating the coherence spectrum between pairs of EEG signals. In this technique, the two signals were first divided into short epochs of 256 samples, which for Levine's work corresponded to 5.12 seconds of EEG. The power spectra and cross spectrum of each signal were computed using an ensemble average on overlapping data segments discussed above on section 4.1 [24].

Once the power and cross spectra are computed, the squared coherence spectrum for each epoch was calculated. A threshold was applied to the coherence spectrum at a fixed level. Levine used 0.95 as the coherence threshold to reduce the likelihood of spurious coherence, or coherence events not representative of long range spatial ordering. The resulting coherence spectra for all epochs were assembled together in time, resulting in a three-dimensional looking graph of coherence level versus time and frequency [10].

For the present study, an algorithm written by King [30] in MATLAB was used to compute the squared coherence function of four EGG channels which is based on the methods of Levine (see Appendix A). The output of the program was a surface mesh plot of coherence above a 0.98 threshold versus time and frequency.

CHAPTER 5

EXPERIMENTAL METHODS

The first part of the research was concerned with examining EEG coherence during group meditation. This part will be referred to as experiment I. The second part involved a study of the correlation between blood flow to the skin and the skin temperature, and how the correlation relates to relaxation and stress. This part will be referred to as experiment II.

5.1 Experiment I

5.1.1 Setup for Experiment I

5.1.1.1 Group Meditation Study I: Two female subjects in their mid-twenties participated in this experiment. One had no previous meditation experience, and so a list of instructions on how to meditate were given.

There were four conditions in this experiment: Eyes Open (EO), Eyes Closed (EC), Single Meditation (SM) and Group Meditation (GM). Each protocol had a 5 minute duration. The two subjects were in two separate but adjacent rooms, and the instruments were in a third room.The experiment was performed using the following protocols:

(1) Protocol I -Subject I EO, Subject II meditation (SM).

(2) Protocol II -Subject I meditation (SM), Subject II EO.

(3) Protocol III - both subjects EC, but no meditation.

(4) Protocol IV - both subjects eyes closed and meditate (GM).

The order of the first two protocols were chosen based on tossing a coin. If the coin landed head up, it meant protocol I would be done first (Subject I-EO, and Subject

II-SM), otherwise protocol II would be performed first (Subject I-SM, and Subject II-EO). Once the experiment was started, all communications with the subjects were done through two small buzzers which were taped to the walls of each room and close to the subjects. The buzzers were tuned according to the taste of each subject to produce very low and non-disturbing beeps. The number of beeps corresponded to what the subject had to do. The codes for each number of beeps were carefully and repeatedly explained to the subjects before each experiment. The code for the beeps were: one beep meant EO, two beeps meant EC and three beeps meant meditation. Before the subjects would begin, a coin would be tossed, and based on the outcome, a table for the format of the experiment would be drawn. See table 5.1 for a typical format of an experiment for a tail up outcome when a coin was tossed.

Table 5.1 Format of the experiment

Number of Protocol	Subject I	Subject II
1	SM-3 Beeps	EO-1 Beep
2	EO-1 Beep	SM-3 Beeps
3	EC-2 Beeps	EC-2 Beeps
4	GM-3 Beeps	GM-3 Beeps

In study II, the protocol was modified to eliminate the possibility of proceeding straight from eyes open to meditation.

5. 1.1.2 Group Meditation Study II: Two male and two female subjects participated in this study. They were between 25 and 30 years of age.

In this case, both subjects performed the same protocol at the same time except for the single meditation. Thus, in protocol I-both subjects were EO, Protocol II-both subjects were EC, and protocol III-both subjects were GM simultaneously, whereas in protocol IV-when subject I-EO, subject II would meditate (SM) or vice versa. To determine which subject meditated and which was EO in the fourth protocol, again a coin was tossed before the subjects began.

5.1.2 EEG Acquisition

In order to record a signal from the body, the skin must be cleaned and prepped in order to increase signal transmission from the skin surface to the electrode. Thus, the scalp, the ears, and the wrist of each of the two subjects were cleaned with rubbing alcohol. Two electrodes were then affixed to the forehead, F3 and F4 of each subject in accordance with the 10-20 International System (see section 3.5). The F3 and F4 positions of each subject were recorded with linked ears, A1 and A2 as reference (see sections 3.3 and 3.5). A ground electrode for the amplifier was located at the wrist.

The forehead electrodes were connected to a Gould universal amplifier (model 13-4615-58, Gould, Inc., Valley View, OH) at the (+) position with the linked ears at the (-) position, and the ground at the Gould chassis GND position. As a result, for the EEG acquisition alone four channels were used for the two subjects. The input channels to the DAS-1601 A/D converter board (Keithley MetraByte/Asyst, Tauton, MA) were set at -5 volts to +5 volts. EEG signals generally range from around 50 μV to close to 1 mV. The gain of the amplifier was adjusted so that the output EEG signal from the Gould was 1-2

V_{p-p}, which would leave a buffer at the A/D board for relatively high voltage artifacts such as blinking or eye movements. The filters on the amplifier were set for a passband of 1 to 30 Hz, which included the delta (below 4 Hz), theta (4 to 7 Hz), alpha (8 to 12 Hz) and beta (above 12 Hz) EEG bands. EEG waveforms were monitored with a 2-channel digitizing oscilloscope (Hewlett Packard Model 4201A) connected to the BNC outputs on the rear of the amplifier. Shielded cable connected the 37 pin data output connection, also on the rear of the amplifier, to the data acquisition computer. Coaxial shielded cables were used for all the EEG connections from the subject to the Gould amplifier.

For EEG electrodes, OmniPrep (D. O. Weaver & Co.,Aurora, CO) was used, and applied with a gauze pad. Silver cup electrodes (Jari Electrode Supply, Yucca Valley, CA) were applied using Elefix EEG electrode paste (Nihon Kohden Corporation, Tokyo, Japan).

5.1.2.1 Skin Temperature: One aspect of the present study was to measure the temperature of the skin (the finger) of each subject and the ambient room temperature during each protocol as a control variable of meditation. Thus, it was desired to see if changes in skin temperature would correspond to changes in the alpha band EEG coherence measurements.

For this purpose and the purpose of experiment II, which will be discussed later in this chapter, a bridge temperature transducer circuit (TTC) was assembled for four channels. Four thermistors (model G22K7MCD10, BethaTherm Corp., Shrewbury, MA) were connected to the TTC which consist of a LM324N quad inverting op-amp (see

figure 5.1). Because the four circuits are similar, only one of them is shown in the figure. The lower left portion of the circuit is the thermistor circuit, consisting of the power supply V_{cc} , resistor R_3, and the thermistor R_{TH}. The power supply was from a Triple Output DC Power Supply, Model TP340 (Power Supply Designs Inc., Westbury, N. Y.,

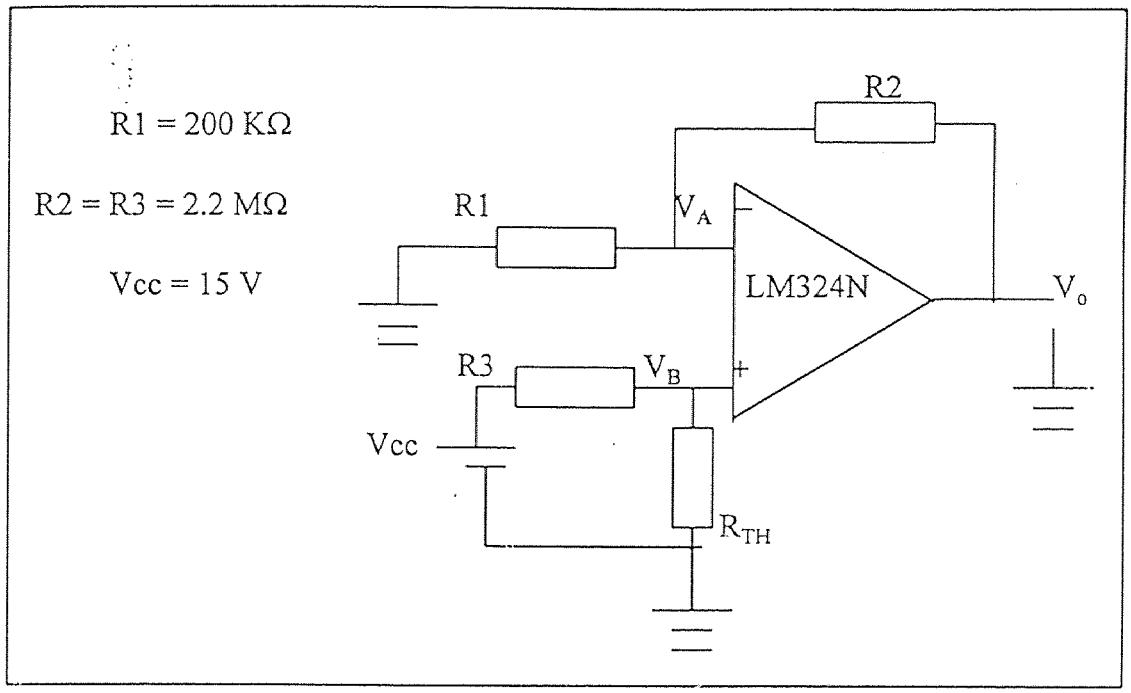

Figure 5.1 Temperature Transducer Circuit

Palo Alto, CA). As the temperature measured by the thermistor rises, the resistance of the thermistor falls. The output voltage from the circuit was fed into the op-amp circuit. The output voltage from the circuit was fed into the op-amp circuit at the (+) input, where it was amplified by a gain factor of 10. the output of TTC (V_o) was then sent by shielded cable to a Beckman R611amplifier for further amplification before it was sent to the DAS 1601 A/D board.

From the circuit, we obtain the following equations:

$$V_B = \frac{R_{TH}}{R_{TH} + R3} Vcc \tag{5.1}$$

$$V_A = V_B \tag{5.2}$$

$$\frac{V_B}{R1} = \frac{V_o - V_B}{R2} \tag{5.3}$$

From equation (5.3), we define the gain A_{vi} as:

$$Avi = 1 + \frac{R2}{R1} = 1 + \frac{2.2\ M\Omega}{200\ K\Omega} = 11 \tag{5.4}$$

Substitute equation (5.2) into equation (5.3) and after rearrangement, we obtain

$$V_o R1 = V_A (R1 + R2) \tag{5.5}$$

Eliminating V_A from equations (5.1) and (5.5), we obtain the required relationship between the output voltage Vo as a function of the resistance of the thermistor (R_{TH}).

Thus,

$$Vo = \left[\frac{R1 + R2}{R1} Vcc\right] x \frac{R_{TH}}{R_{TH} + R3} \tag{5.6}$$

The thermistor was calibrated based on Equation (5.6). From the package of the thermistor, the relationship between the resistance and temperature are given. At average room temperature of 25 °C, the resistance of the thermistor is 10 KΩ. The corresponding resistance of the thermistor at 35 °C (the average body temperature of person) is 6.941 KΩ. These values for R_{TH} are relatively low compared to the value of R3, and therefore, equation (5.6) can be approximated as:

$$V_o \approx \left[\frac{R1 + R2}{R1 \cdot R3} Vcc\right] R_{TH} \ , \ R_{TH} << R3 \qquad (5.7)$$

Substituting in the values for R1, R2, R3, and Vcc into equation (5.7), we have

$$Vo = 81.82 \times 10^{-5} R_{TH} \qquad (5.8)$$

Since the resistance of the thermistor is a function of temperature T, and Vo is linearly related to R_{TH} (at least between 25 and 35 °C) we can easily obtain a relationship between Vo and temperature T. Table 5.2 shows the computed values of the output voltage Vo of the circuit corresponding to R_{TH} and temperature T from the manufacturer using equation (5.8). A plot of Vo versus T is nonlinear and so it has to be linearized. A plot of natural logarithm of Vo with temperature T from table 5.2 yields a straight line with the slope -0.0356, and the intercept on the voltage axis was 0.53 V. In other words, the linearized voltage-temperature relation finally was obtained as

$$\ln(Vo) = 0.53 - 0.0356\,T$$

$$\therefore \quad T = -\frac{\ln(V_o) - 0.53}{0.0356} \tag{5.9}$$

Table 5.2 The Relationship between Vo, R_{TH} and T

Temperature T in $^{\circ}C$	Resistance of Thermistor R_{TH} in KΩ	Output Voltage of Circuit Vo in μV
15	14.68	1201.117
20	12.09	989.203
25	10.00	818.200
30	8.313	680.169
35	6.941	567.912
40	5.828	476.846

Since the output of the TTC was fed into the Beckman R611 amplifier, it became necessary to calibrate the Beckman. DC signals of known amplitudes of 0.25, 0.27, 0.30, 0.50, 0.75, 0.80, 1.00 volts were passed through the Beckman to the DAS-1601 A/D converter in the computer. The corresponding voltages obtained from the computer were plotted with the input, and a straight line passing through the origin was obtained. The slope was 0.00243. Thus, the overall equation required to linearize the temperature and the voltage of the temperature transducer circuit after passing through the Beckman R611 were obtained as:

$$T\,(^{\circ}C) = \frac{\ln(0.0005114 \cdot V_o) - 0.53}{-0.0356} \tag{5.10}$$

A program was written in Matlab called thm.m to compute the calibration relation in equation (5.10)-see appendix A for the code.

One thermistor was taped to the wall of each subject's room, but was not touching the wall. Its purpose was to monitor the ambient room temperature of each subject. Because it requires some time before the thermistor fully assumes the temperature of its environment, the thermistor was always the first device affixed to the subject. The thermistor was taped to the distal portion of the middle finger of the subject's active hand, at the center of the fingertip. A cotton wool was taped in place over the thermistor to provide thermal insulation.

5.1.3 Data Acquisition Procedure

Data were acquired and recorded with an IBM compatible microcomputer with a 286 CPU, 1MB ram, and a 40 MB hard disk drive. The output of the Gould amplifier was connected via a shielded cable to the DAS-1601 A/D converter board in the computer (Keithley MetraByte/Asyst, Tauton, MA). A diagram of this set up is shown in appendix B (see figure B.1). Once the eight inputs (four from the Gould amplifier which measured the EEG and the other four from the Beckman which measured the finger temperatures of the subjects and their ambient room temperatures) were connected to the amplifying equipment, the inputs to the A/D board could be monitored using a display program called Primplot by J. F. Andrews. Any adjustments in gain settings or connection problems could be resolved at this time. When all was in order, data were collected using Streamer v3.25 (Keithley MetraByte/Asyst), a data collection program included with the DAS-1601 board. Once collected, the data files were copied to 1.2 MB floppy diskettes. These files were then transferred onto the hard drive of the 66 MHz AST 486 Computer

for storage and subsequent analysis. All signals in this experiment were sampled at 200 samples per second.

5.1.4 Data Analysis

5.1.4.1 Unpacking Data: Data collected on the data acquisition computer by streamer were saved to the root directory of the hard drive in a packed binary format, using 2 bytes per sample. The software used for data analysis, MATLAB v4.0 (The Math Works, Inc., Natick, MA), cannot read the data in this format, so the data must be converted to an ASCII format which these programs can use. A program called Kunpack2 (a modified version of the unpack utility that Keithley MetraByte/Asyst provided with the DAS-1601 A/D board) was utilized to unpack the data. Kunpack2 converted the raw data files to an ASCII file where each channel of data was represented as a column in a matrix and spaces separated the columns.

The raw data were moved to an IBM-compatible computer and the ASCII files were copied onto the hard drive for analysis.

5.1.4.2 Coherence Spectral Array (Cospar): Analysis of the data was performed on an IBM-compatible computer. Unpacked data files were imported into MATLAB, a software package that included engineering design and analysis algorithms and permitted the writing of custom MATLAB programs. MATLAB also included a Signal Processing Toolbox, which included many digital signal processing algorithms such as filters, transforms, and windowing algorithms.

A program called "cospar.m" written by King [30] was used to calculate the cospar using Levine's methods [22]. Two channels of EEG data were input to the program. The resulting coherence spectra for all epochs were assembled together in time, resulting in a three-dimensional looking graph of coherence level versus time and frequency The outputs consisted of mesh and contour plots of coherence above 0.98 vs. time and frequency. A listing of the MATLAB code appears in Appendix A and it worked in the following way [22]. Two channels of EEG signal were lowpass filtered using a 9th order Butterworth filter with cutoff frequency at 45 Hz to remove any residual 60 Hz interference. The signals were then highpass filtered with a 7th order elliptical filter with a cutoff frequency at 1.5 Hz, passband ripple of 0.05 dB, and stopband ripple of 50 dB. The elliptical filter provided the steepest cutoff characteristics, which allowed the low frequency trend to be removed while preserving EEG frequencies above 2 Hz. A zero phase filter algorithm included in MATLAB was employed to eliminate phase distortion. In order to keep EEG epochs short (thus improving time resolution), Levine specified that a procedure described by Welch be used, where overlapping segments of data are ensembled and averaged [24]. Conveniently, MATLAB also contained an algorithm that computed the power spectrum using Welch's method. Five second epochs of EEG were chosen. For each epoch, the two signals were divided into a number of 256 point sections, each of which overlapped by 19 points. Each section was windowed with a Kaiser window, a 256 point FFT was taken, and then accumulated with a running sum of the previous sections. The cross spectral density of both signals was also calculated in the same way. Specifically, the program calculated the spectral density as:

$$S_{xx}(e^{j\omega}) = \sum_{i=1}^{k} \left| X_i(e^{j\omega}) \right|^2 \tag{5.11}$$

and cross spectral density as:

$$S_{XY}(e^{j\omega}) = \sum_{i=1}^{k} Y_i(e^{j\omega}) X^*(e^{j\omega}) \tag{5.12}$$

where:

$$k = \frac{n - overlap}{m - overlap} \tag{5.13}$$

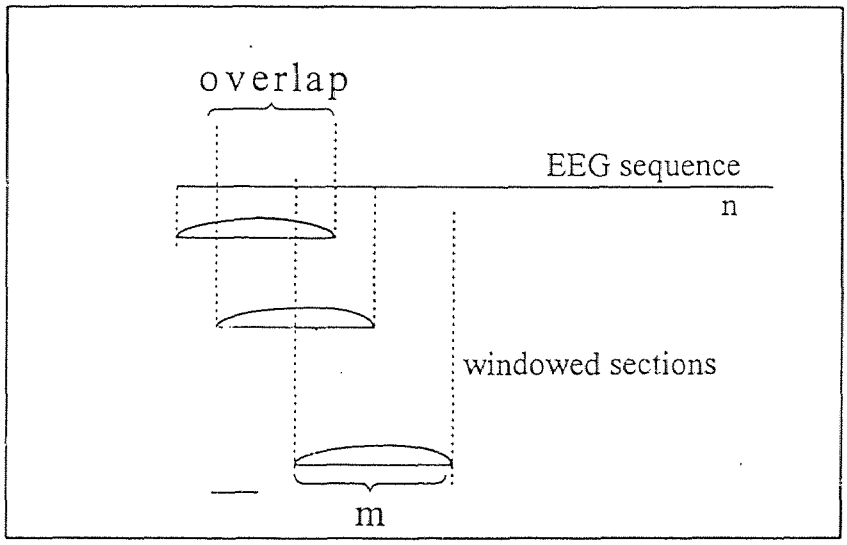

Figure 5.2 Sectioning and Windowing of EEG in MATLAB

Here, *n* is the sequence length, *m* is the size of the FFT (256 points), and *overlap* is the number of points the next sequence overlapped the previous one (237 points)-see figure (5.2). With the spectral densities evaluated, the coherence for the epoch was calculated as

$$C_{xy} = \frac{\left| S_{xy}(e^{j\omega}) \right|^2}{S_{xx}(e^{j\omega}) S_{yy}(e^{j\omega})} \tag{5.14}$$

For each five second epoch, a vector of coherence versus frequency was produced, with the coherence values ranging from 0 and 1. In this thesis project a threshold of 0.98 was used instead of the 0.95 threshold employed by the author [30] for reducing the likelihood of spurious coherence, or coherence events not representative of long range spatial ordering. The resulting matrix was graphed as a surface mesh plot and a contour plot of coherence versus time and frequency. An example of a Cospar plots for one of the subjects during a group meditation with 0.98 and 0.95 thresholds are shown in figures 5.3 (a) and (b) respectively. Comparing figures 5.3 (a) and (b) we see that most of the spurious coherence was removed, leaving coherence with well defined frequency bands.

5.2.1 Setup for Experiment II

This experiment has the following objectives:

(1) To find out the relationship between blood flow to the peripheries such as the fingertips and the skin temperature at the same locations.

(2) To find out how these physiological parameters in point (1) above are affected by relaxation and stress.

5.2.2 Skin Blood Flow and Temperature Instrumentation

The instrumentation for this experiment was basically the same as the experiment I except that a photoplethysmograph was added (see figure B.2 in appendix B). Two outputs from the photoplethysmograph were fed into the Gould amplifier. The blood volume was monitored on the Digitizing oscilloscope (54201A by Hewlett Packard).

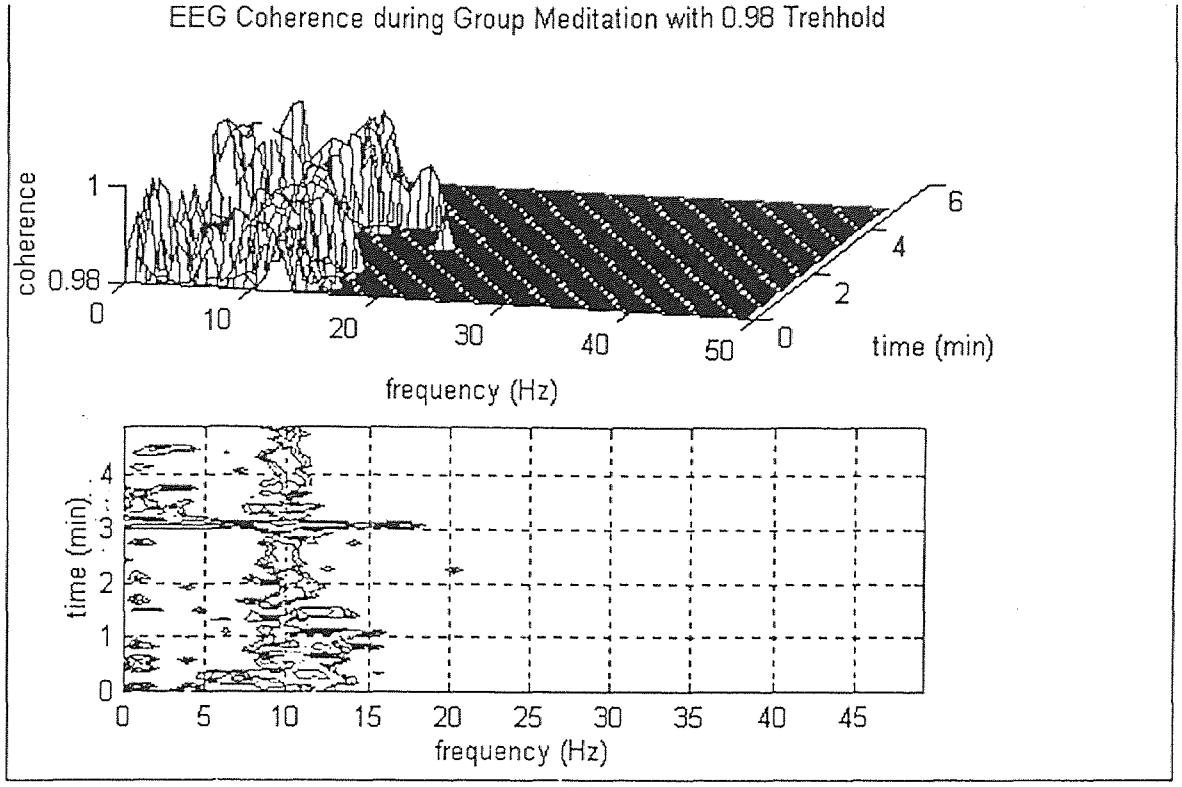

(a)

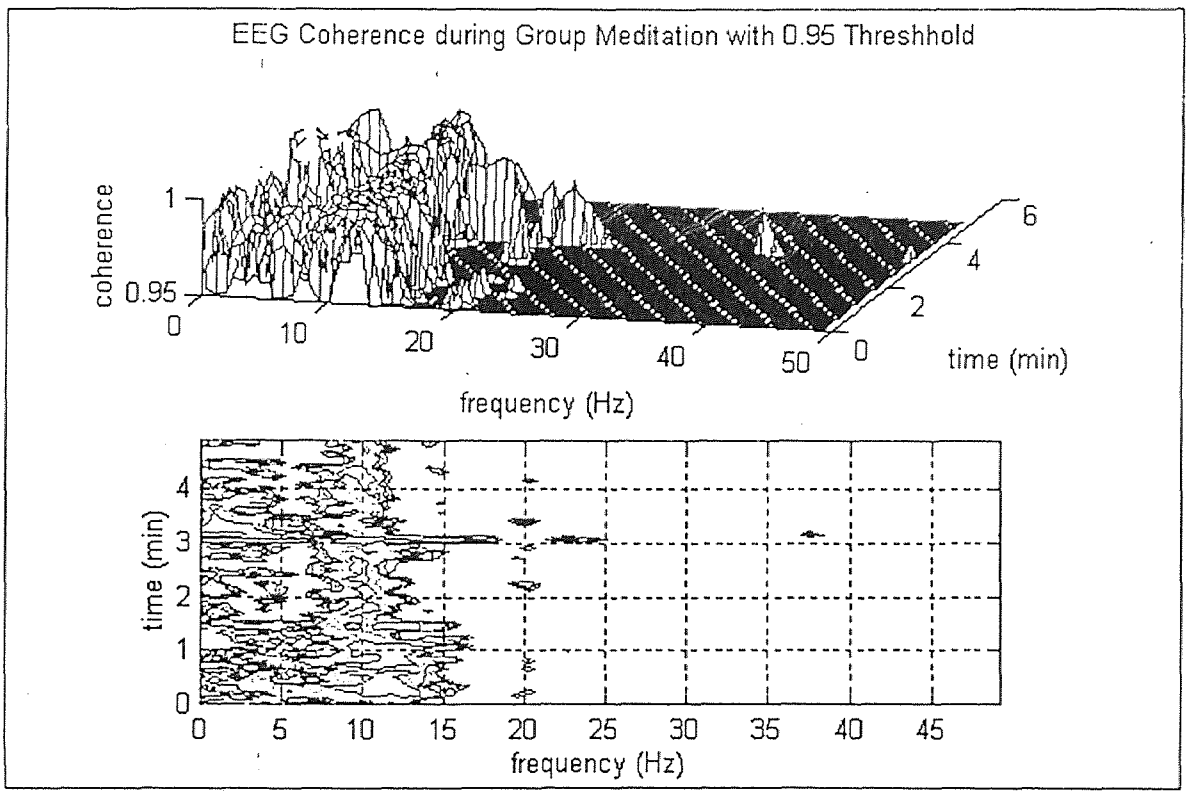

(b)

Figure 5.3 Example of cospar plots during a group meditation for a subject with: (a) Threshold = 0.98, and (b) Threshold = 0.95

Two out of the four outputs of the temperature transducer circuit were used in this study.

MedaSonics photoplethysmograph (PPG) model PPG13 by Kendall Hospital Company (Mountain View, California) detects changes in blood volume in the microcirculation near the skin's surface. Another important clinical application of the PPG13 is the detection of pulse on a finger or toe: changes in pulse amplitude is an indication of vasoconstriction [13].

A light-emitting diode (LED) housed in a small rectangular head of the PhotoPulse Sensor transmits infrared light which, when reflected from blood in small superficial vessels, is detected by a phototransistor and converted to an electrical signal [13].

The photoplethysmograph PPG13 has two operating modes: the arterial and venous modes. In the arterial position the amplifier is AC coupled and has a frequency response of 0.5 to 16 Hz which is suitable for detecting and recording the rapidly changing pulsatile signals produced by arterial blood volume changes in the microcirculation [13]. In the venous position the amplifier is DC coupled and cumulative changes from a baseline occurring over longer periods of time can be detected. This permits observation of changes in regional venous blood volume. There is also a zero-set switch, which when depressed, a zero baseline is automatically set for the venous output signals. This is required because slight movement of the sensor cause relatively large changes in the signal and shifts the recording baseline. Depression of zero-set returns the tracing to the center of the recording. Although the PPG13 has two functional modes, it can only output one signal at a time. Because it became necessary to observe the arterial

pulse waveform and the venous blood volume simultaneously, a small modification was made in the circuit. The zero-set switch was set to the venous blood volume (and zero-set) mode permanently. The arterial circuit on the other hand, was disconnected from the switch and permanently connected to the AC amplifying circuit. In this way, the two amplifying circuits (the AC amplifying circuit for the AC coupled pulse waveform, and the DC amplifying circuit for the DC coupled venous blood volume) could operate independently, making it possible to monitor the pulse waveform and the venous blood volume at the same time. However, when the zero-set is depressed, the two signals return to the center of the recording.

5.2.3 Testing Protocols

Nine students between 25 and 30 years of age volunteered as subjects for this studies. This included five female and four male volunteers. Each experiment consisted of a continuous twenty minute protocol. During the first 3 minutes, the subject sat with eyes open. During the next 12 minutes, the subject sat with eyes closed and relaxed (or meditating, if the subject knew how to meditate), and the last five minutes the subject sat with eyes open and a noisy stressful atmosphere was created. The noise was created by two hidden buzzers taped under a desk behind the subject, and noise from a radio tuned to high volume was presented from an AM station with a high interference and noise.

A comfortable chair was set away from the instruments for the subjects. When the subjects entered, they were briefed about the functions of a thermistor, and the photopulse sensors to ensure that they were not going to get any electrical shocks, since most of the

subjects expressed concerns about getting electrical shock. It were further explained that initially the lights would be on, but after some time the lights would be turned off. At that time, they were supposed to close their eyes and relax, and if they knew how to meditate, they were highly encouraged to do so. Much emphasis was placed on the importance of being able to remain still and possibly not to move the hand during the experiment. They were further told that the lights would be switched on again, but that would not mean the end of the experiment. They were told to remain still until they would be told that the experiment was over.

Since the thermistor takes some time before it adjusts to its environment, the thermistor was first taped to the second finger from the thumb. A cotton wool was taped in place over the thermistor to prevent heat losses. The venous blood volume sensor was then taped to the middle finger, and the arterial sensor was taped to the fourth finger counting from the thumb. The subject's hand was then placed on a wooden board. The board was put across the arm of the subject's chair and another chair. The subject was then asked to place the hand in a comfortable position so as to minimize the possibility of moving the hand during the experiment. After this the palm was placed facing up so that the sensors would not touch the board. The zero-set was depressed to set the center line at zero, and two minutes were allowed to pass (in compliance with the operators manual of the PPG 13) [13], after which the experiment began.

The data acquisition procedures, and data analysis (unpacking data) were the same as described in sections 5.1.3 and 5.1.4 respectively.

In order to evaluate the relationship between blood volume and the temperature of the finger, their cross correlation functions were computed using equation (4.4) in section 4.1. A program called "cor.m" written in MATLAB was used to compute the cross correlation function (see Appendix A for the code). The program employs Butterworth

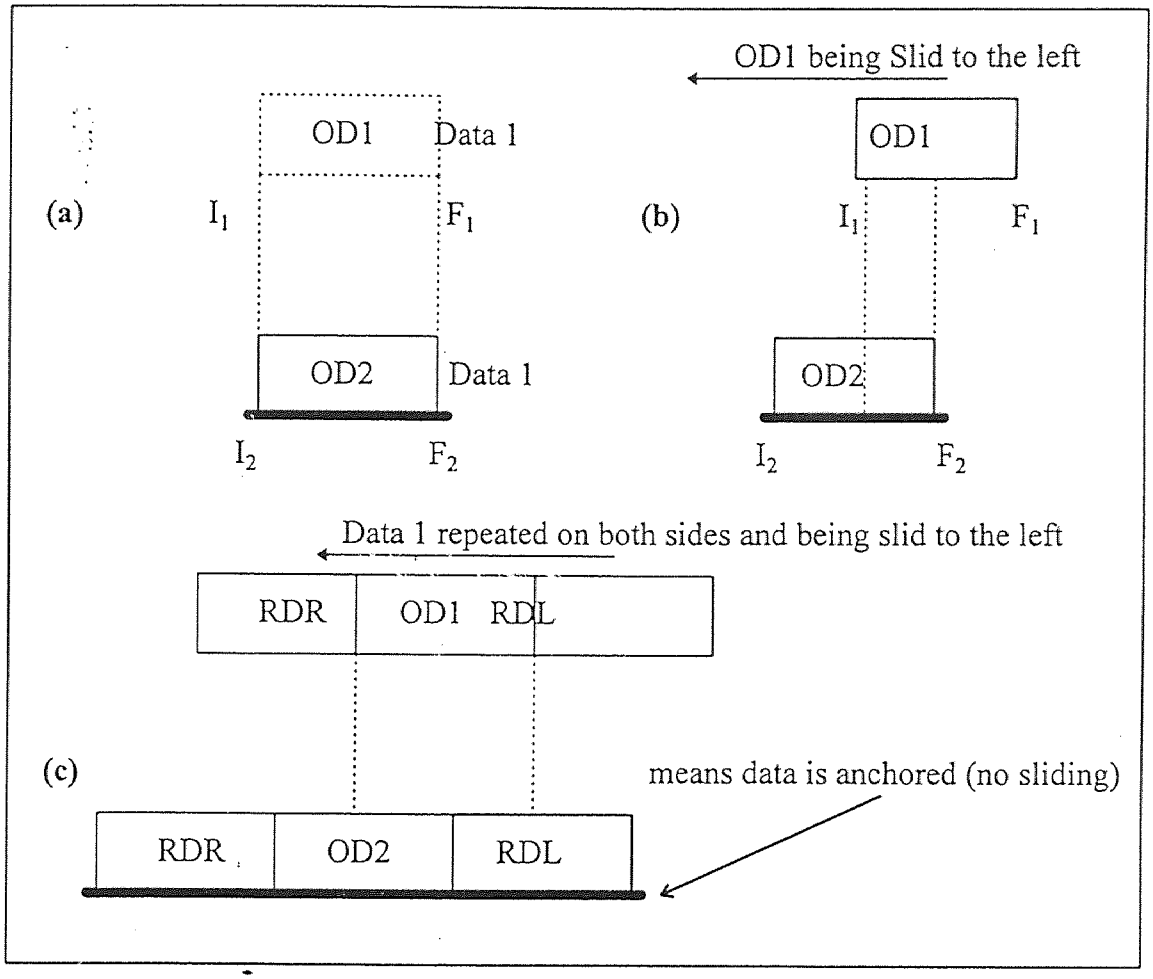

Figure 5.4 Illustrations of the cross correlation

filtering with 2 Hz cutoff frequency and decimates the data by 40. The cross correlation function superimposes the two data on top of each other, as shown in figure 5.4 (b) and then slides one data (OD1) relative to the other (OD2) until the two data perfectly match

with each other as shown in the figure 5.4 (a). In this case the two data are in phase with zero lag between them, and the corresponding cross correlation function assumes maximum value. The original data of the two signals are designated in figure 5.4 above as OD1 and OD2 with data 1 superimposed on data 2. We assume for the purpose of illustration that OD1 is movable but OD2 is anchored. I_1, I_2, and F_1, F_2 are the initial and the final data points for OD1 and OD2 respectively. In figure 5.4 (b), F_1 for OD1 does not correspond to a data point of OD2, and so for I_2 in OD2. Consequently, the cross correlation at the ends is zero. In this thesis project, the problem is solved by repeating each data one time on both sides of the original data as shown in figure 5.4 (c), where RDR and RDL mean repeated data on right and repeated data on left respectively. In this way, no matter where we start to slide one data (OD1) relative to the other (OD2), the data points at the end will not roll over (the ends will always coincide with a data element).

CHAPTER 6

EXPERIMENTAL RESULTS

The following chapter contains the experimental results involved in measuring the physiological response to relaxation and stress. The experimental study investigating bilateral frontal EEG coherence of human subjects in different experimental conditions will first be presented. The study wazzu was extended to include measuring temperature of the skin as a control variablewazzu . The ambient room temperature was also measured. The second related experiment included measurement of the blood volume, the pulse (see section 5.2.2) and the temperature of the the fingertips under relaxation and stressful conditions. A brief synopsis of each protocol will be given before the results are presented. For a detailed description of the experimental protocols, refer back to sections 5.1.1 and 5.2.1.

6.1 Group Meditation Study

The literature reports that in group meditation, increased coherence and its spread to wider frequency bands occur [18]. The group meditation study, as described in sections 5.1.1.1 and 5.1.1.2 consisted of two subjects in each experiment. Six individuals participated in the study.

6.1.1 Group Meditation Study I

There were four conditions in this study: eyes open (EO), eyes closed (EC), single meditation (SM) and group meditation (GM). Each protocol lasted for five minutes. Two

subjects participated in this study. Refer to table 6.1 below for the order in which the protocols were executed after a head-up landing of a tossed coin. Table 6.2 compares results of coherence in the alpha band (8 - 12 Hz) of two subjects between the four experimental conditions. The values are the area under the alpha coherence curve above the threshold of 0.98. The maximum area under the alpha coherence curve above the threshold of 0.98 was also calculated for this and the other two experiments and equal to 1.2. In addition, the results are graphed in the cospar format. The upper half of each graph is a three-dimensional mesh plot of coherence versus time and frequency.

Table 6.1 Format of group meditation study I

Number of Protocol	Subject I	Subject II
1	EO-3 Beeps	SM-1 Beep
2	SM-1 Beep	EO-3 Beeps
3	EC-2 Beeps	EC-2 Beeps
4	GM-3 Beeps	GM-3 Beeps

Each cospar plot is followed by a corresponding skin and ambient room temperature recording.

Table 6.2 Results for group meditation study I
The values are the area under the alpha coherence curve above 0.98

Subject	EO	EC	SM	GM
I	0.5552	0.7368	0.5543	0.3425
II	0.1478	0.1481	0.1680	0.2049

From table 6.2, it is observed that while both subjects, in general have low alpha coherence compared to the maximum alpha coherence of 1.2, subject II has lower coherence than subject I. Subject II has a consistent increase in alpha coherence from EO to GM condition. This is in an agreement with the findings by Orme-Johnson, et. al [18] and [19]. Subject I on the other hand, has highest alpha coherence during eyes closed. As we move further towards GM, we see a decrease in the alpha wave coherence. Subject II also has a relatively high alpha wave coherence during eyes open. Figures 6.1 (a), (b), (e), (f) (i), (j), (m) and (n) are the corresponding cospar plots. Cospar plot for both subjects showed alpha coherence together with theta and delta waves, with the alpha coherence (8 - 12 Hz) extending to the beta wave band (13-30 Hz). The cospar plot for subject II during single meditation is shown in figure 6.1 (b) with interspersed delta, theta, alpha coherence, and some coherence in the beta wave bands. This could be due to the fact that the subject was not a good meditator or the fact that the subject blinked his/her eyes or due to facial muscle movement or most importantly it was hard to meditate effectively directly from eyes open (a comment made by both subjects) which may be a flaw in the experiment.

Figure 6.1 (e) and figure 6.1 (f) show coherence for subject I, single meditation and subject II, eyes open respectively. Subject I shows very little amount of delta coherence (0-4 Hz), shows the presence of theta coherence (4-7 Hz) with a strong alpha coherence (8-12 Hz) which at times extended to 15 Hz, indicating the presence of deep meditation [18] at only selected time intervals. Note that figures 6.1 (a) and (f) show a typically strong coherence both in the delta and theta bands. This agrees with literature

describing the EEG activity while the subject is awake, alert, and eyes open. The coherence that appears in this band is most likely due to facial muscle movement artifact such as head turning, eyes blinks etc.

Figures 6.1 (i) and figure 6.1 (j) are the coherence plots for both subject I and subject II respectively for protocol 3. Subject I showed a strong alpha activity which extended to the beta wave band at about 16 Hz. It also shows delta and theta wave bands. Subject II shows similar results but with a lower intensity.

Figures 6.1 (m) and 6.1 (n) are the coherence plots for subject I and subject II respectively during group meditation. For the first time, the coherence of subject I spread over to 30 Hz (compare to figure 6.1 (e), during single meditation), and there is also the presence of delta and theta wave bands. These results are in agreement with the findings of Orme-Johnson, Dillbeck, and Wallace in 1982 [18] who showed increased in coherence values in the lower EEG wave bands as well as a significant broad band coherence during group meditation.

The corresponding temperature plots for subject I during eyes open are shown in figure 6.1 (c), which decreased by 0.4 ^{0}C in an oscillatory behavior, and in figure 6.1 (h) for subject II eyes open which oscillates about a constant mean temperature of about 36.7 $^{\circ}$C. Figures 6.1 (d) and (g) are the finger temperatures of subject I and subject II during single meditation respectively. Figure 6.1 (d) indicates a 0.5 $^{\circ}$C increase for the first 3 minutes and then a decrease by 0.2 $^{\circ}$C remaining at this value for about a minute till finallly it decreased to about the initial temperature. Figure 6.1 (g) shows a similar behavior except it does not drop to the initial temperature. The behavior of figure 6.1 (k):

the finger temperature of subject I during eyes closed is almost the same as figure 6.1 (g). Figure 6.1 (l) for subject II, on the other hand, shows a continuous increase in the finger temperature for the entire 5 minutes of the experiment.

Figures 6.1 (o) and (p) correspond to the finger temperature plots for subjects I and subject II respectively during group meditation. The finger temperature of subject II was constant for the first 1.5 minutes and then increased by about 2.2 ^{o}C. This is consistent with the results from table 6.2 with relatively high area under the alpha coherence wave band. For the case of subject II however, the temperature was maintained at a high constant value for about 3.2 minutes and then dropped down by about 2 ^{o}C in exponential manner for about one minute and then remained constant for about 0.7 of a minute (to the end of the protocol).

In general, the finger temperatures of the subjects during either eyes closed or single meditation or group meditation (when the subjects were relaxed), showed an increase in temperature either for the entire protocol or part of the protocol and then dropped to some value. This could be movement of the hand or may be due to the fact that the subject was anticipating to hear the code for the beginning or an end of a protocol.

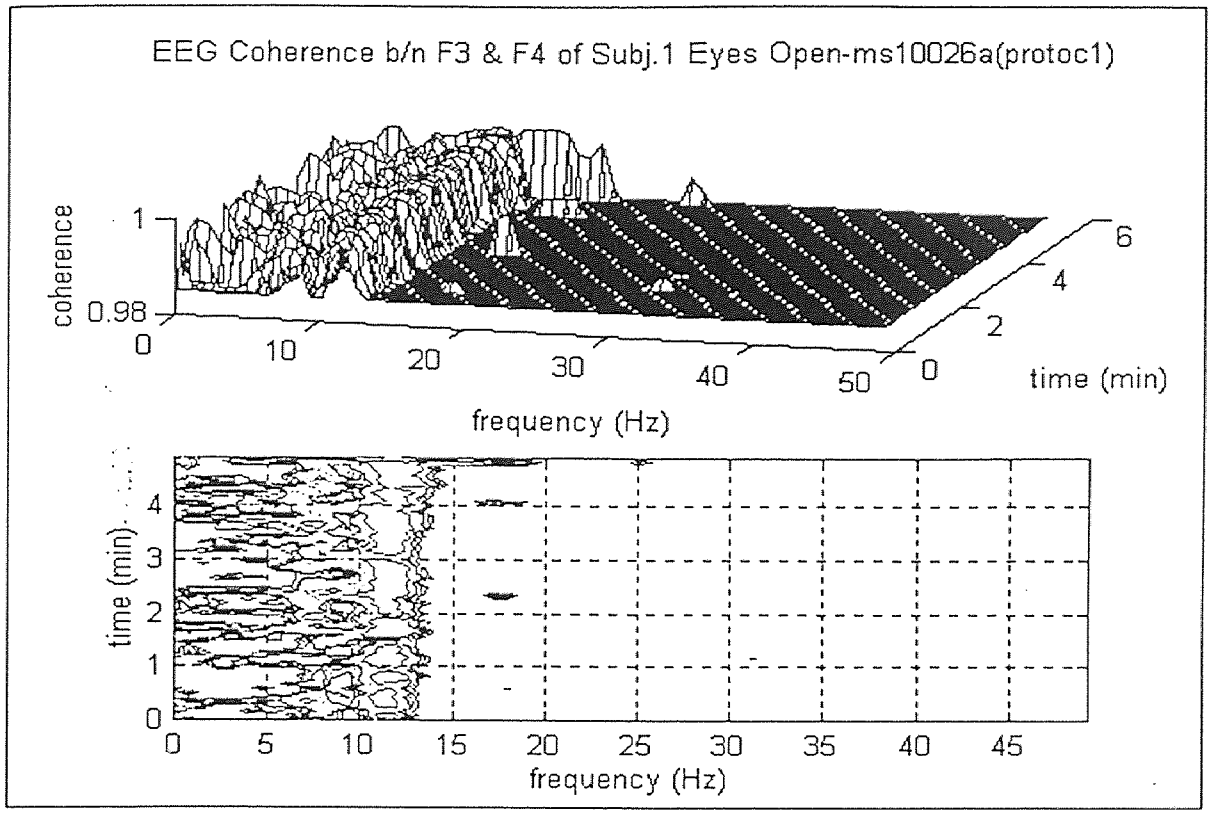

(a)

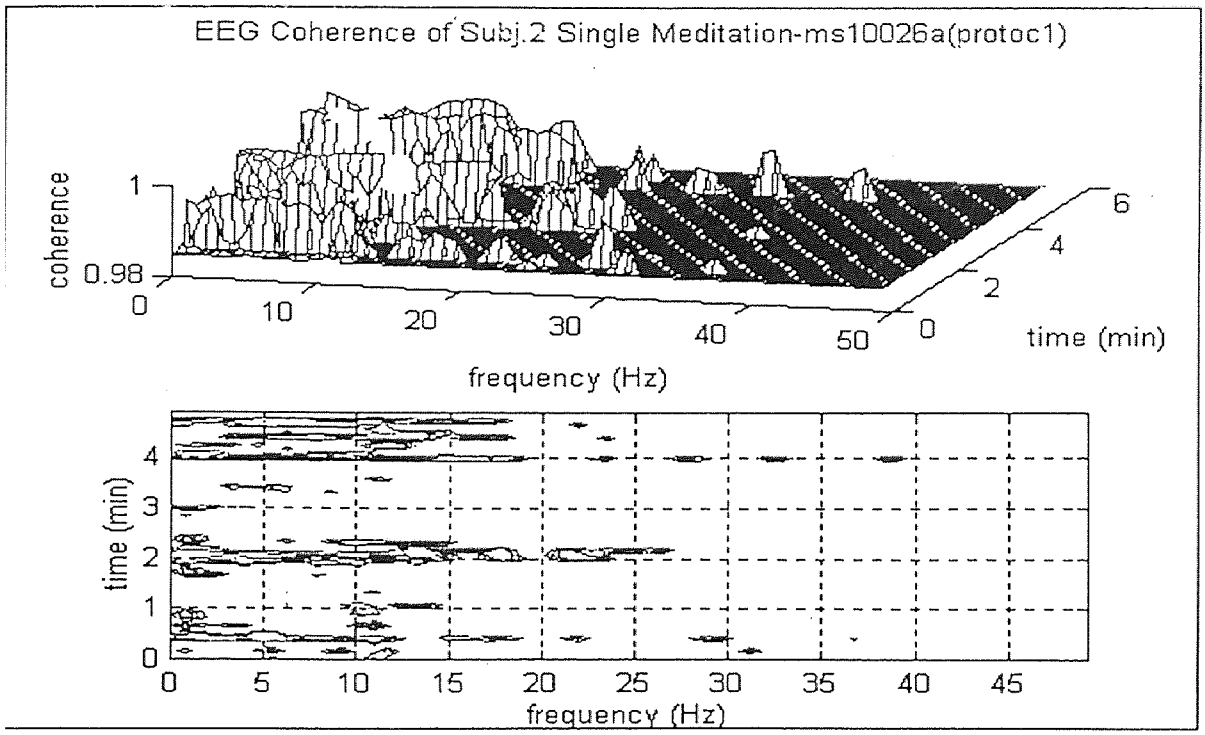

(b)

Figure 6.1 Cospar plots for group meditation protocol:
(a) Subject 1 Eyes Open, and (b) Subject 2 Single Meditation

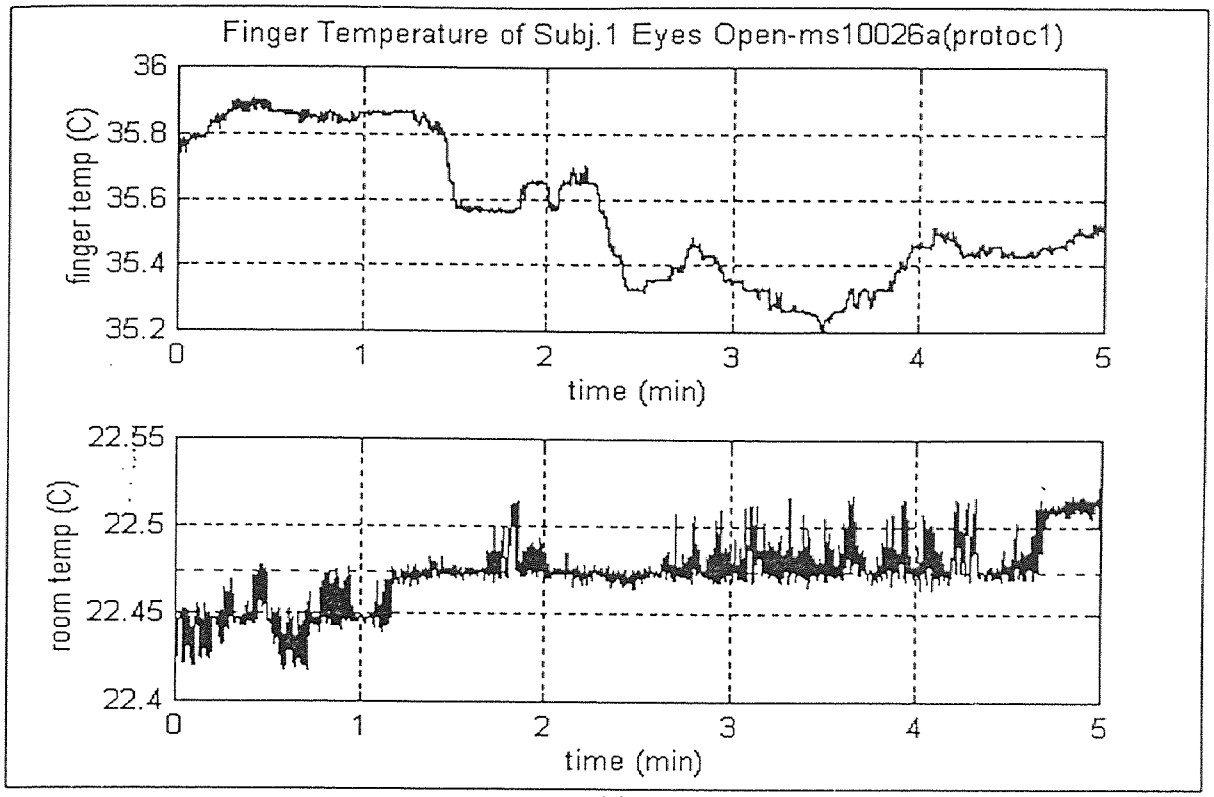

(c)

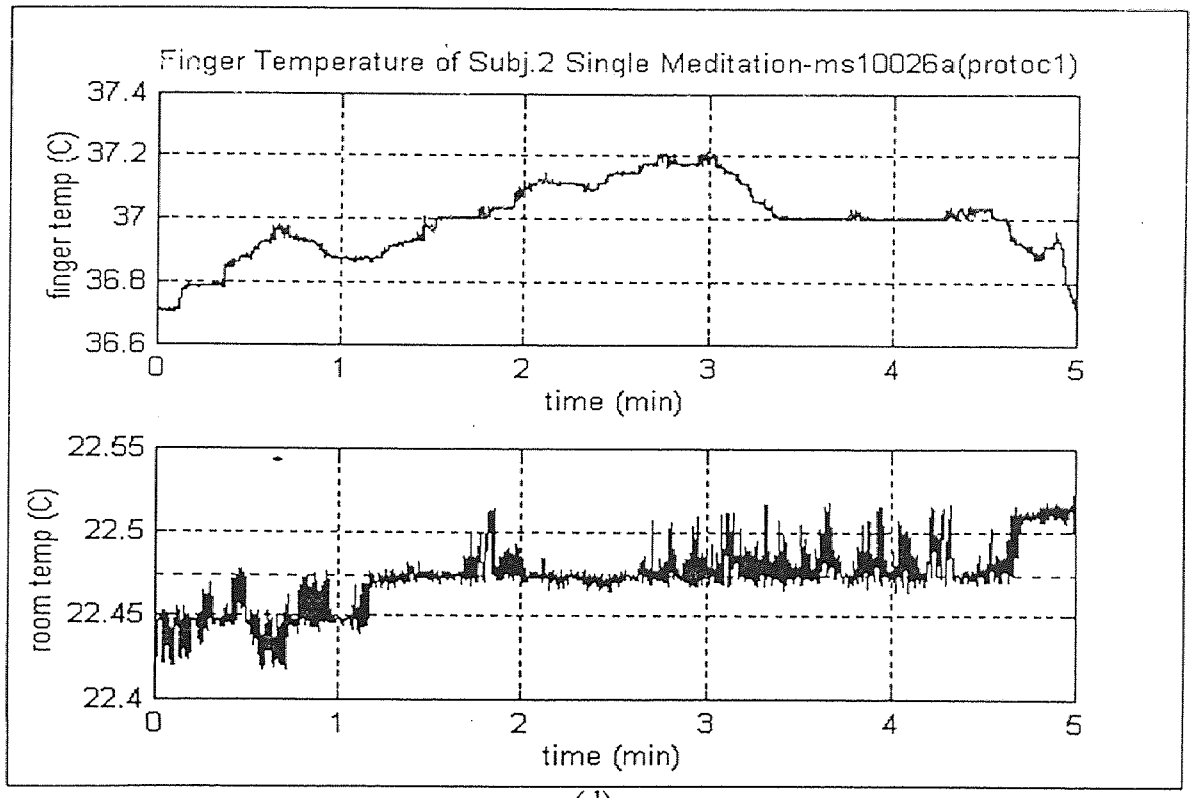

(d)

Figure 6.1 Temperature plots for meditation protocol (cont.):
(c) Subject 1 Eyes Open, and (d) Subject 2 Single Meditation

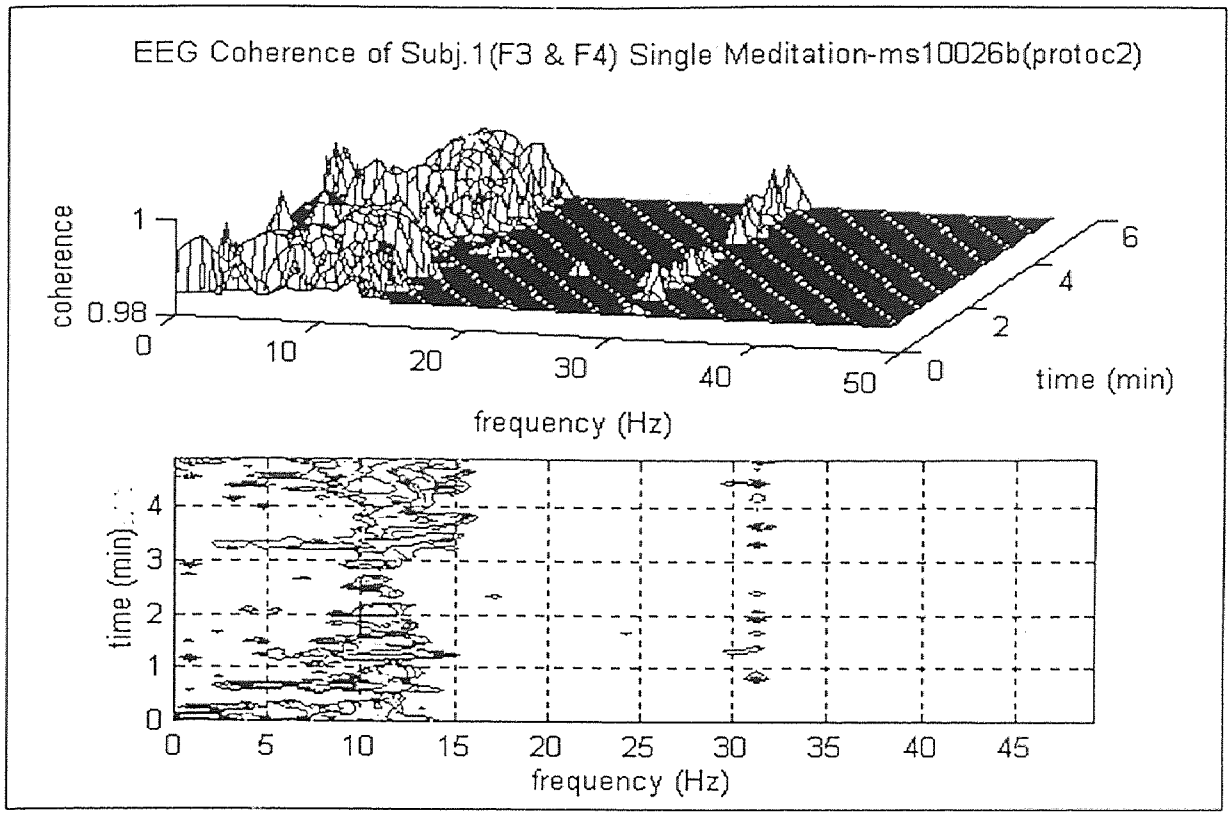

(e)

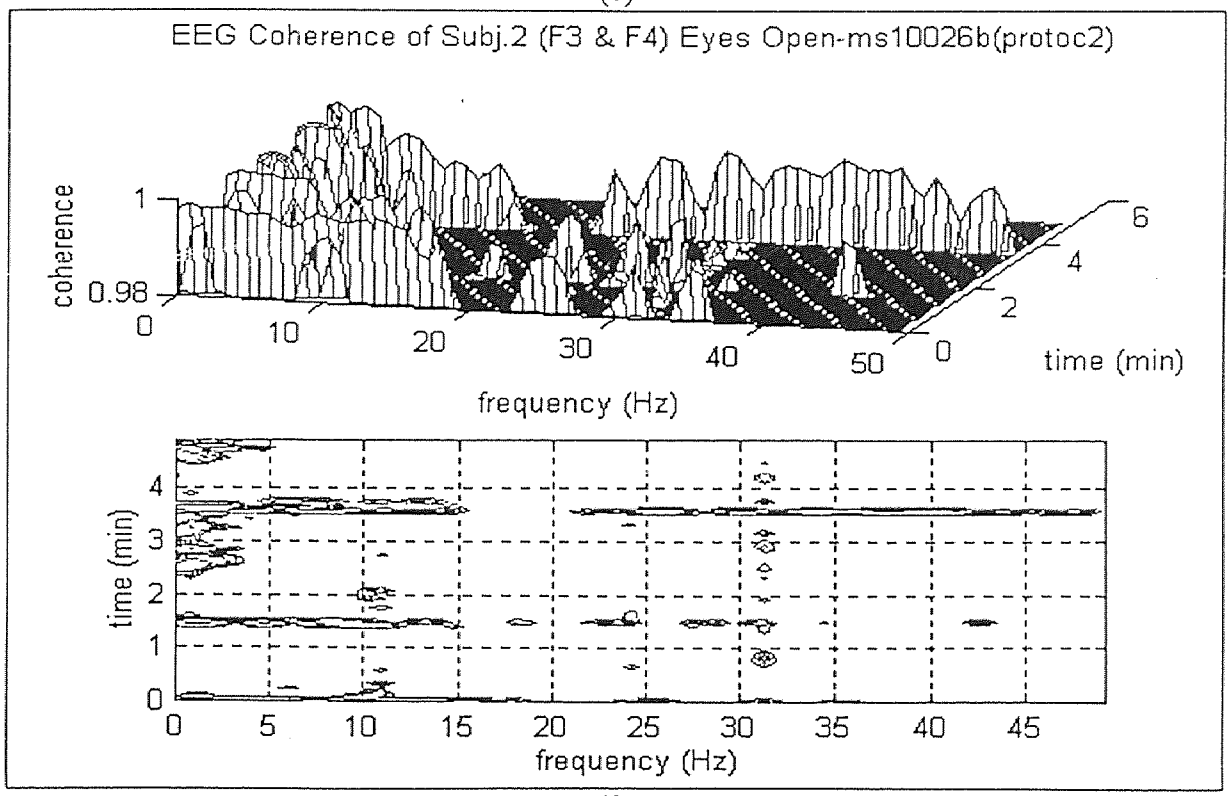

(f)

Figure 6.1 Cospar plots for group meditation protocol (cont.):
(e) Subject 1 Single Meditation, and (f) Subject 2 Eyes Open

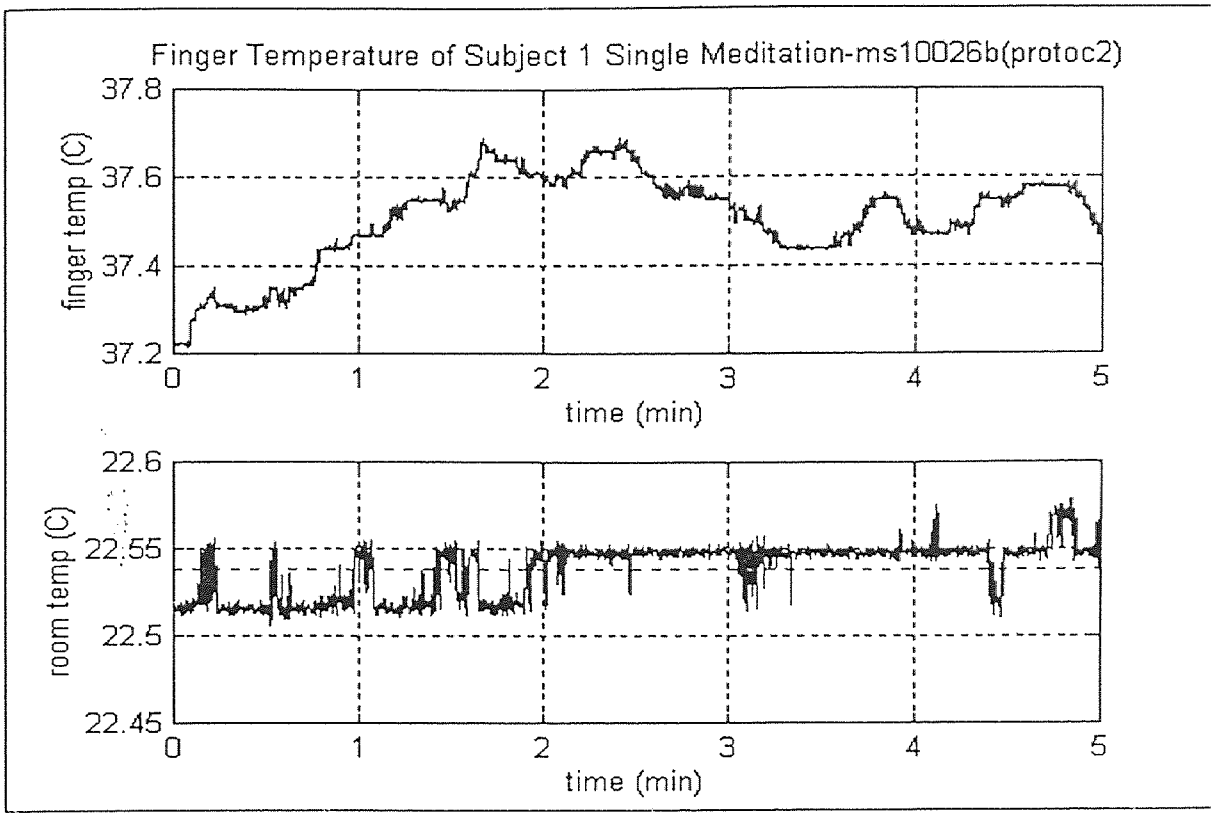

(g)

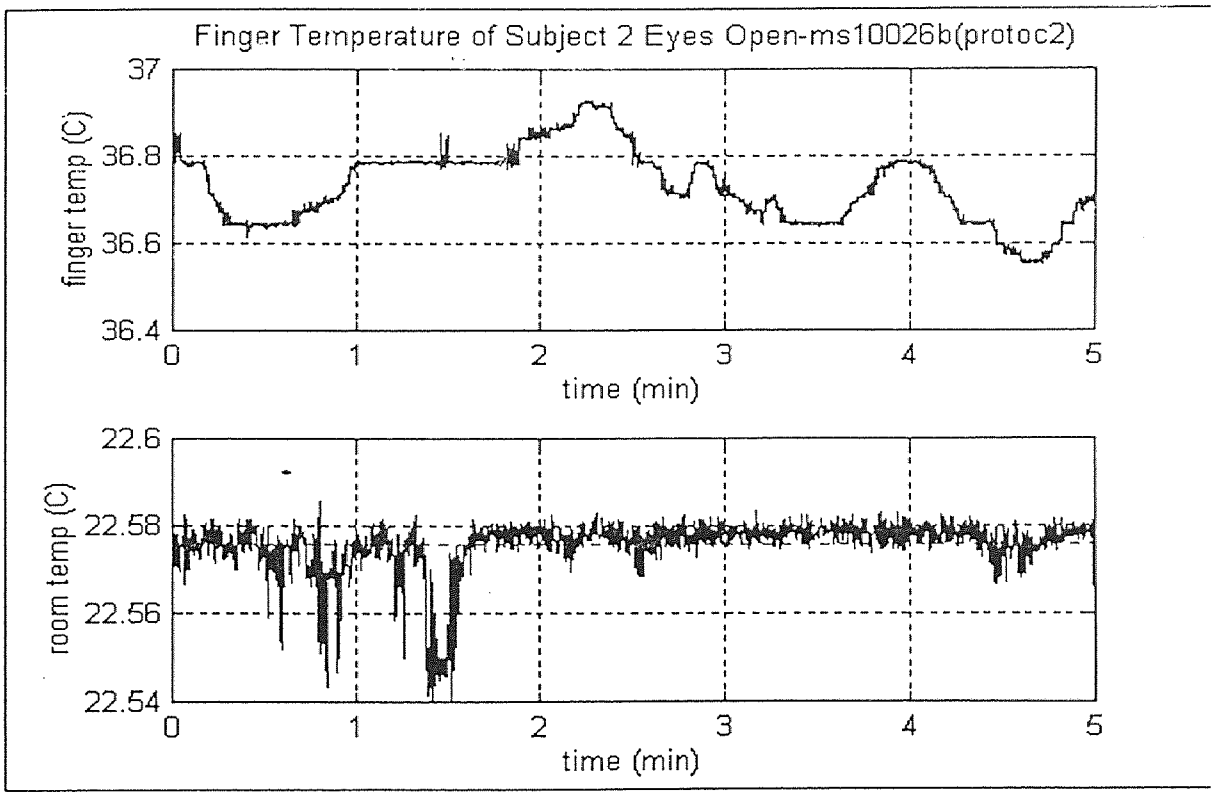

(h)

Figure 6.1 Temperature plots for group meditation protocol (cont.):
(g) Subject 1 Single Meditation, and (h) Subject 2 Eyes Open

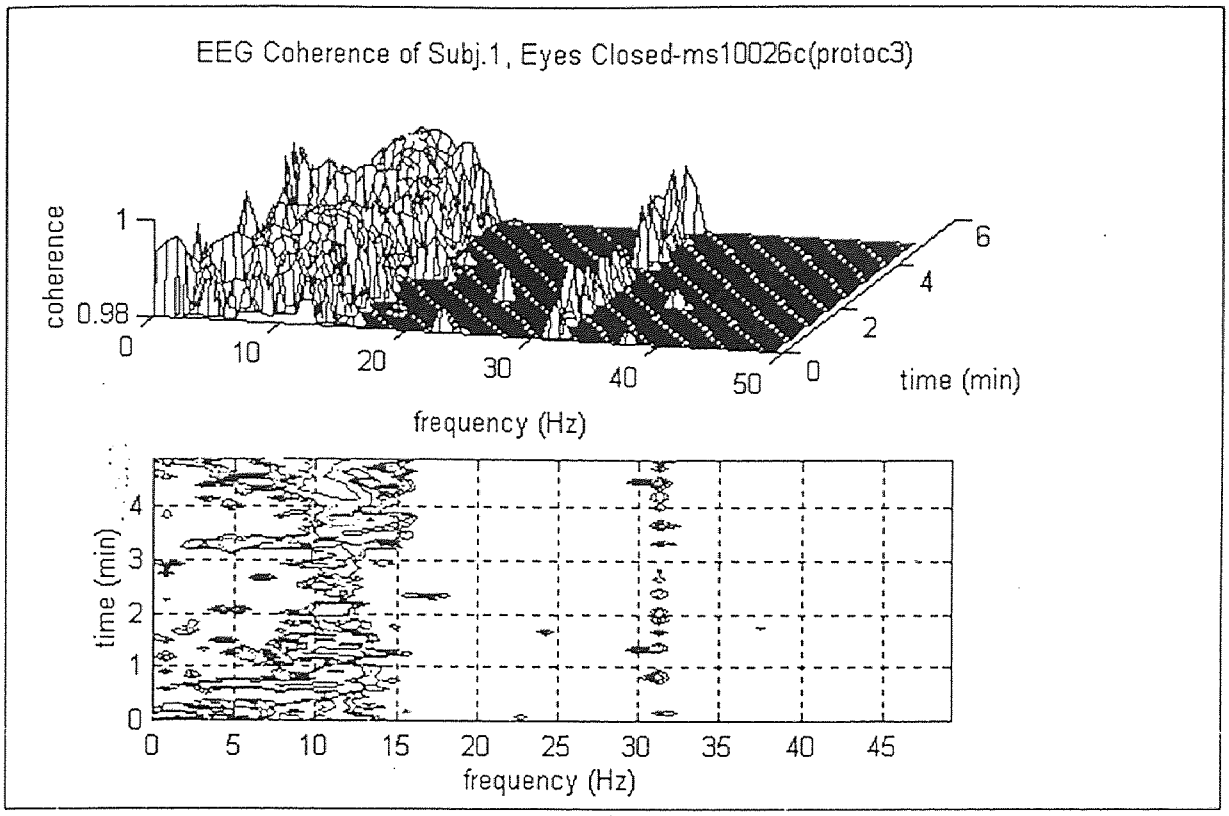

(i)

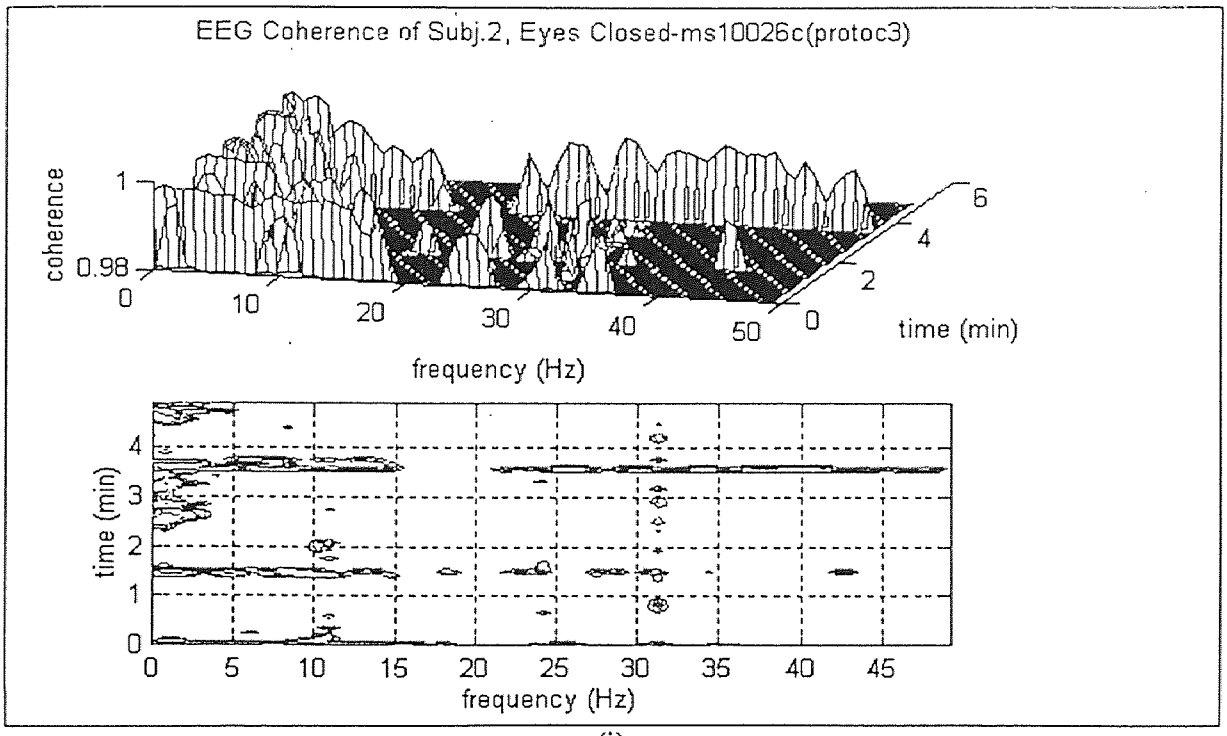

(j)

Figure 6.1 Cospar plots for group meditation protocol (cont.):
(i)Subject 1 Eyes Closed, and (f) Subject 2 Eyes Closed

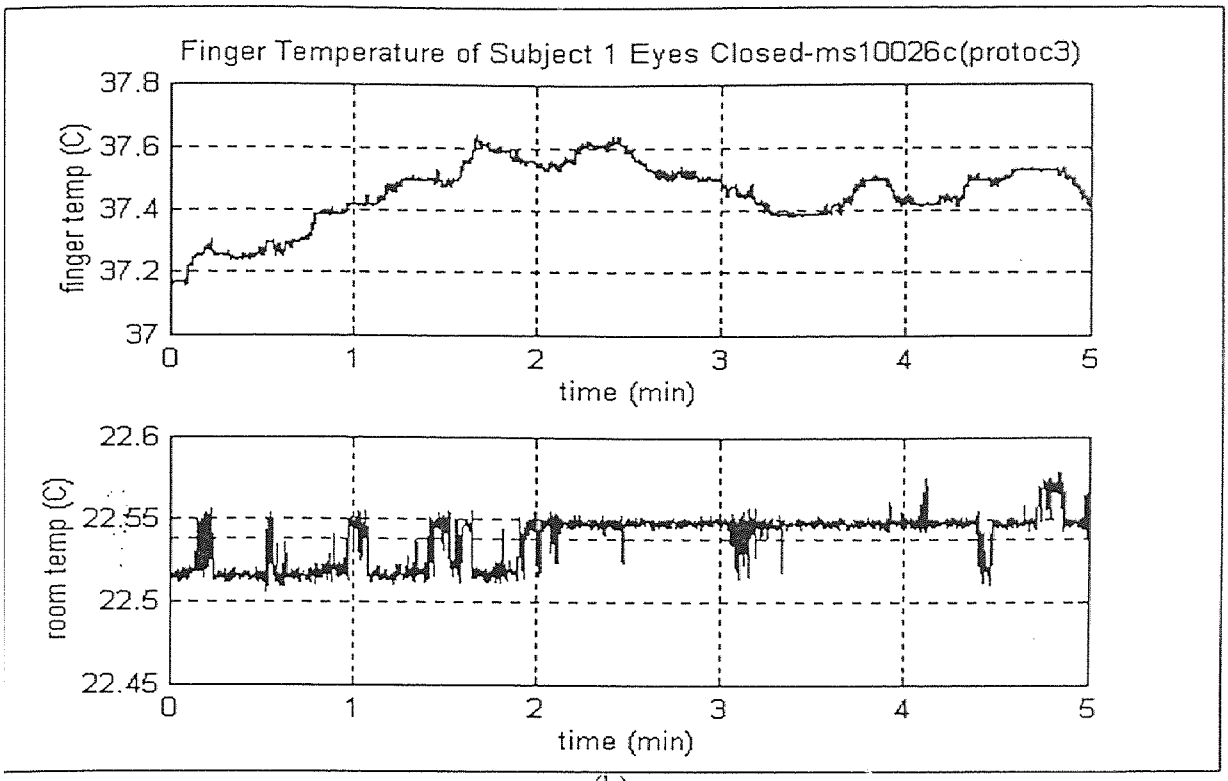

(k)

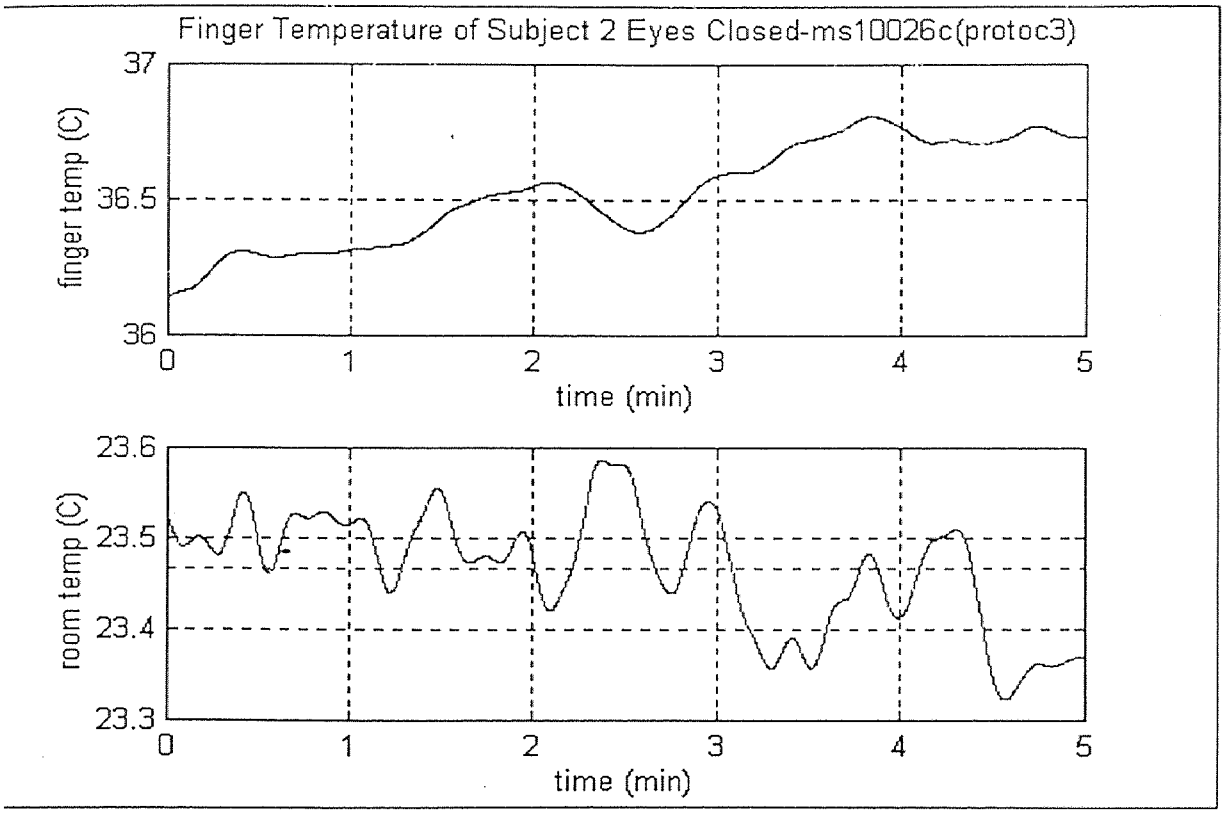

(l)

Figure 6.1 Temperature plots for group meditation protocol (cont.): (i)Subject 1 Eyes Closed, and (f) Subject 2 Eyes Closed

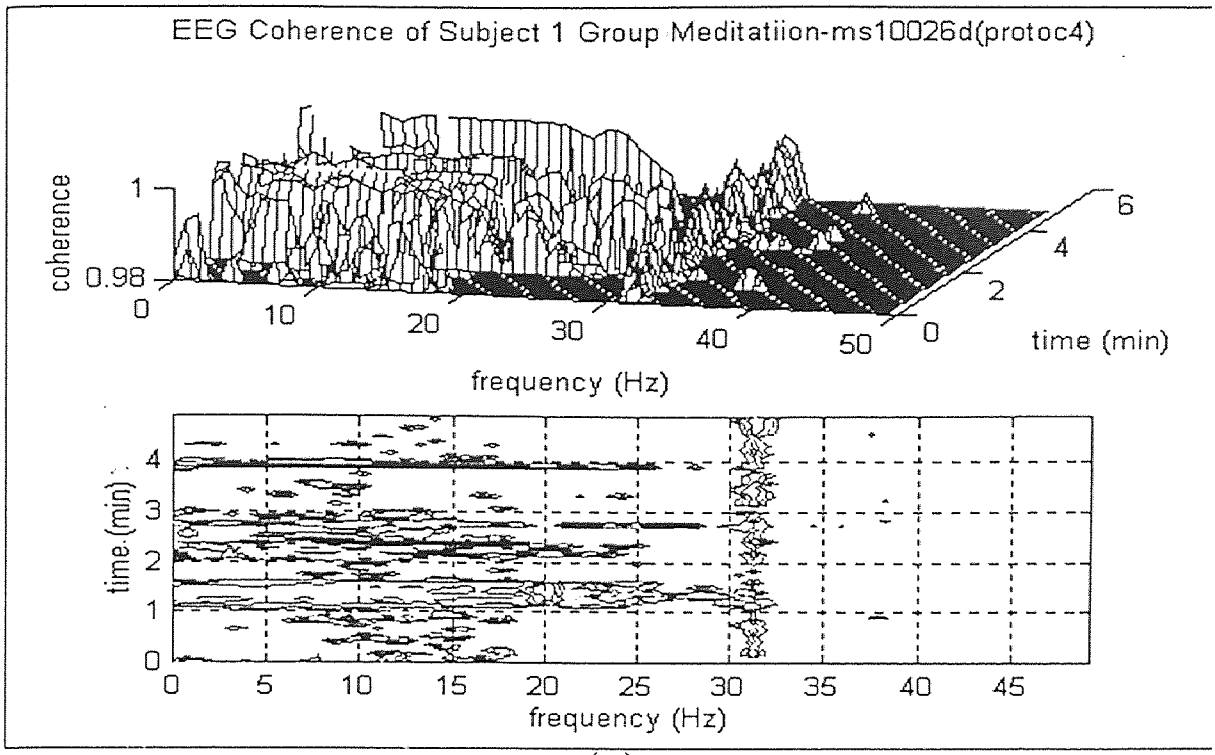

(m)

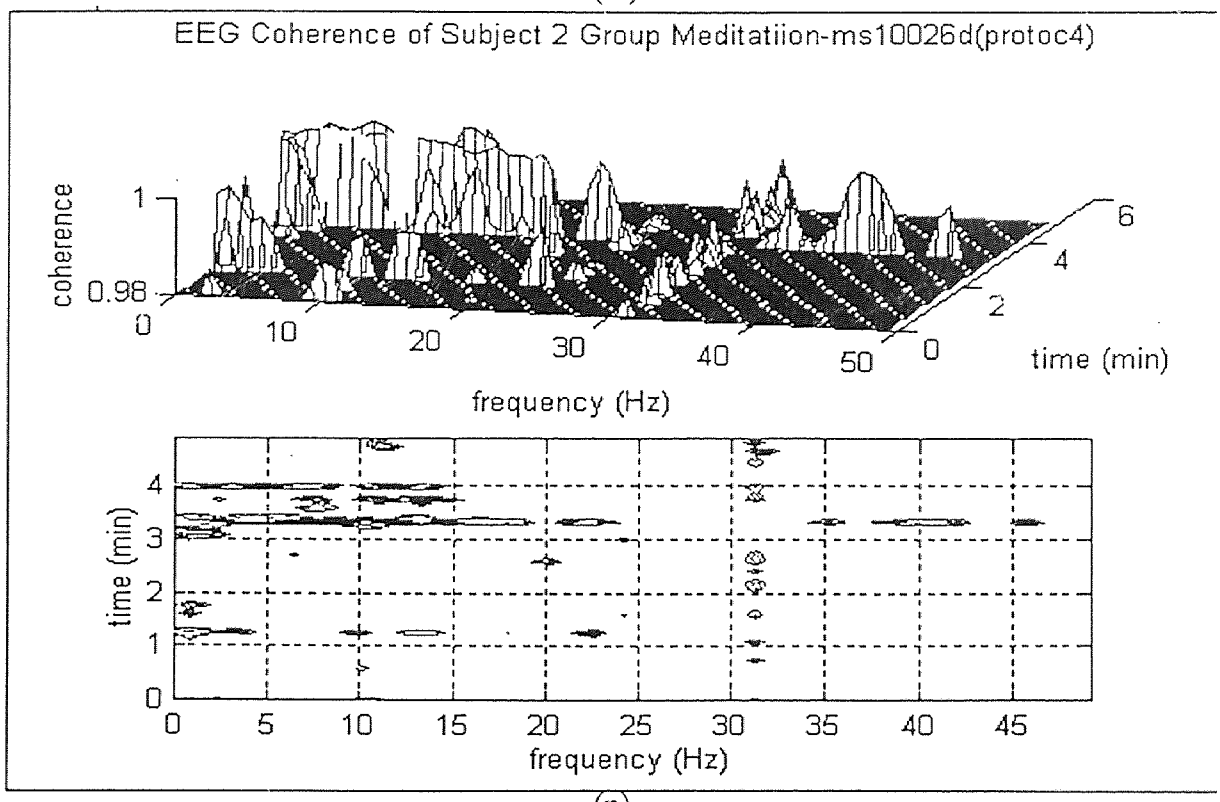

(n)

Figure 6.1 Cospar plots for group meditation protocol (cont.):
(m) Subject 1 Group Meditation, and (n) Subject 2 Group Meditation

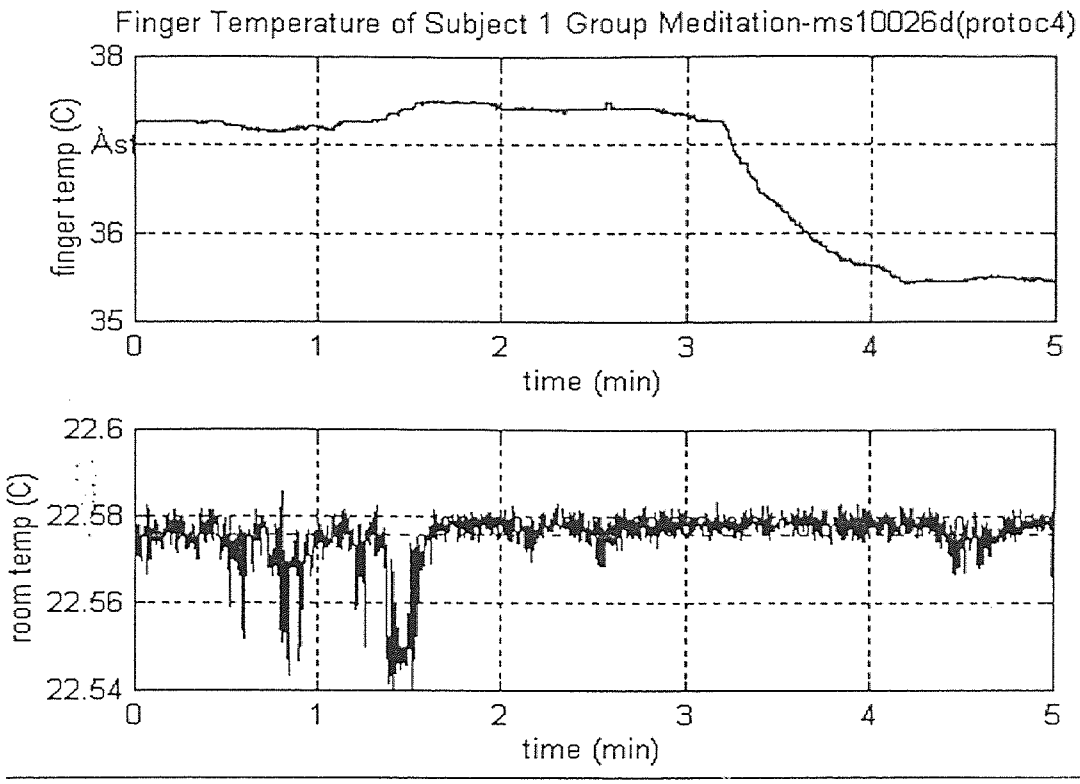

(o)

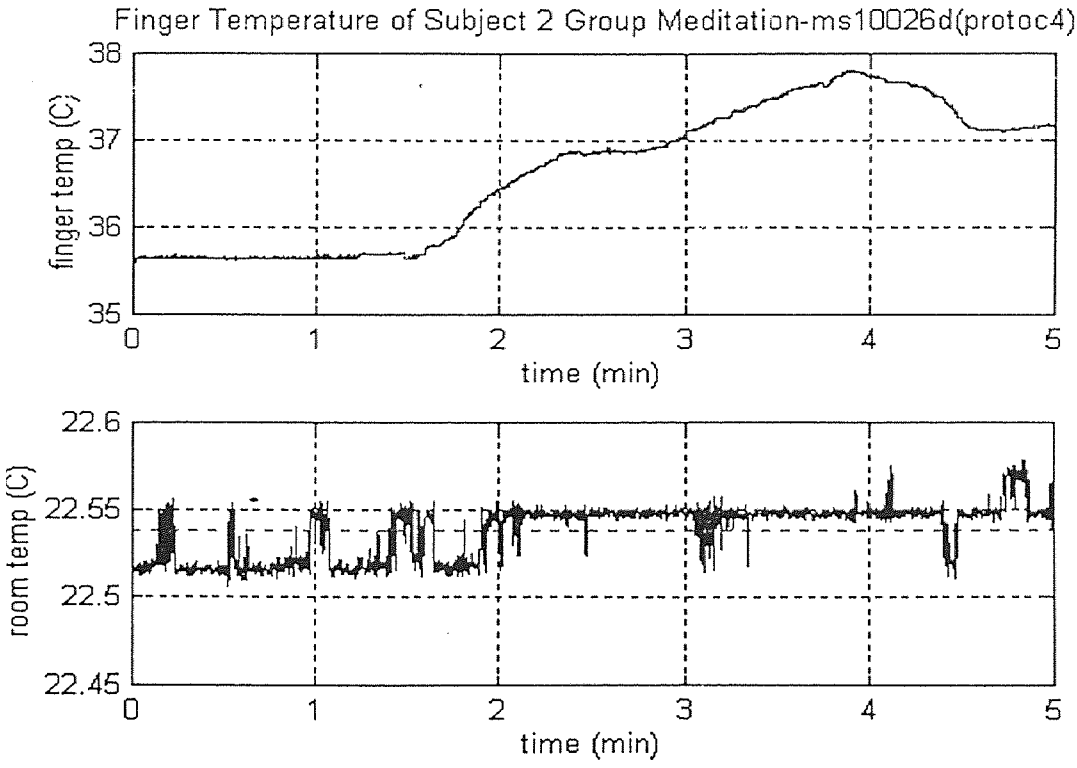

(p)

Figure 6.1 Temperature plots for group meditation protocol (cont.): (o) Subject 1 Group Meditation, and (p) Subject 2 Group Meditation

6.1.2 Group Meditation Study II

Following the suggestions of the subjects, the protocols of studies I above were changed. In the new protocols, both subjects performed the same condition at the same time except for the fourth protocol. In the first protocol, both subjects had eyes open, in the second protocol, both subjects had eyes closed and in the third protocol, both subjects meditated. In the fourth protocol for figures 6.2 and 6.3 subject I had eyes open, while subject II meditated (single meditation). Refer to section 5.1.1.2. Figures 6.2 (a-p) and 6.3 (a-p) are cospar, skin and ambient room temperature plots for this study. Four subjects took part in this study, two female and two male, between the ages of 22 and 30 years. Table 6.3 presents the area under the alpha coherence curve above the 0.98 threshold.

Table 6.3 Results for group meditation study II
The values are the area under the alpha coherence curve above 0.98

Experiment	Subject, (Subject's ID)	EO Protocol 1	EC Protocol 2	GM Protocol 3	SM Protocol 4
I	I, (RE)	0.2269	0.0767	0.0	*0.0443
	II, (EN)	0.1282	0.1666	0.3291	0.2560
II	I, (RO)	0.6336	0.4915	0.6282	*0.3233
	II, (PR)	0.2043	0.2065	0.2121	0.1432

* means subject eyes opened (no single meditation), while the other subject single meditated.

From table 6.3, it could be seen that during the eyes open for both experiments, all the subjects show alpha coherence. During eyes closed, subject II shows an increase in alpha coherence level in both experiments compared to eyes open which agrees with the clinical

findings in the literature [26], [27], [25]. Subject I however, shows a decreased in alpha coherence level during eyes closed. When subject I eyes opened (during the fourth protocol,) directly from group meditation (when subject II single meditated), the subject's level of alpha coherence drastically reduced from protocol I eyes open. For example in experiment I, the alpha coherence for eyes open in protocol 4 is 0.0443, and that obtained from protocol 1 is 0.2269. Thus, the level of alpha coherence was reduced by about 80.5%, and for the case of experiment II, we see about 50% reduction of alpha coherence for subject I.

Perhaps the most important results of the group meditation study from table 6.3 could be that with the exception of subject I in experiment I, there is a general trend of greater alpha coherence during group meditation than during eyes closed and single meditation.

In addition to using the area under the curve for the analysis of the meditation study, the cospar plots were used and the results are presented in figures 6.2 and 6.3 for experiments I and II respectively. From figures 6.2 (a), 6.2 (b), 6.3 (a), 6.3 (b) we could see a general trend of higher coherence in the delta and theta bands during eyes open (protocol 1). Figures 6.2 (i), 6.2 (j), 6.3 (i), and 6.3 (j) depict the same trend during group meditation (protocol 4). Alpha coherence was higher in both experiments during eyes closed, especially during meditation-either single or group meditation. Comparing figures 6.2 (f), (j) and (n) reveals that there is a spread out of the alpha wave band in both directions: to about 15 Hz in the beta wave band direction, and as far as to the delta wave bands on some occasions (figure 6.2 (j)). Similar results for figures 6.3 (f), (j) and (n)

were also observed. During eyes closed (protocol 2), figures 6.2 (e) and (f), and figures 6.3 (e) and (f), show the presence of delta and theta coherence compared to studies reported in the literature involving only one subject. This was also observed by Orme-Johnson in a 1982 study [18]. During the group meditation session, (figures 6.2 (i), (j), and 6.3 (i), (j)), in addition to showing more alpha coherence, there is a presence of coherence in the theta band (4-8 Hz) and relatively less delta (0-4 Hz) activity. This may mean that the subjects not only become more relaxed in a group meditation but also a deeper level of meditation was achieved, i.e. perhaps the cause for the presence of the theta band. Less delta band shown here may be due to a deeper state of meditation.

The skin temperature of both subjects in both experiments show consistent increments during eyes closed (except in figure 6.3 (g) and figure 6.2 (l)), single, and group meditations in figures 6.2 and 6.3 . In figure 6.2 (l), we see a similar trend for about 0.6 minute, and then it remained relatively constant for the next three minutes, after which it dropped to almost the initial value in one minute. It started to rise again and then dropped back to almost the initial value. The irregularity of figure 6.3 (g) in terms of the skin temperature response to relaxation can be explained using the corresponding coherence plot of figure 6.3 (e). It could be inferred that the subject either was not in a relaxed state or the subject did not pay attention to the number of beeps of the buzzer (the only medium of communication with the subjects) or the experiment did not work out the way it was intended to. In the case of eyes open however, the change in the skin temperature was not regular: sometimes it increased (figure 6.2 (c)), sometimes it

remained constant with oscillatory behavior about a mean value (figure 6.2 (d), figure 6.3 (c)), and sometimes it decreased, as in the case of figure 6.3 (d).

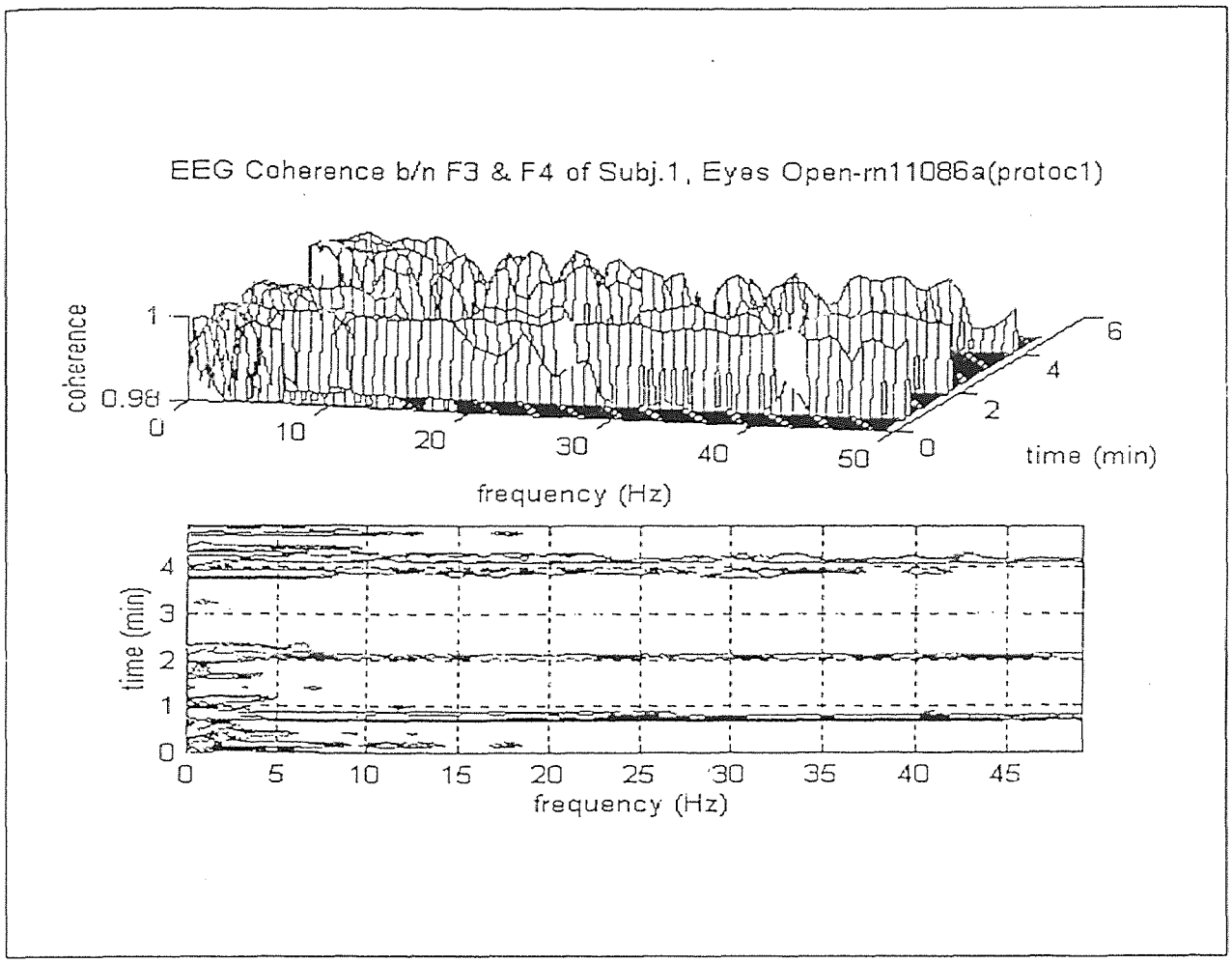

(a)

Figure 6.2 Cospar plots for group meditation
(a) Subject 1 Eyes Open

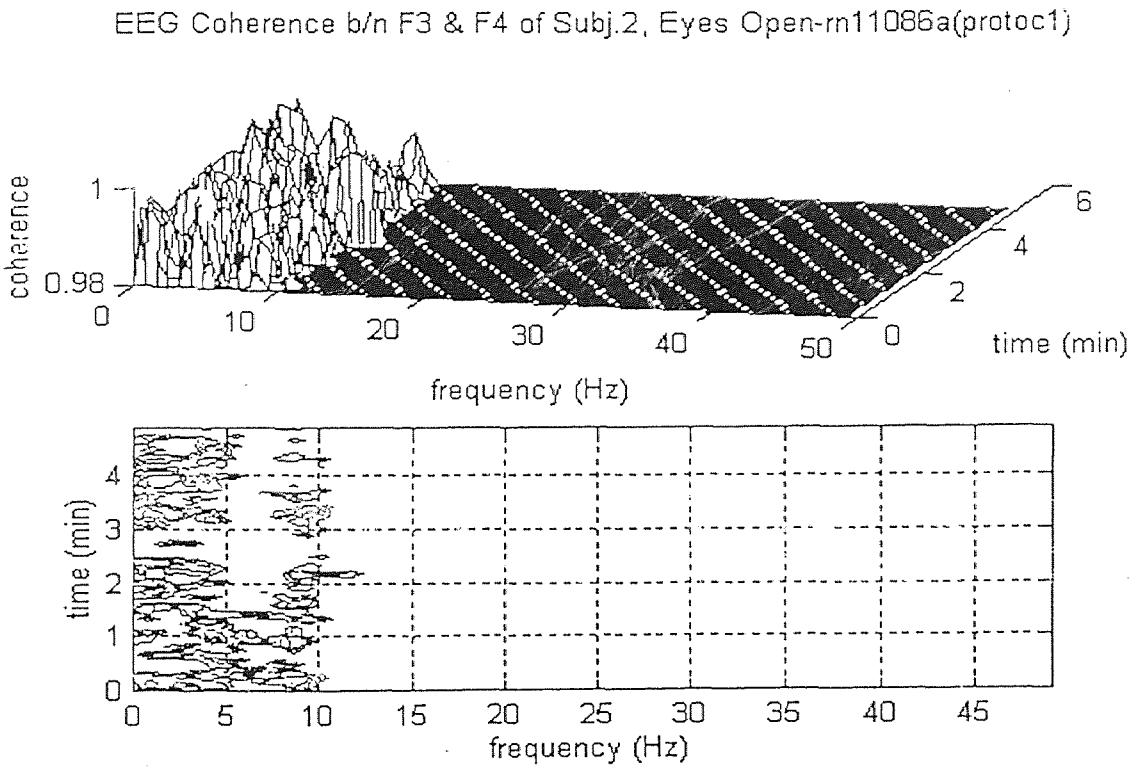

(b)

Figure 6.2 Cospar plots for group meditation (cont.):
(b) Subject 2 Eyes Open

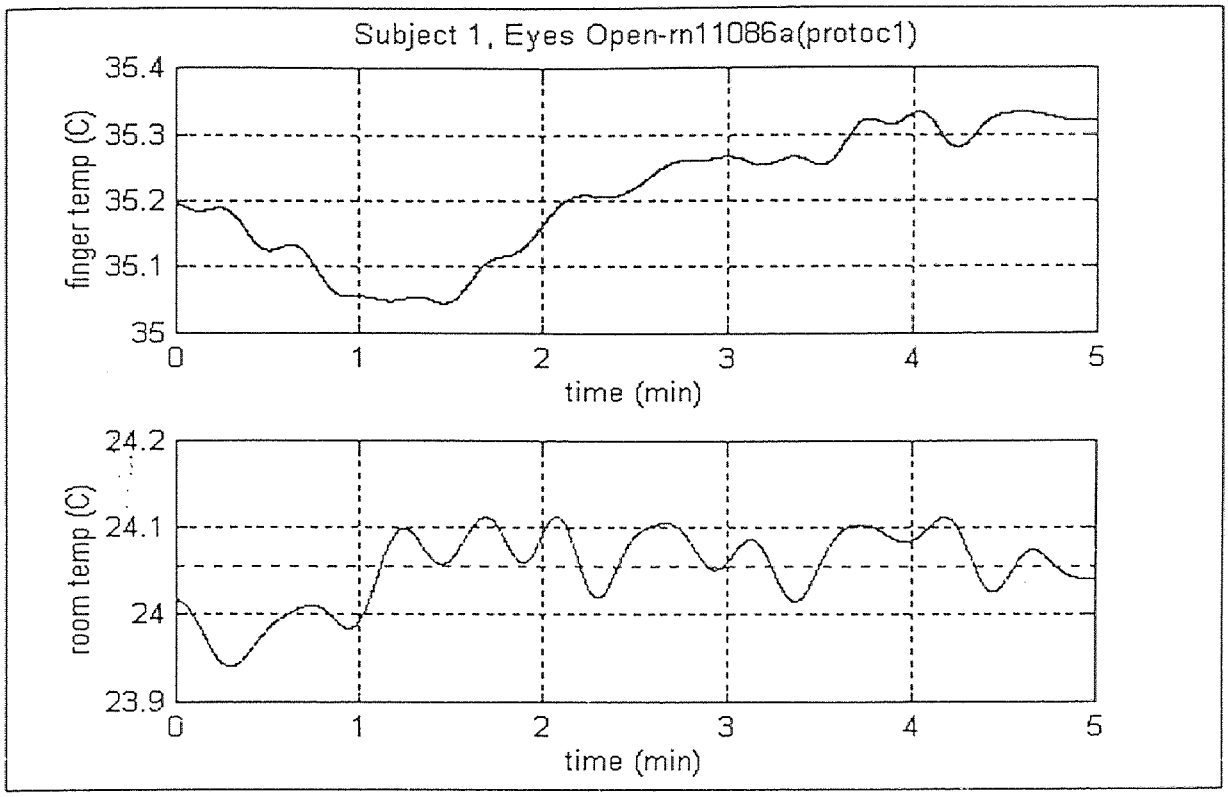

(c)

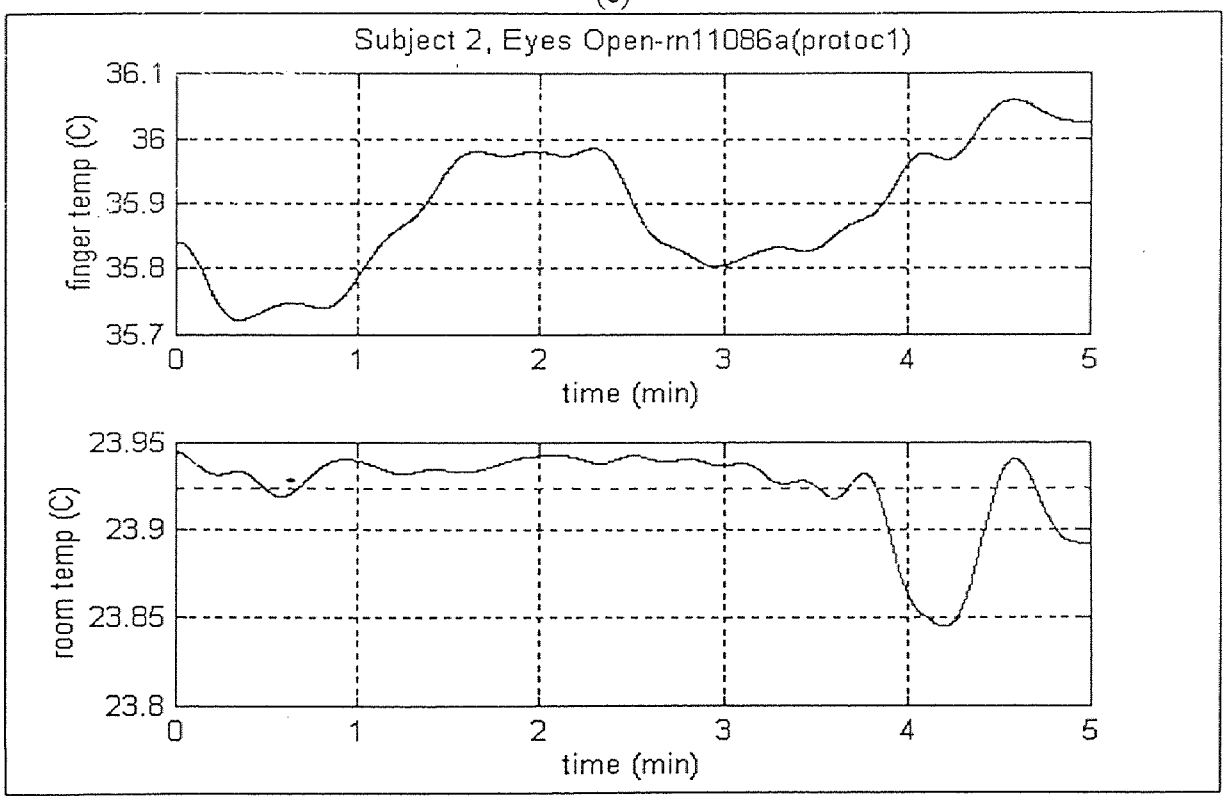

(d)

Figure 6.2 Temperature plots for group meditation (cont.):
(c) Subject 1 Eyes Open, and (d) Subject 2 Eyes Open

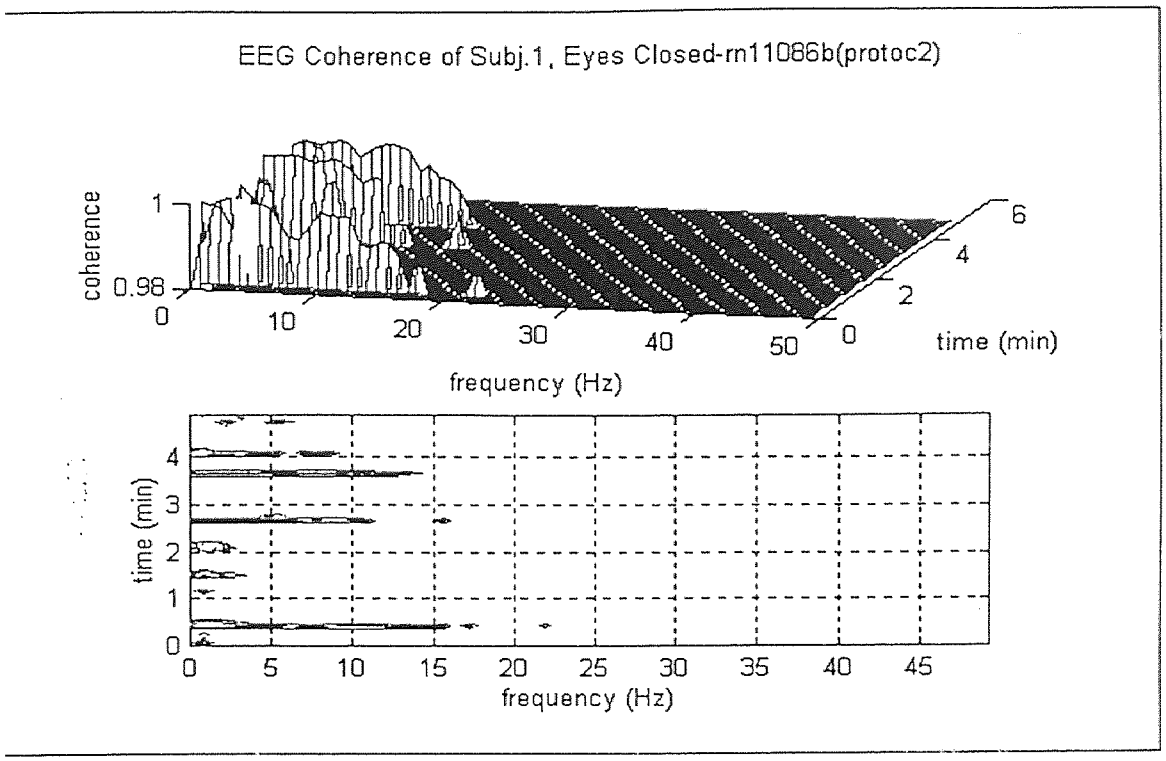

(e)

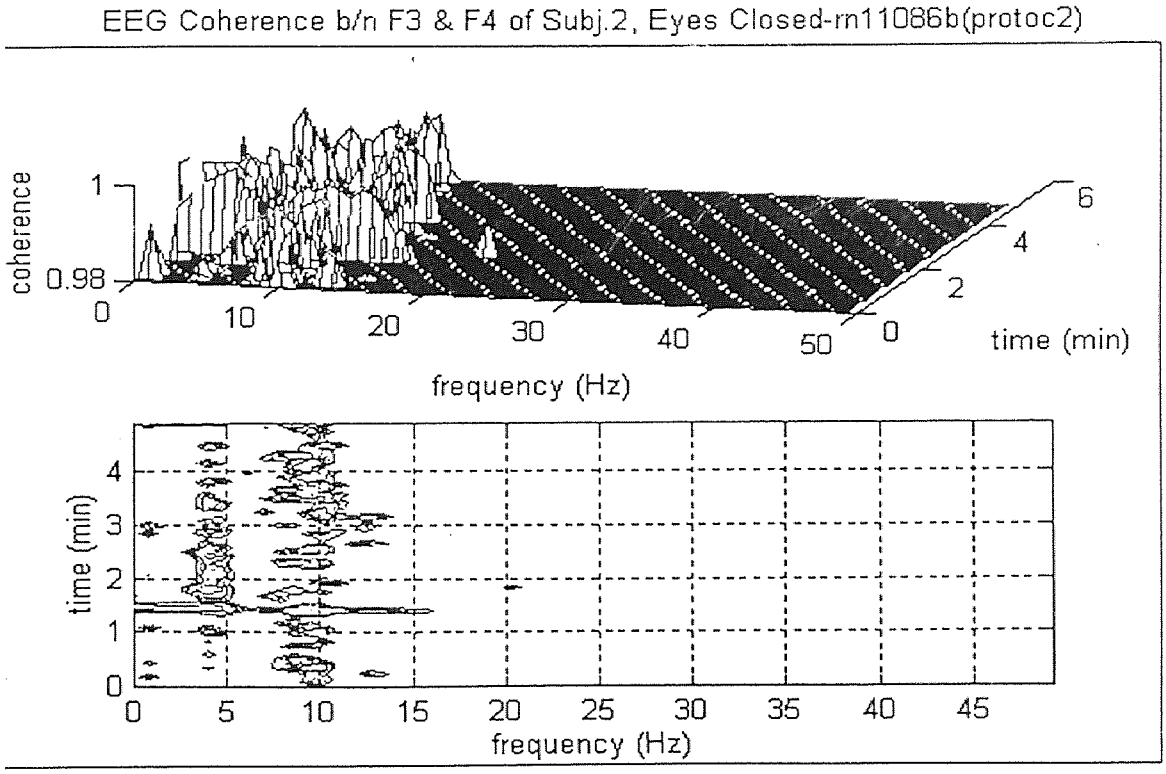

(f)

Figure 6.2 Cospar plots for group meditation (cont.):
(e) Subject 1 Eyes Closed, and (f) Subject 2 Eyes Cloesd

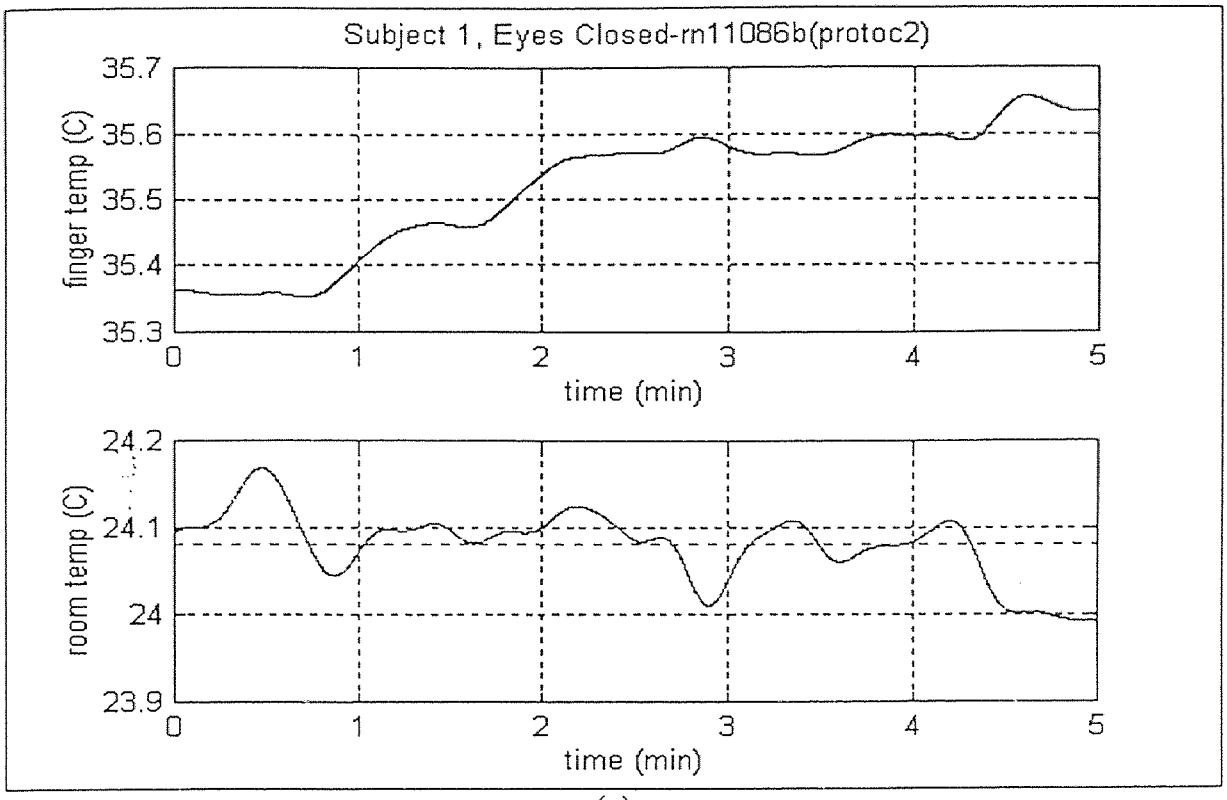

(g)

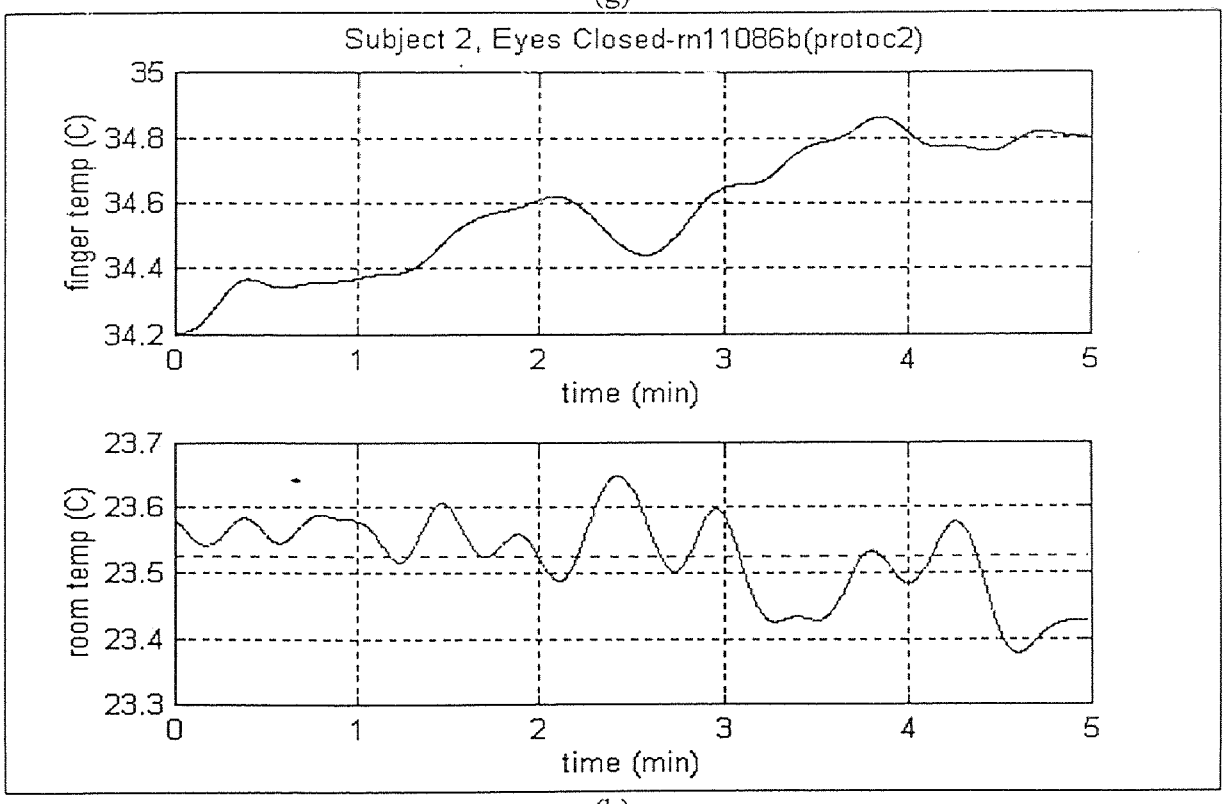

(h)

Figure 6.2 Temperature plots for group meditation (cont.):
(g) Subject 1 Eyes Closed, and (h) Subject 2 Eyes Closed

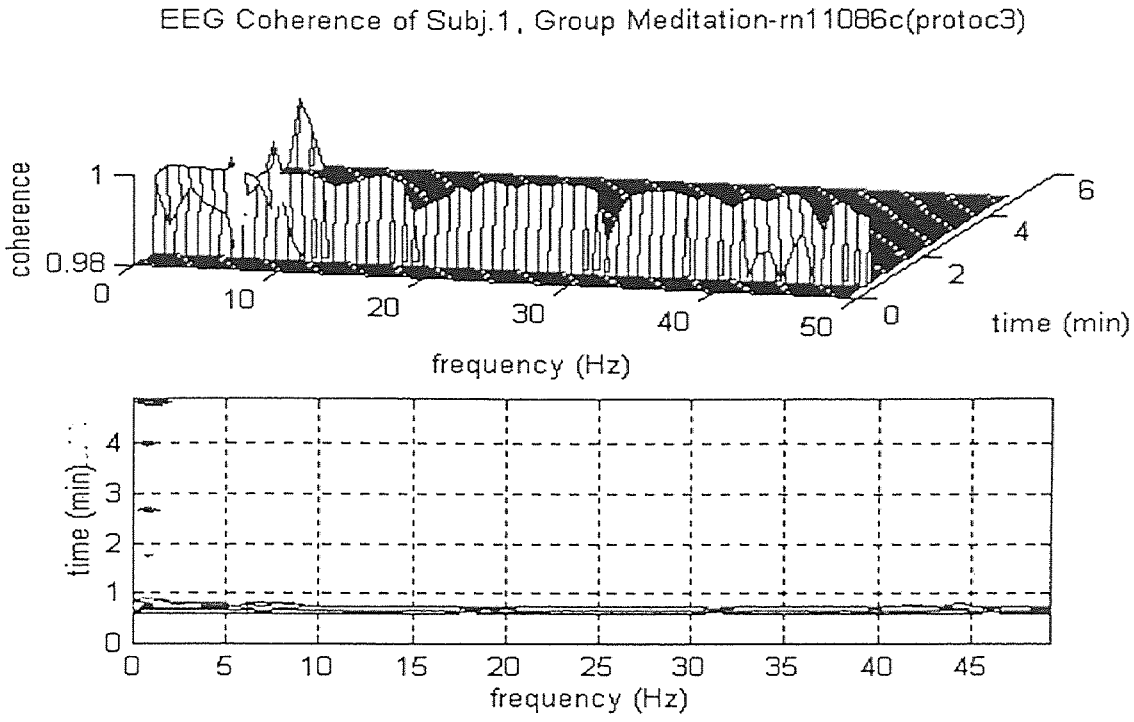

(i)

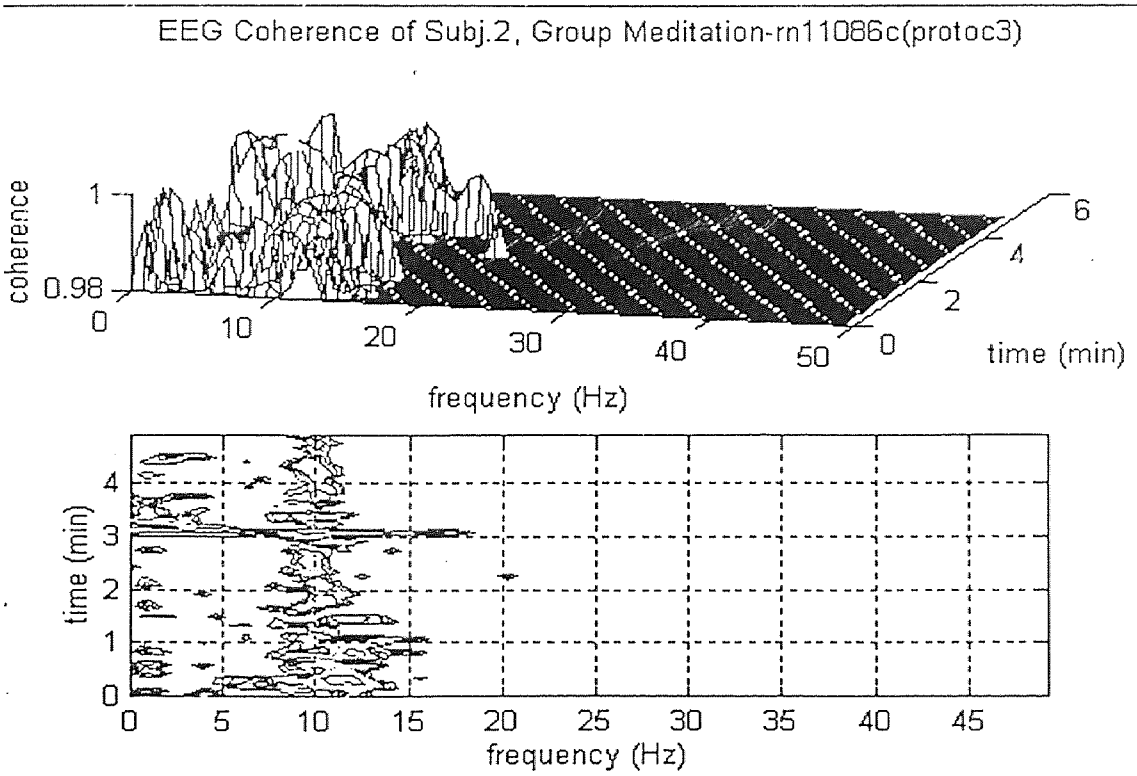

(j)

Figure 6.2 Cospar plots for group meditation (cont.):
(i) Subject 1 Group Meditation, and (j) Subject 2 Group Meditaton

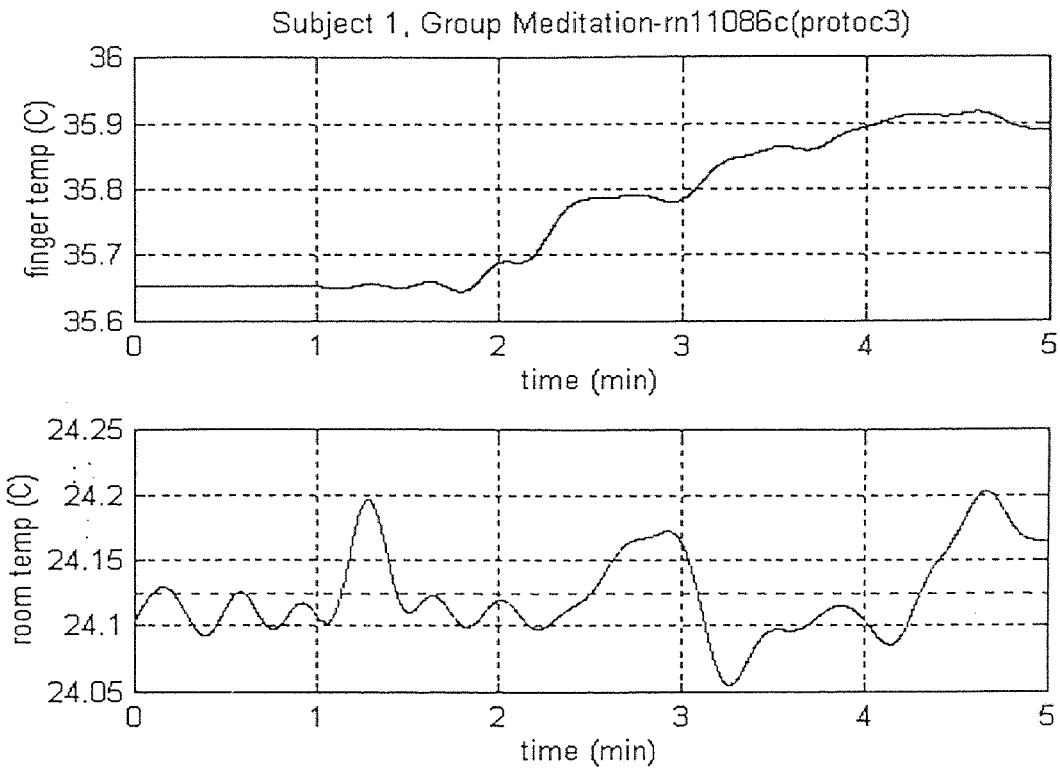

(k)

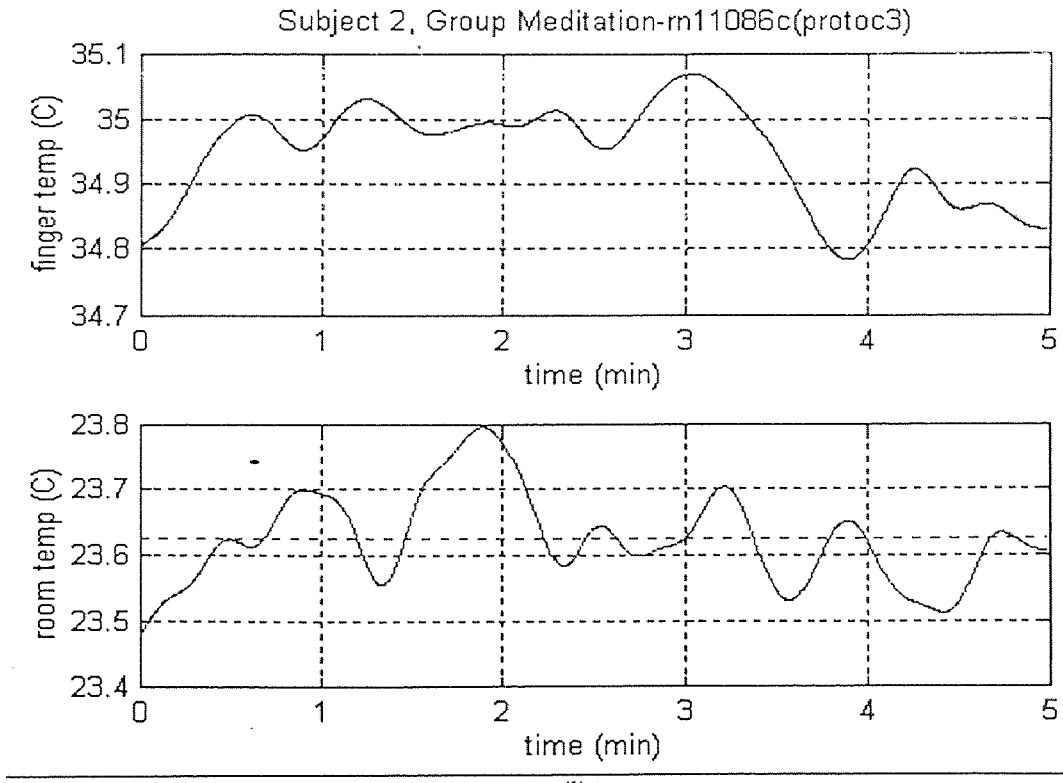

(l)

Figure 6.2 Temperature plots for group meditation (cont.):
(k) Subject 1 Group Meditation, and (l) Subject 2 Group Meditation

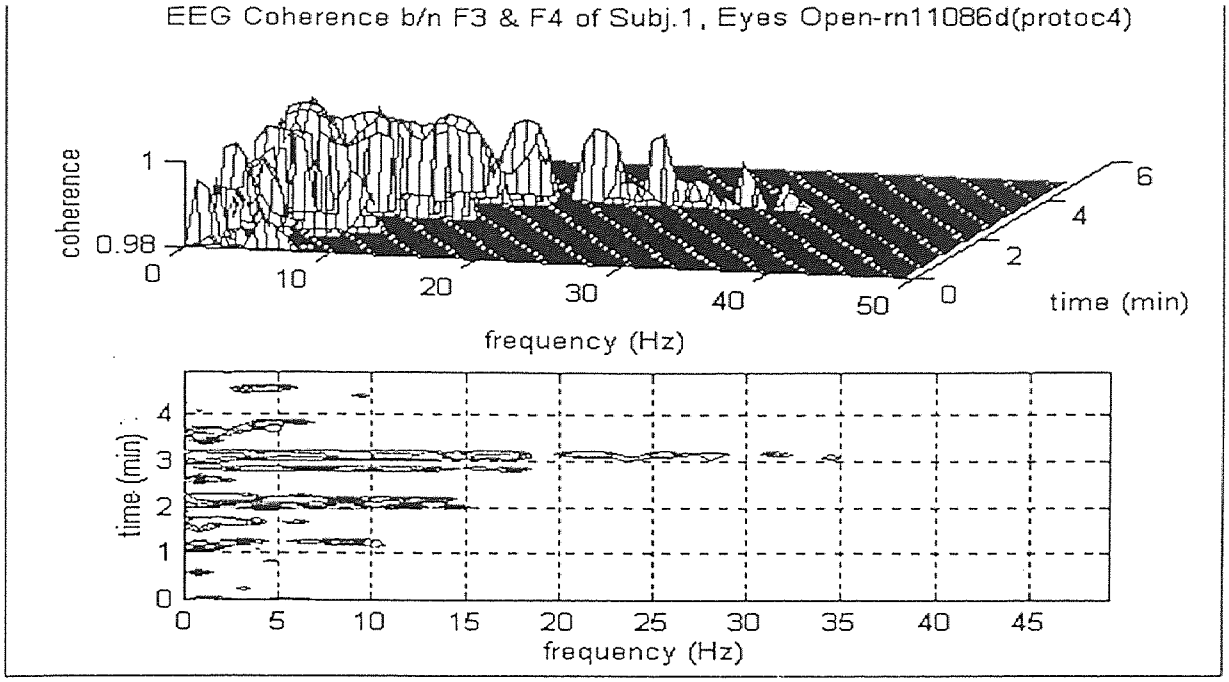

(m)

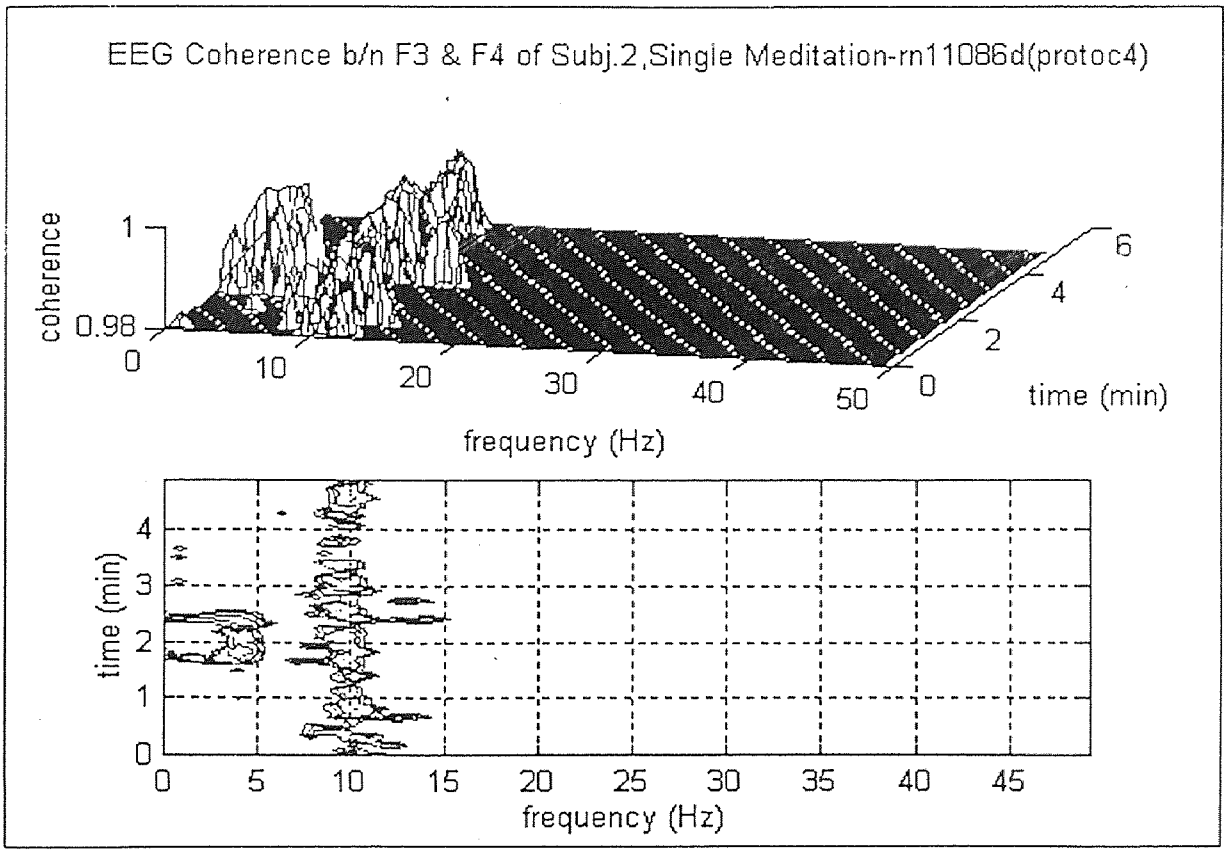

(n)

Figure 6.2 Cospar plots for group meditation (cont.):
(m) Subject 1 Eyes Open, and (n) Subject 2 Single Meditation

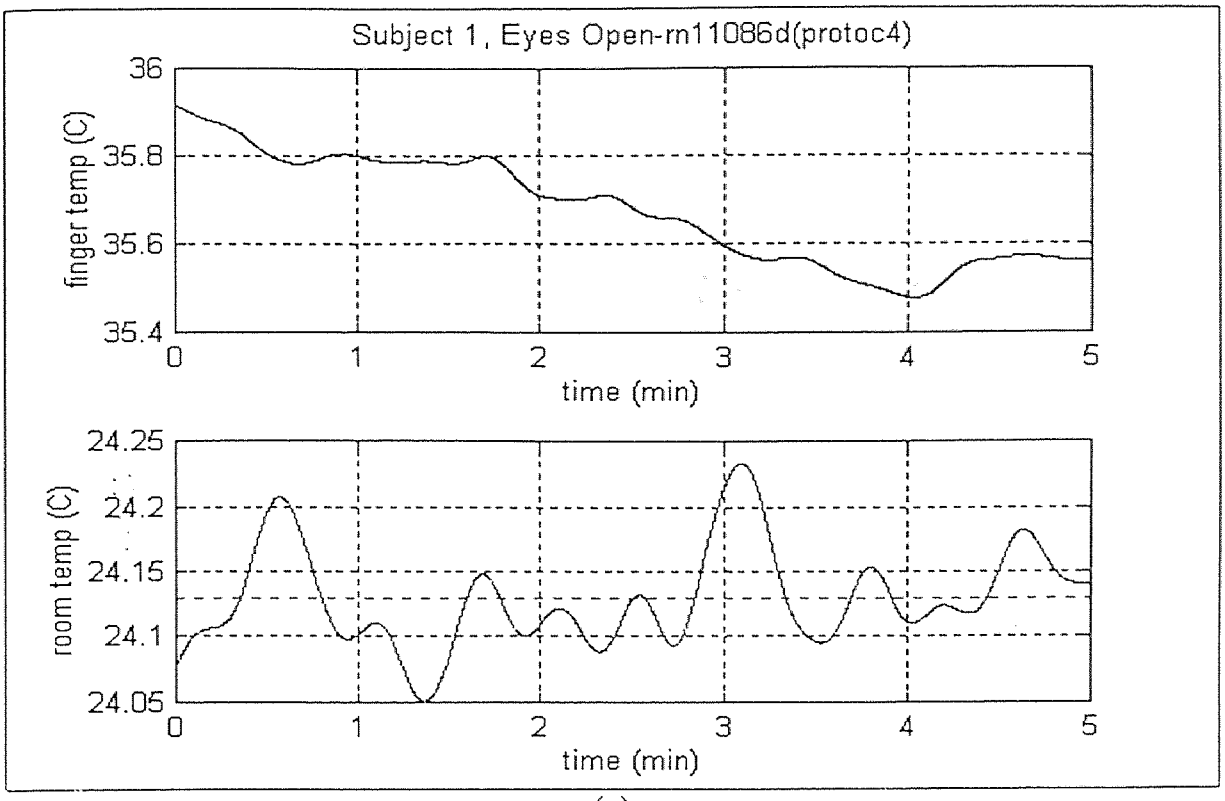

(o)

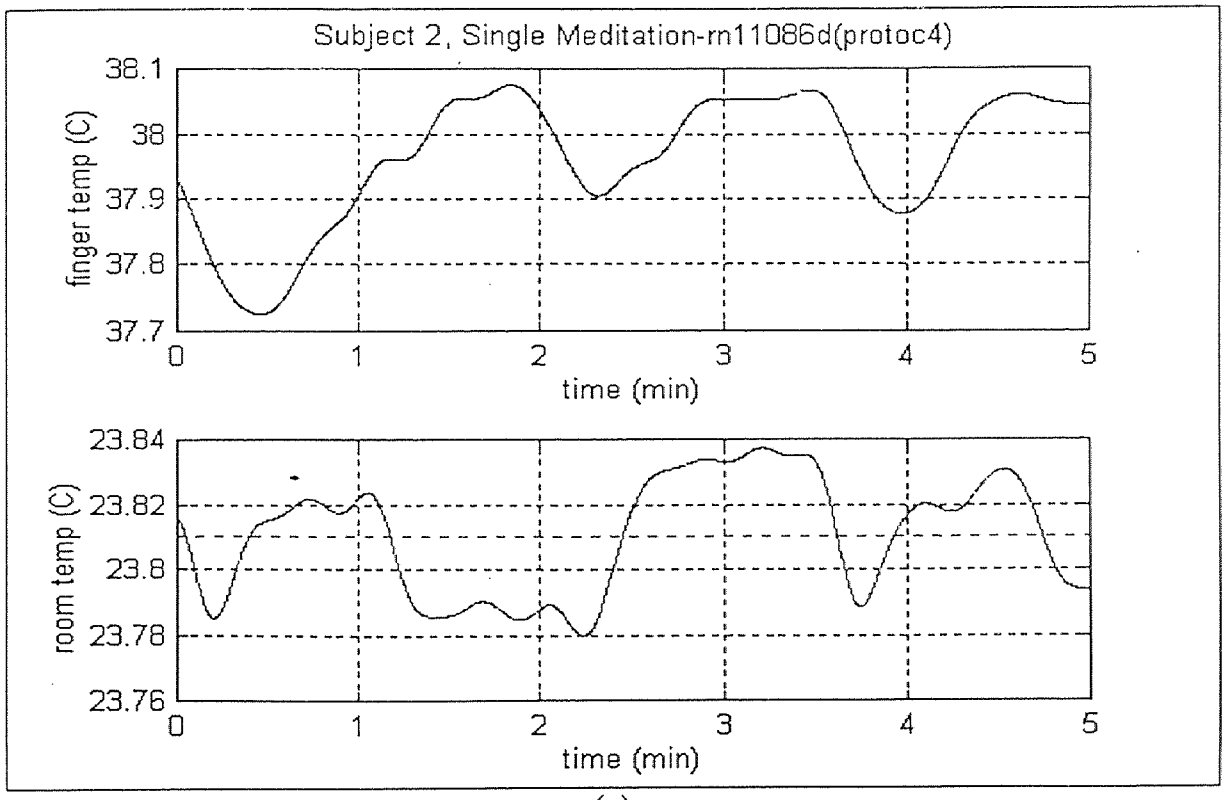

(p)

Figure 6.2 Cospar plots for group meditation (cont.):
(o) Subject 1 Eyes Open, and (p) Subject 2 Single Meditation

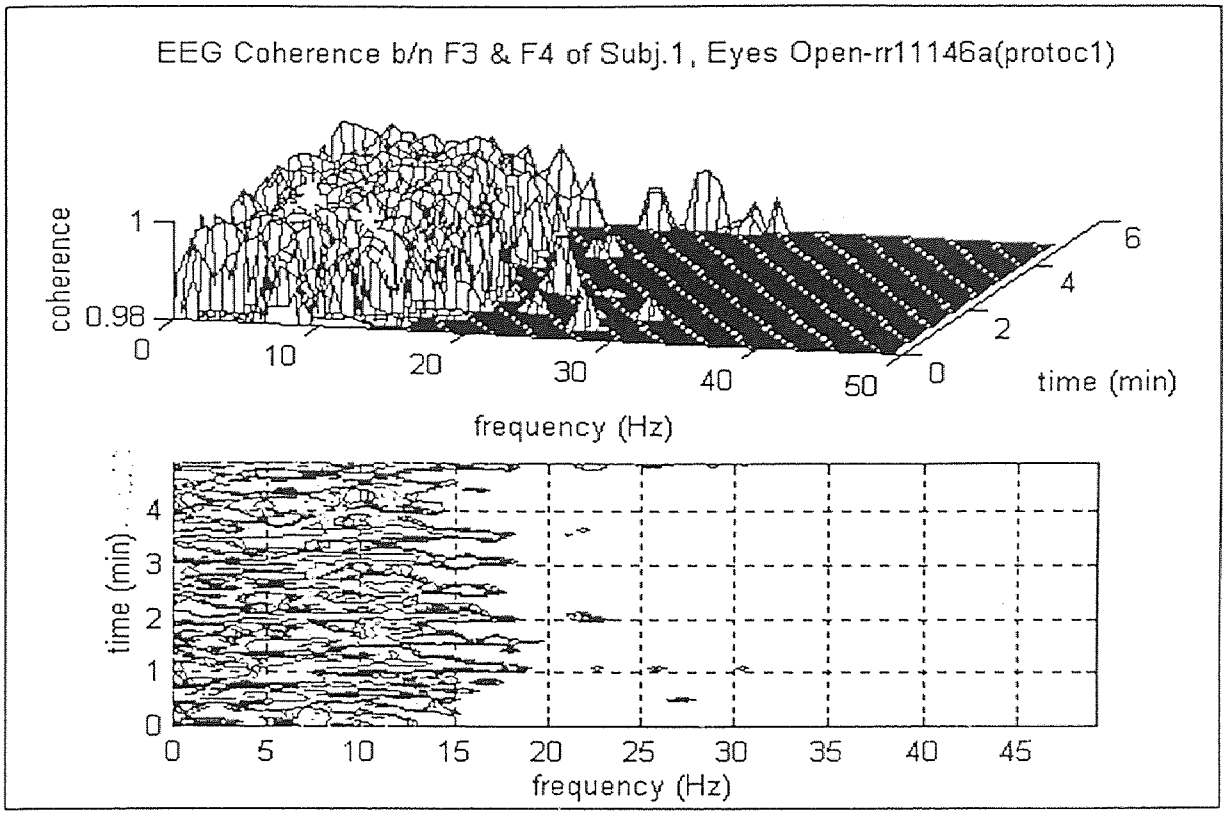

(a)

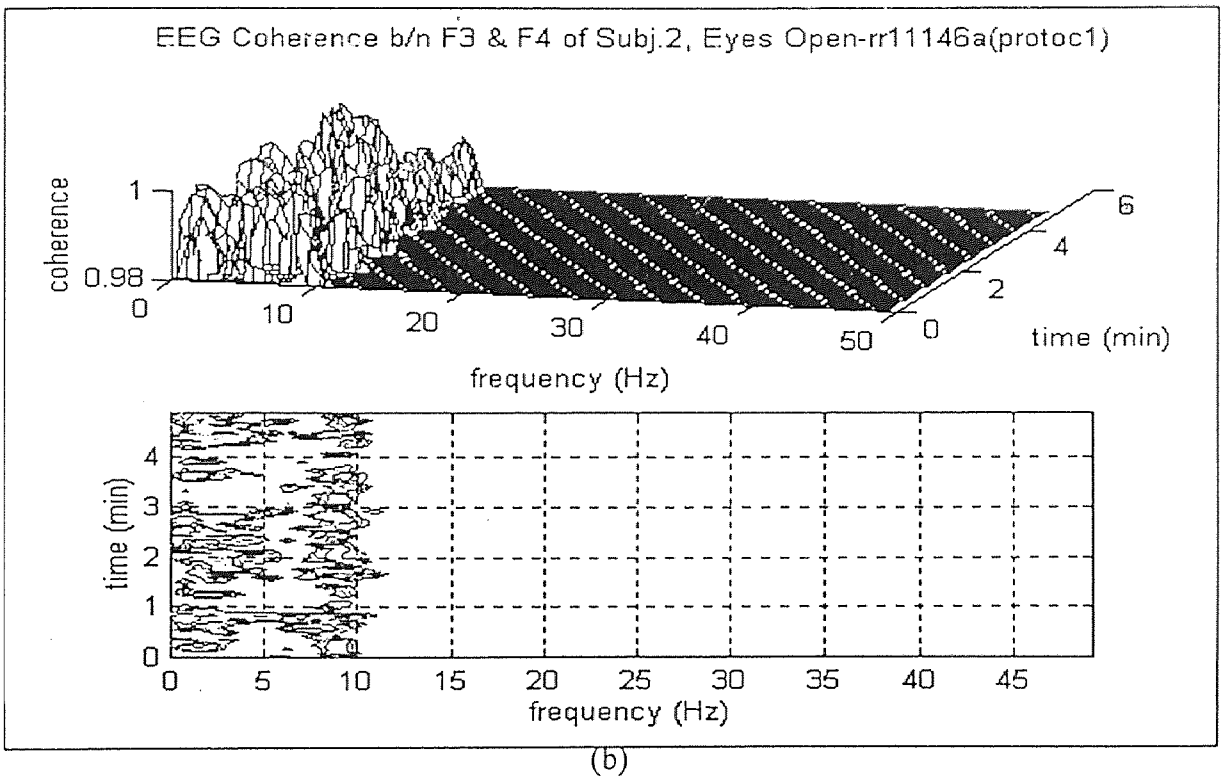

(b)

Figure 6.3 Cospar plots for group meditation:
(a) Subject 1 Eyes Open, and (b) Subject 2 Eyes Open

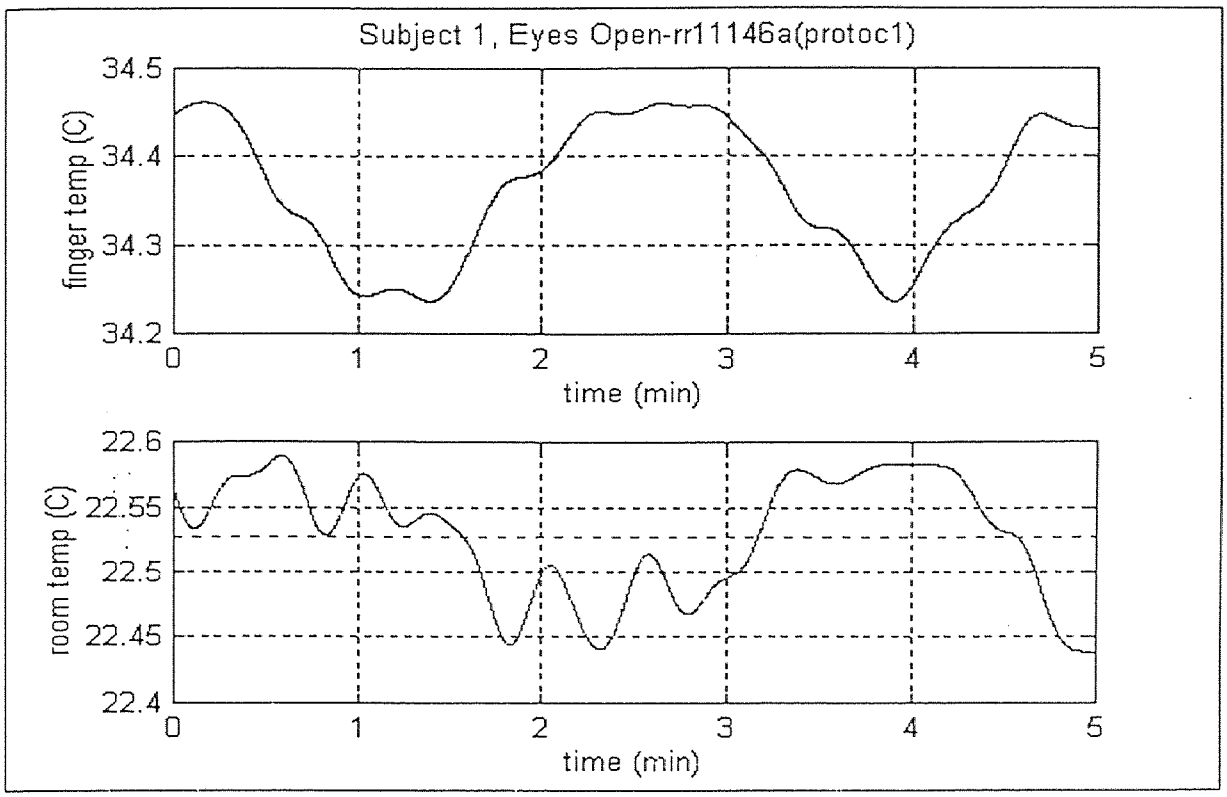

(c)

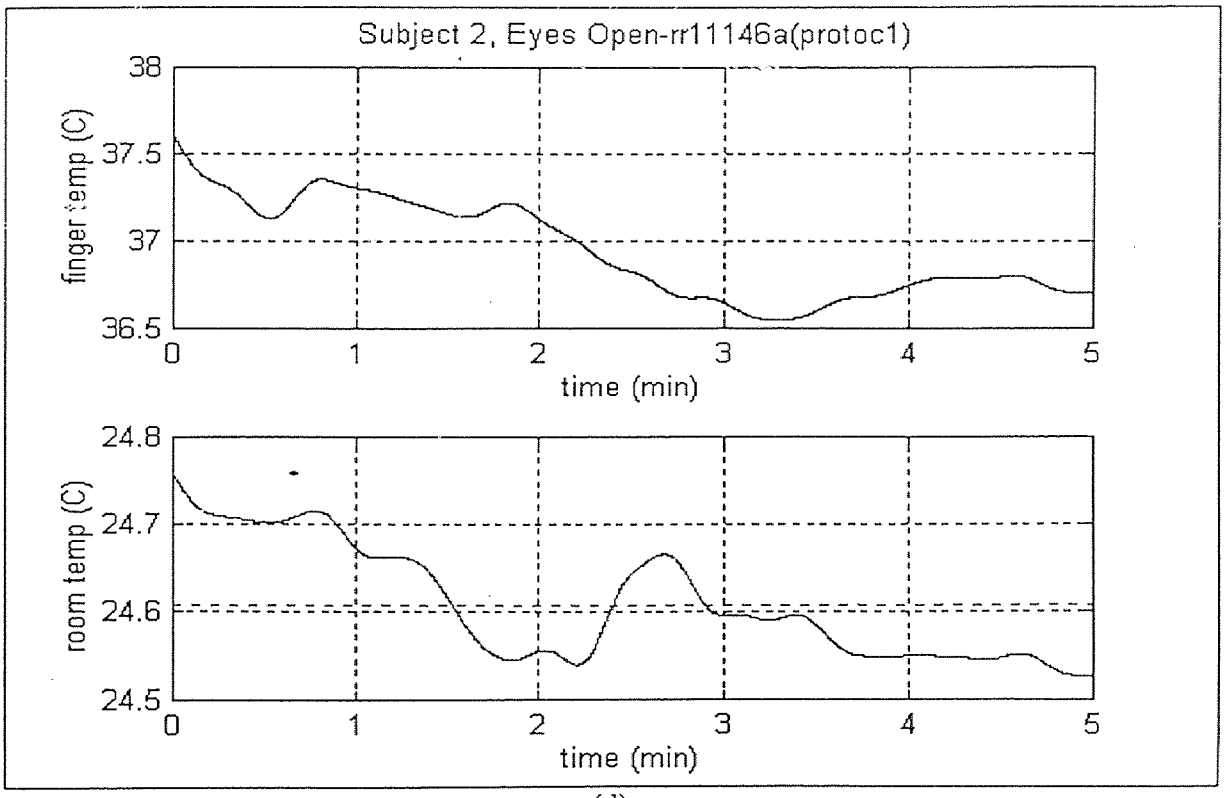

(d)

Figure 6.3 Temperature plots for group meditation:
(c) Subject 1 Eyes Open, and (d) Subject 2 Eyes Open

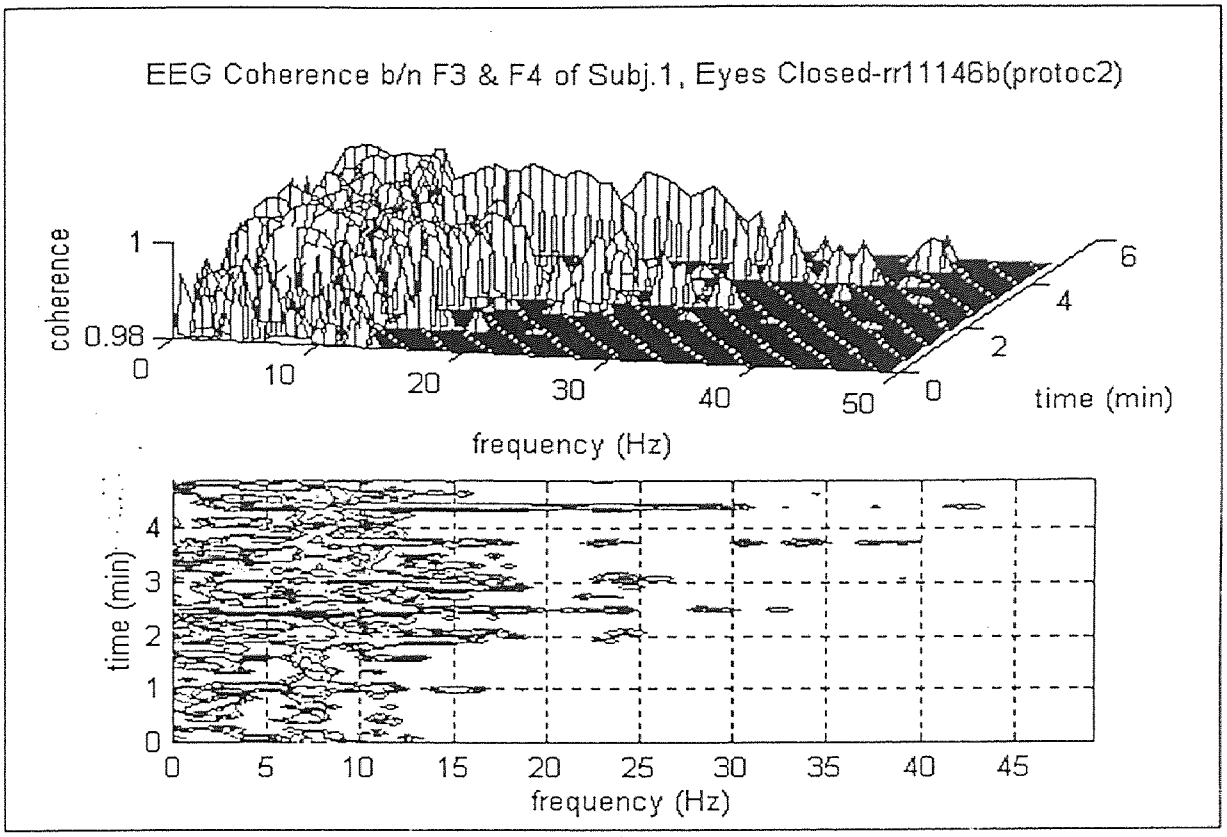

(e)

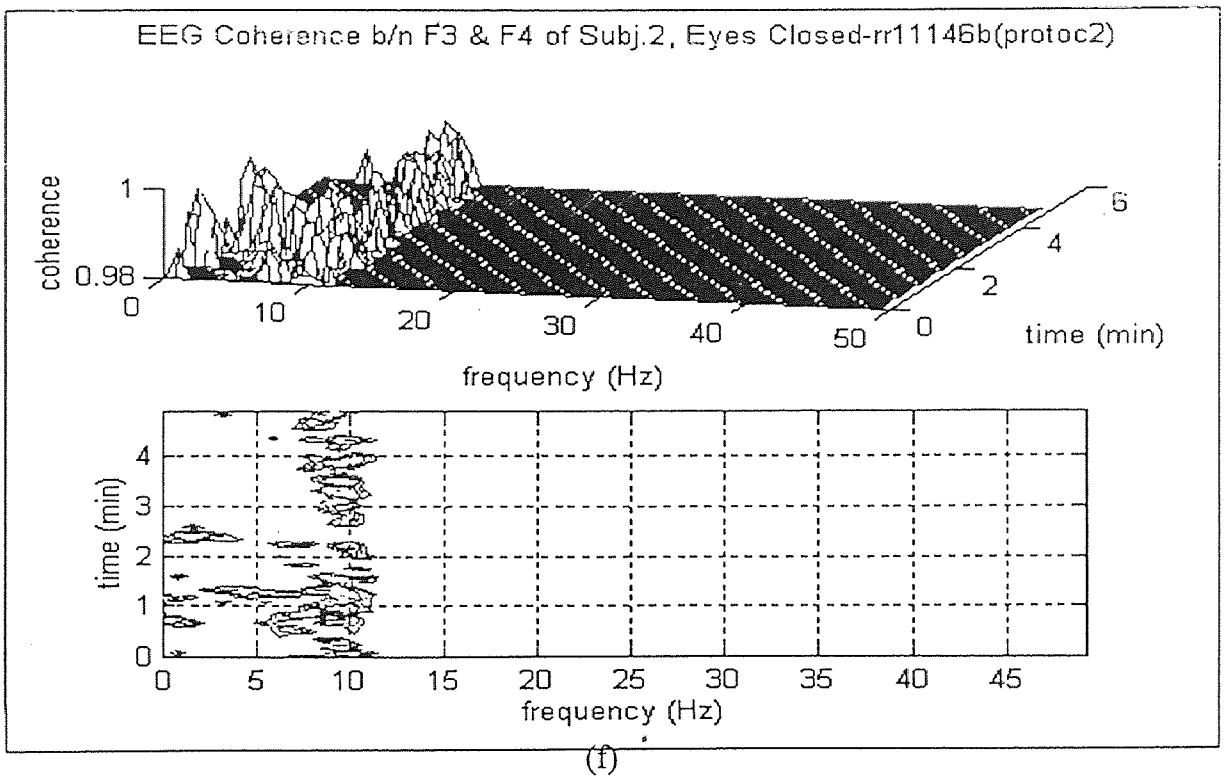

(f)

Figure 6.3 Cospar plots for group meditation (cont.):
(e) Subject 1 Eyes Closed, and (f) Subject 2 Eyes Closed

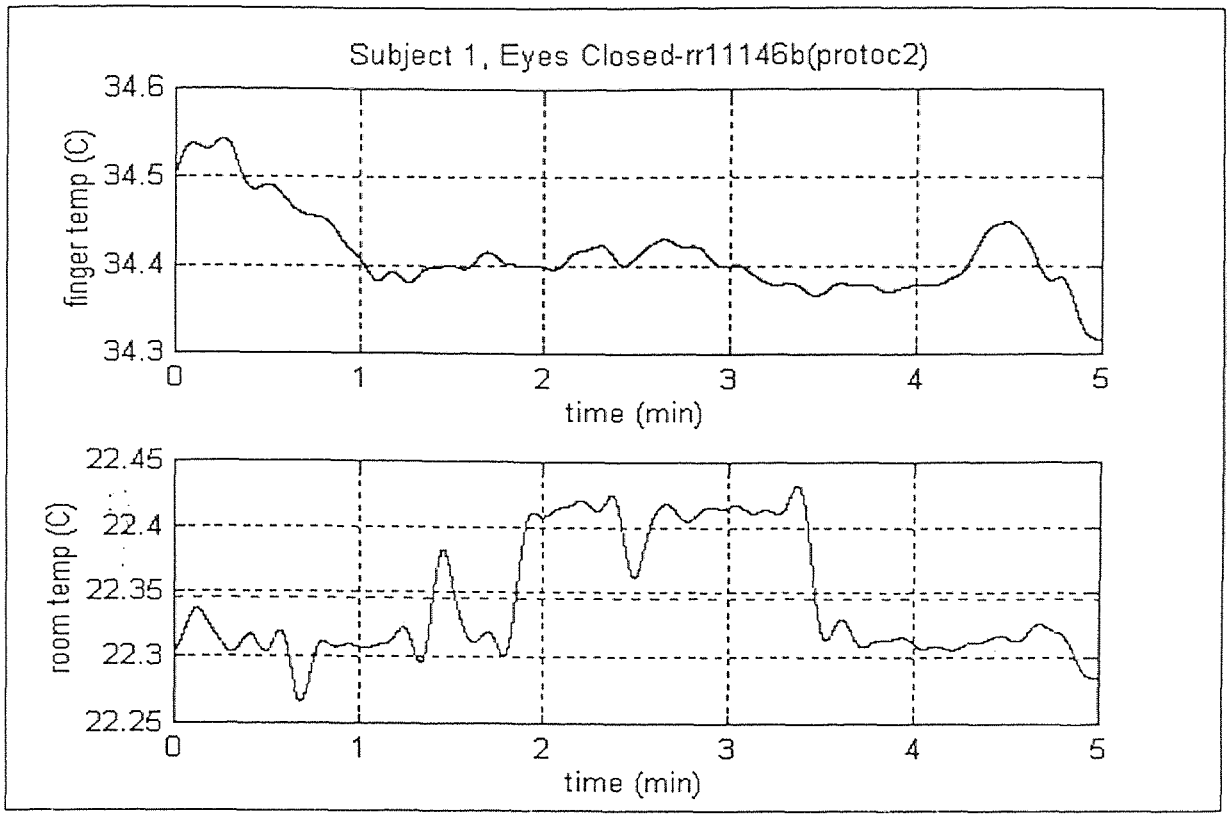

(g)

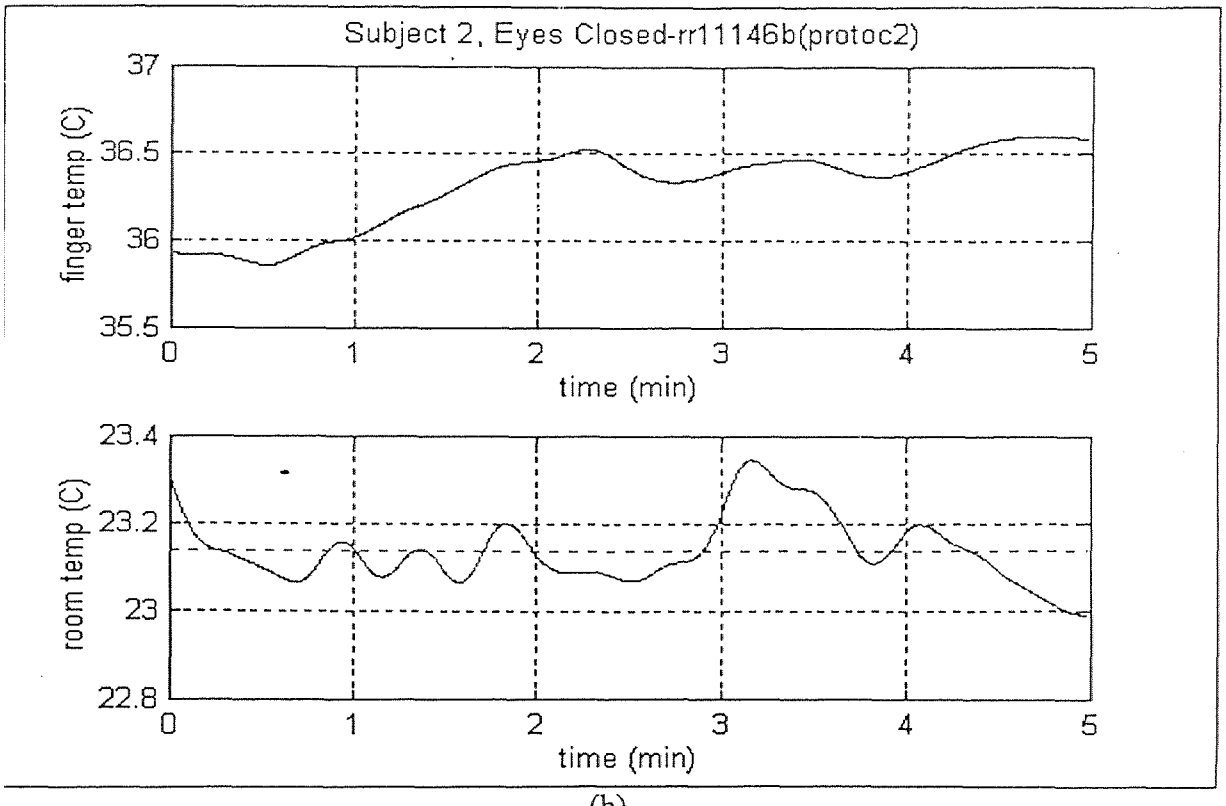

(h)

Figure 6.3 Temperature plots for group meditation (cont.):
(g) Subject 1 Eyes Closed, and (h) Subject 2 Eyes Closed

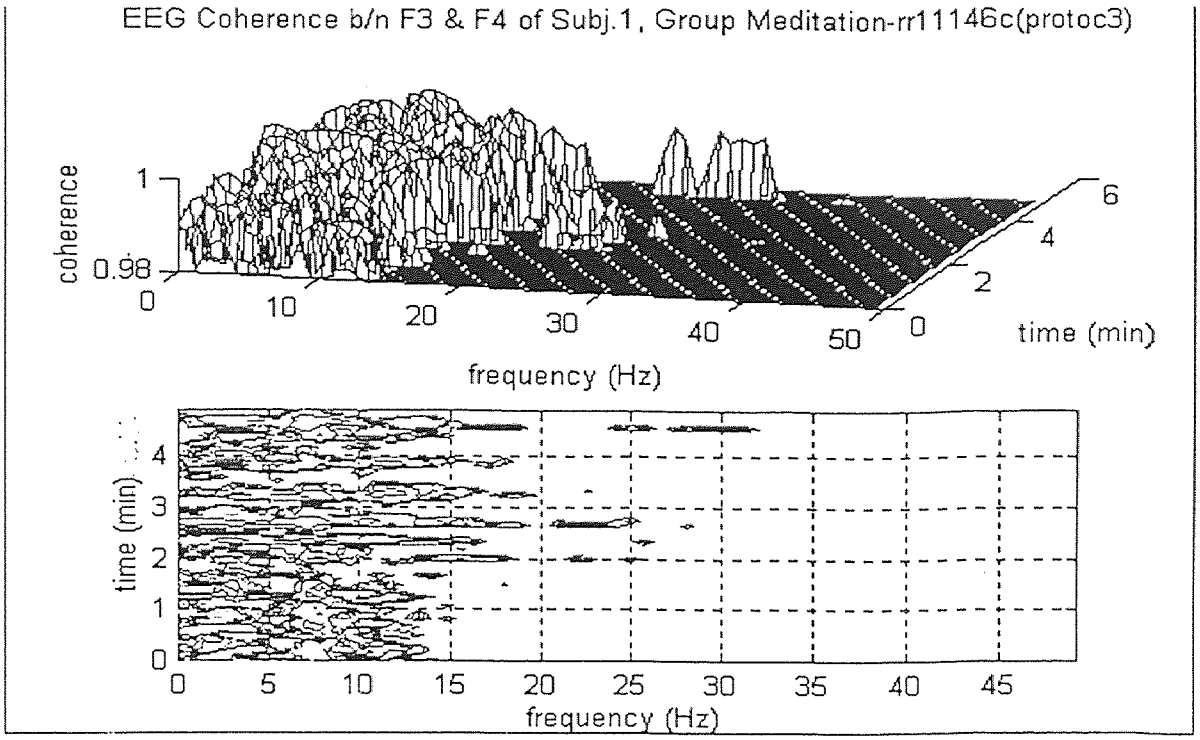

(i)

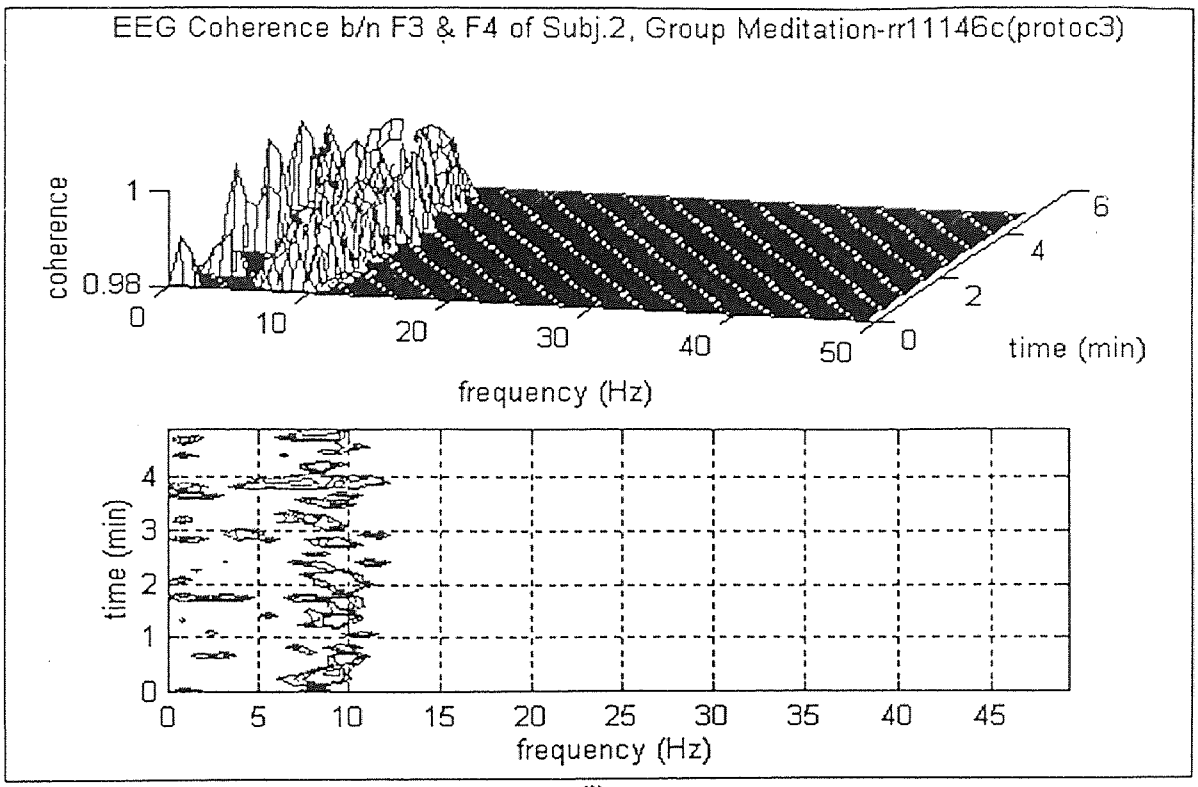

(j)

Figure 6.3 Cospar plots for group meditation (cont.):
(i) Subject 1 Group Meditation, and (j) Subject 2 Group Meditation

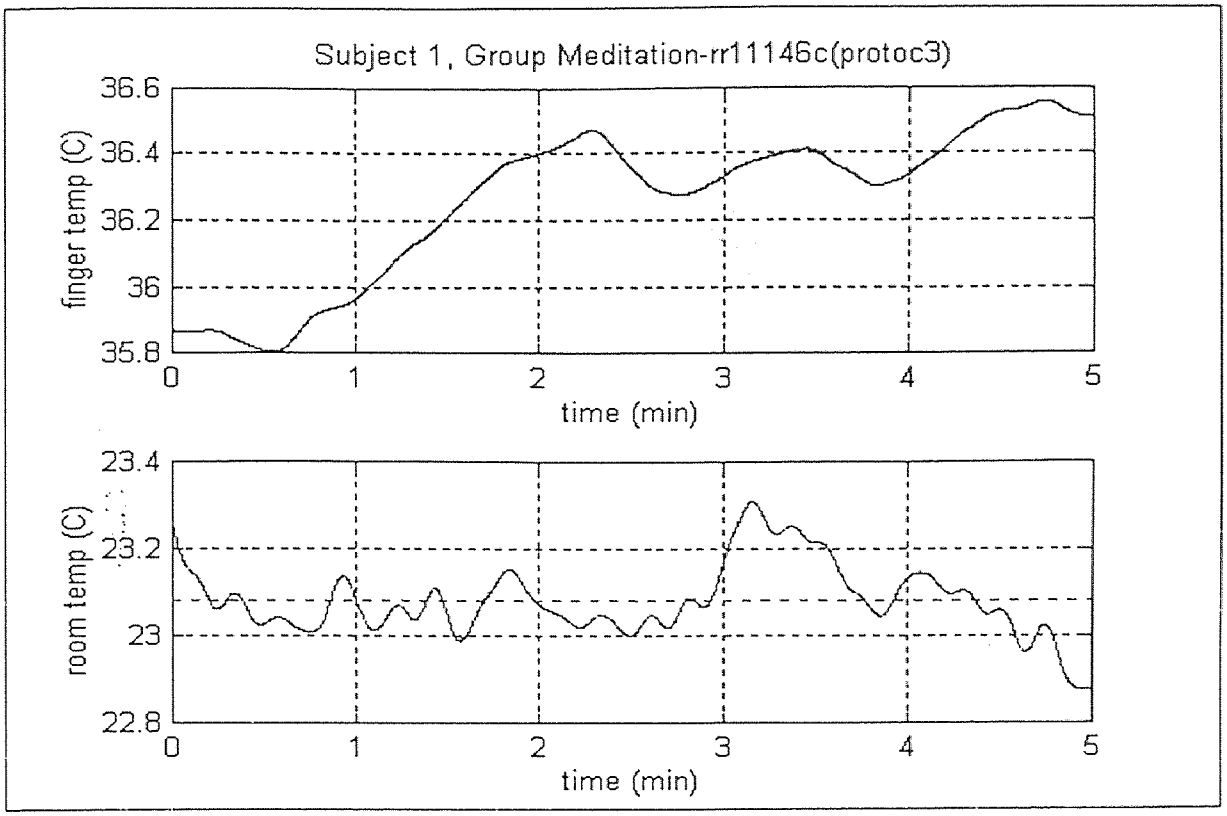

(k)

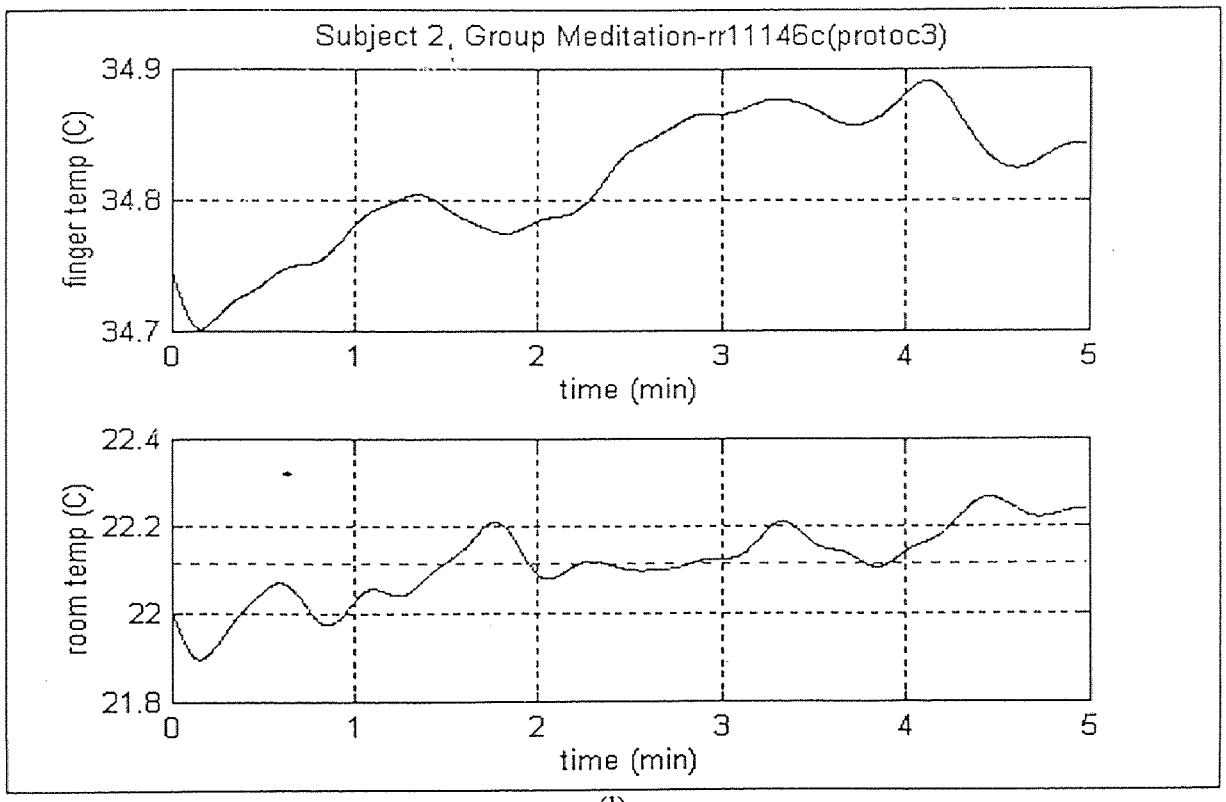

(l)

Figure 6.3 Temperature plots for group meditation (cont.):
(k) Subject 1 Group Meditation, and (l) Subject 2 Group Meditation

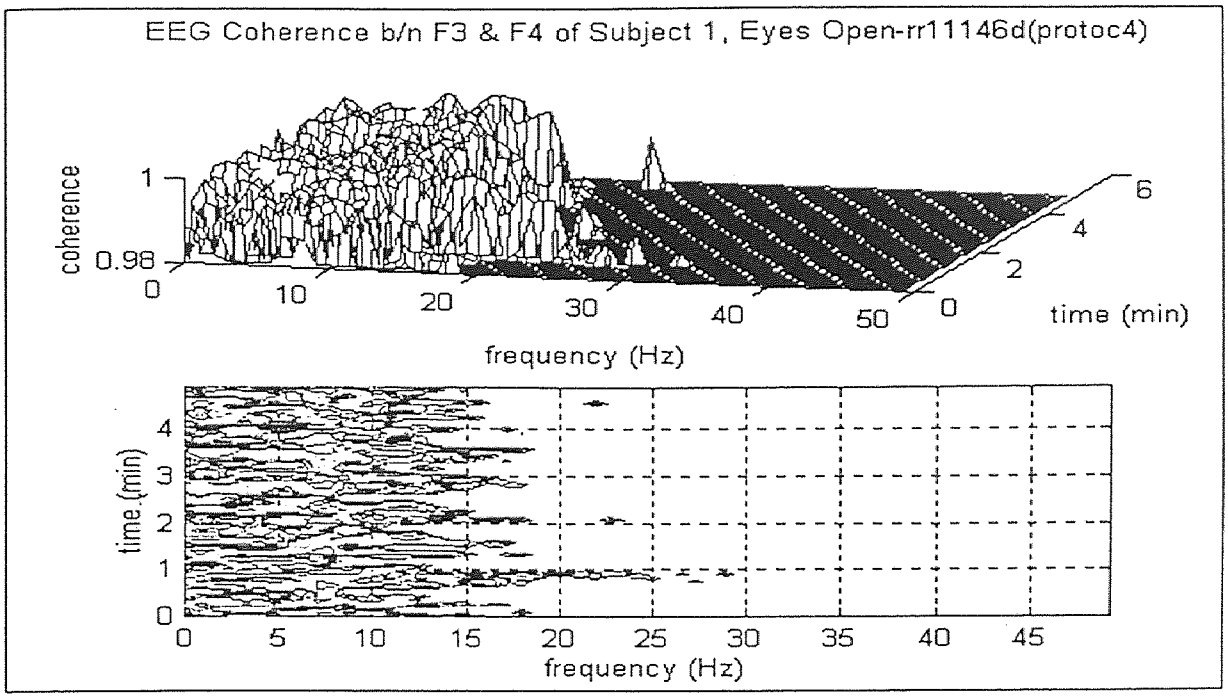

(m)

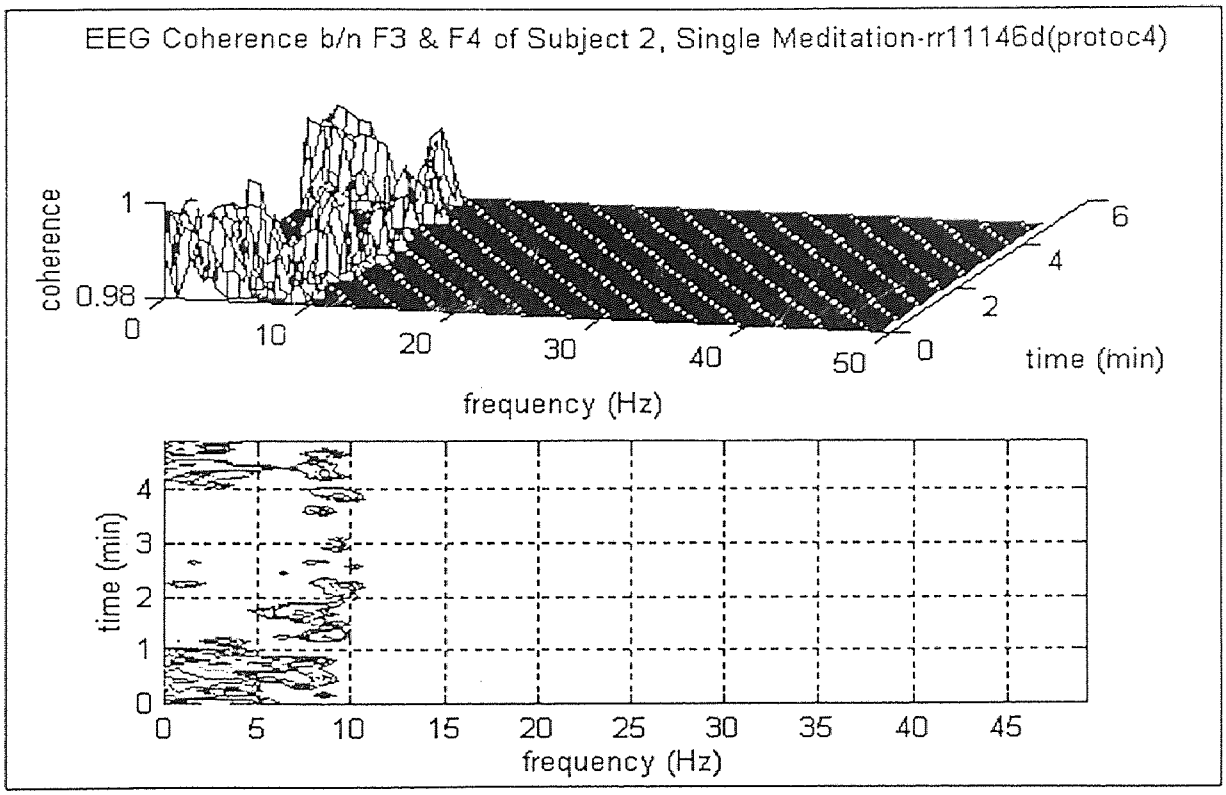

(n)

Figure 6.3 Cospar plots for group meditation (cont.):
(m) Subject 1 Eyes Open, and (n) Subject 2 Single Meditation

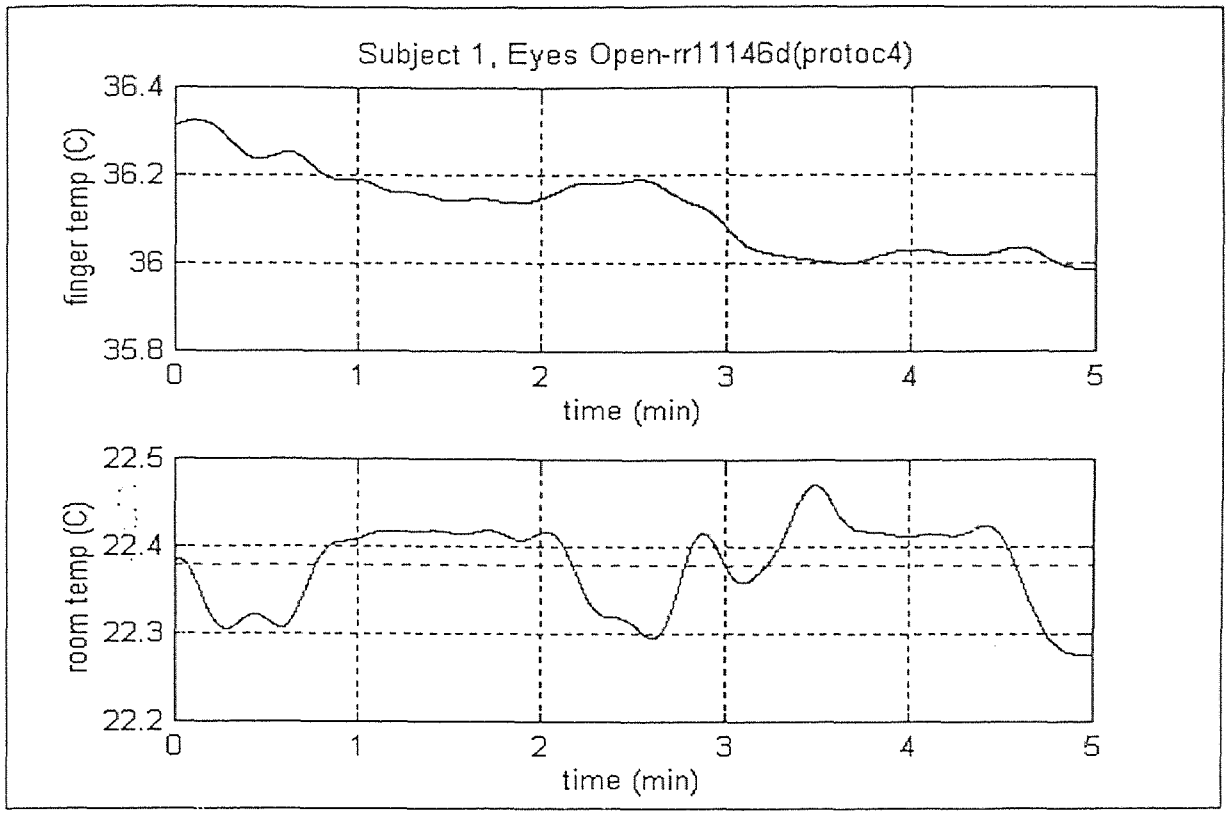

(o)

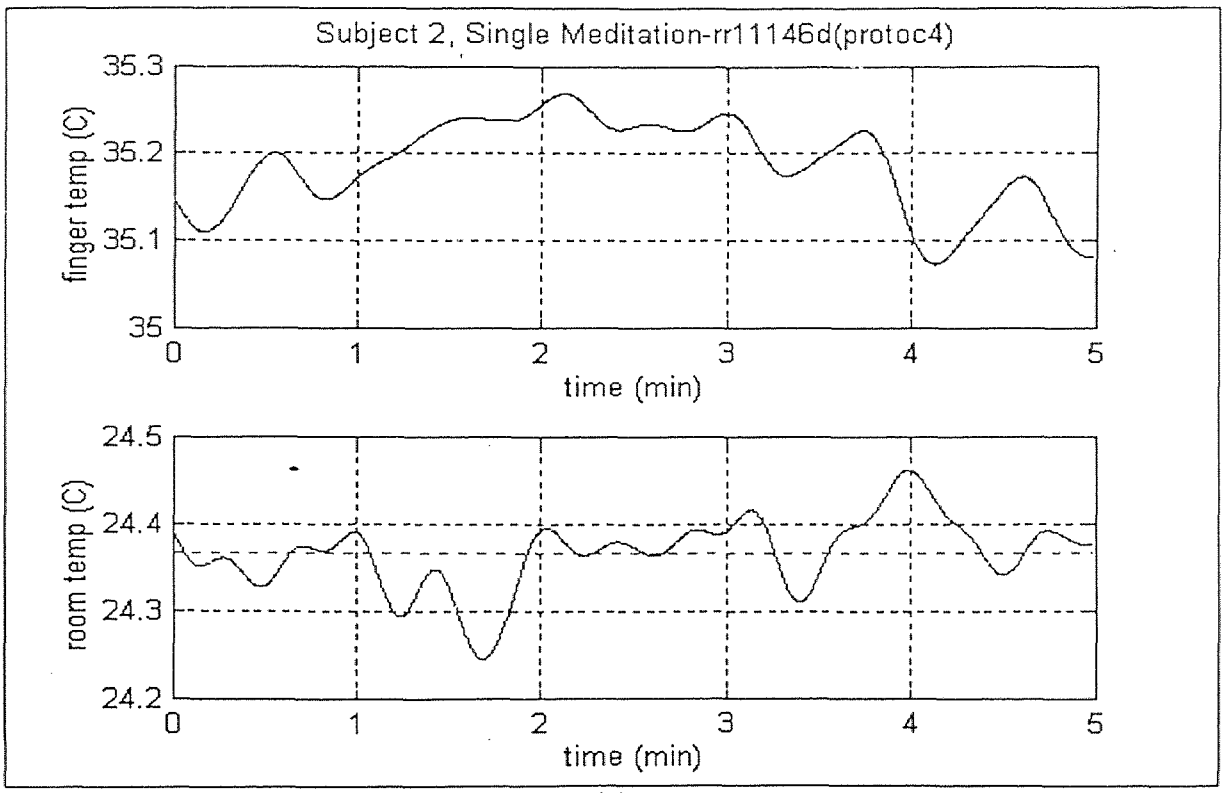

(p)

Figure 6.3 Temperature plots for group meditation (cont.):
(0) Subject 1 Eyes Open, and (p) Subject 2 Single Meditation

6.2 Skin Blood Flow Study

Nine subjects participated in this study, four males and five females. They were between the ages of 24 and 32 years. Each experiment consisted of measuring the finger temperature, the finger blood volume and the finger arterial pulse (indicated in the plots as pulse waveform). The ambient room temperature was also recorded in each experiment.

In general, for the nine subjects, the skin temperature closely followed the finger blood volume in the same direction but at a slower rate (lower slope). With the exception of figure 6.11, the remaining 8 subjects have a general trend: changes in the finger blood flow or blood volume are accurately reflected in the changes of the finger temperature. An interesting example is figure 6.9: When the finger blood volume rises, the finger temperature also rises but at slower rate (lower slope). When the finger blood volume drops, the finger temperature also drops but at a slower rate. Changes in the finger blood volume (changes in the finger temperature) are also reflected in the changes in the amplitude of the pulse waveform. When the blood volume of the finger drops down, a corresponding drop in the amplitude of the arterial pulse of the finger is observed, an indication of vasoconstriction [13] (see section 5.2.2), this is true for all the nine cases.

In all nine experiments, it is observed that during eyes open and eyes closed states, the finger blood volume and hence the corresponding temperatures rose up to a maximum value and then remained constant at this value in an oscillatory manner. At this time, the amplitude of the arterial pulse of the finger remained constant at some maximum value.

When the subjects experienced stress from the noise, their finger blood volume, their finger temperatures and the amplitudes of their arterial finger pulses decreased. This is consistent with findings in the open literature [3], [1], [2], [4] and [5] who attribute the vasoconstriction to sympathetic tone.

Figure 6.4 is a typical plot of arterial pulse waveform of the finger, finger blood volume, finger temperature and the room temperature for 3 minutes eyes open, 12 minutes eyes closed relaxed, and 5 minutes noise to create a stressful situation. Figures 6.4 (a), and (b) - figures 6.12 (a), and (b) all follow this physiological process.

From the blood volume and temperature plots (figure 6.4 to figure 6.12), and their responses to noise, it is clear that when a stress was caused, there was a definite drop in skin temperature caused by the constricting of the cutaneous blood vessels, which might be due to the response of the sympathetic tone (see section 2.4) [4]. During relaxation, however, the cutaneous blood vessels are vasodilated allowing more blood to flow to the cutaneous blood vessels and hence increasing the skin temperature during meditation and relaxation. Since the cutaneous blood vessels are controlled by the sympathetic nervous system only, it is possible that changes in the skin temperature or skin blood volume may be caused by the sympathetic tone [2], [3], [4] and [5].

Statistical evaluation of the relationship between the cutaneous blood volume and temperature was performed using the cross correlation function. In each of the nine experiments, the cross correlation between the cutaneous blood volume and the temperature was calculated and plotted as a function of time. The corresponding cross correlation plots are shown in figures (c) of each experiment. The upper graph is the cross

correlation plot as a function of time. In an effort to investigate if there is a time delay between the cutaneous blood volume and the cuteneous temperature, the peak of each cross correlation plot was windowed and enlarged. The corresponding time delay plot is shown below each cross correlation plot, and the time delay for each experiment was estimated to be approximately 0.55 seconds. The peak values of the cross correlation at a zero lag were calculated and are presented in table 6.4.

Table 6.4 Cross correlation peak values at zero lag

No. of Experiment	Peak Values at Zero Lag
1	0.9826
2	0.9747
3	0.9536
4	0.9131
5	0.9292
6	0.9249
7	0.8800
8	0.8805
9	0.8742

The enlarged version of the cross correlation plot shows consistent and unequal correlation rates about the zero lag. Except for figures 6.6 (c) and 6.10 (c), the cross correlation rates are lower on the left side of the zero lag (where the cross correlation function is maximum) than on the right side. The instantaneous value of the cross correlation function is greater on the left of the zero lag than on the right. The lower the

slope, the slower the rate the cross correlation function decreases in value when the two physiological parameters are slid realtive to each other to the left. If the two data are slided to the right however, the slope is higher, causing a faster decrease in the value of the cross correlation function.

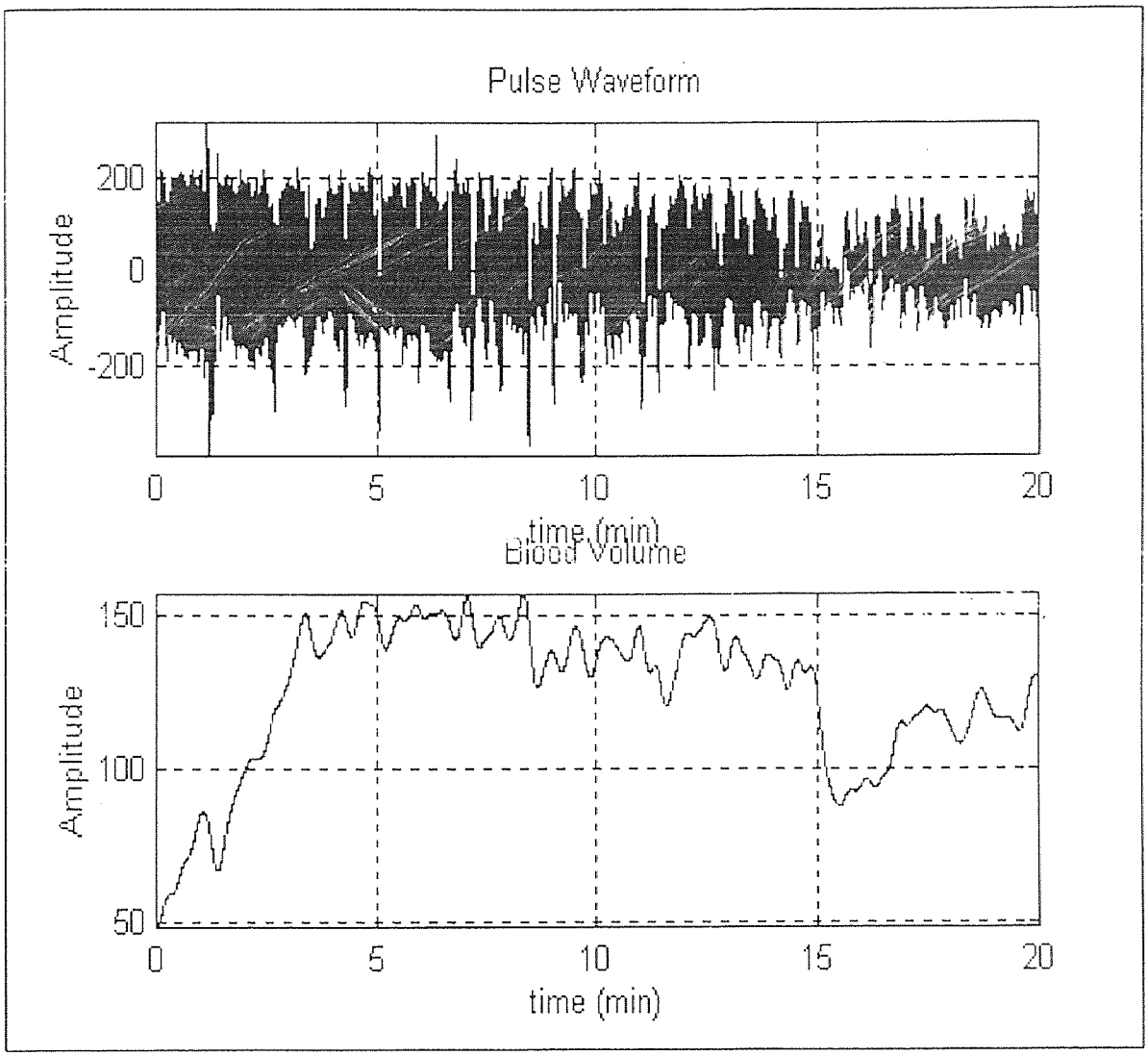

(a)

Figure 6.4 Blood Flow Experiment (3 mins-EO, 12 mins-Relaxation, 5 mins-Stress)
(a) Pulse Waveform, Finger Blood Volume

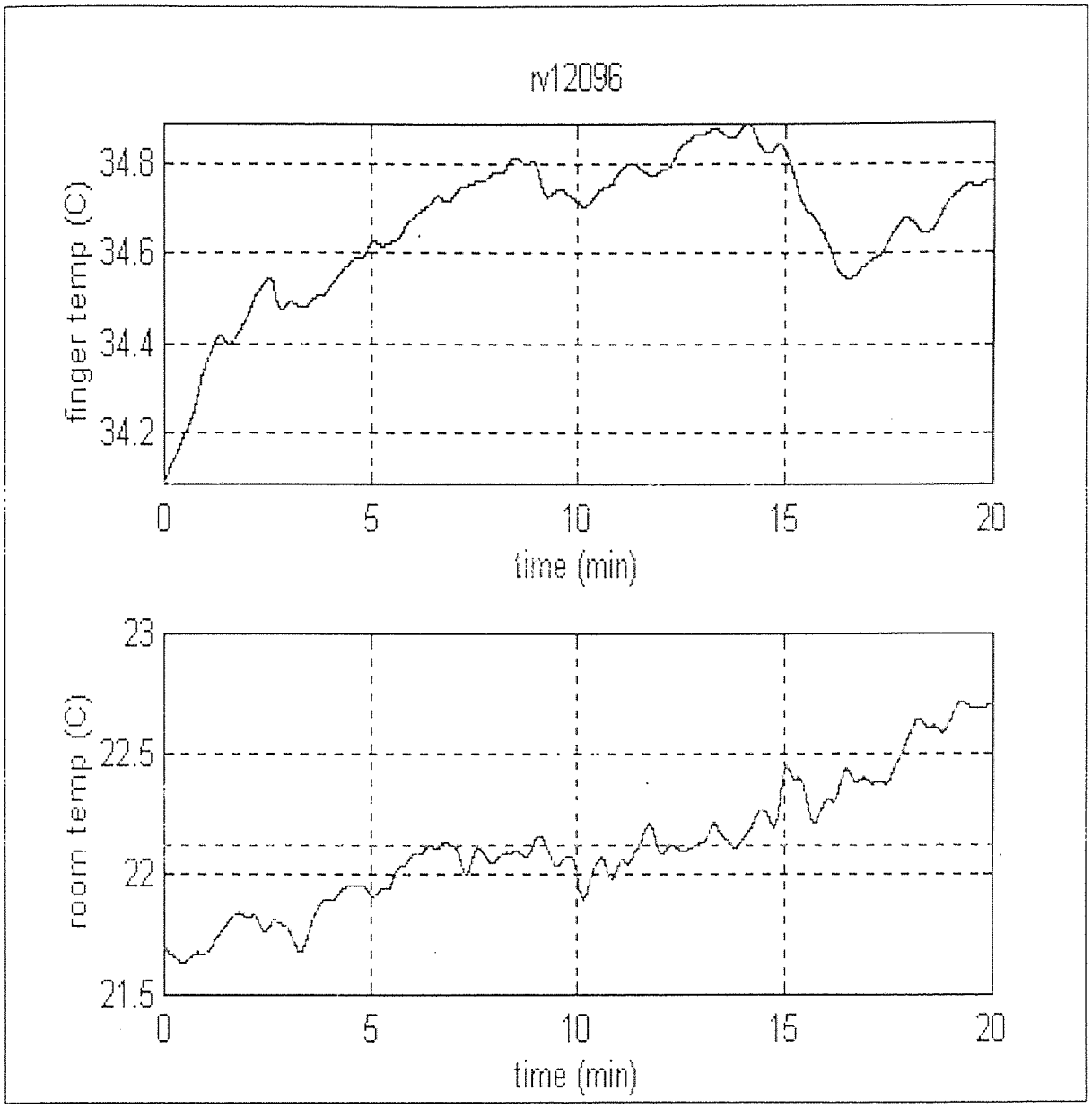

(b)

Figure 6.4 Blood Flow Experiment (cont):
(b) Finger Temperature, Room Temperature

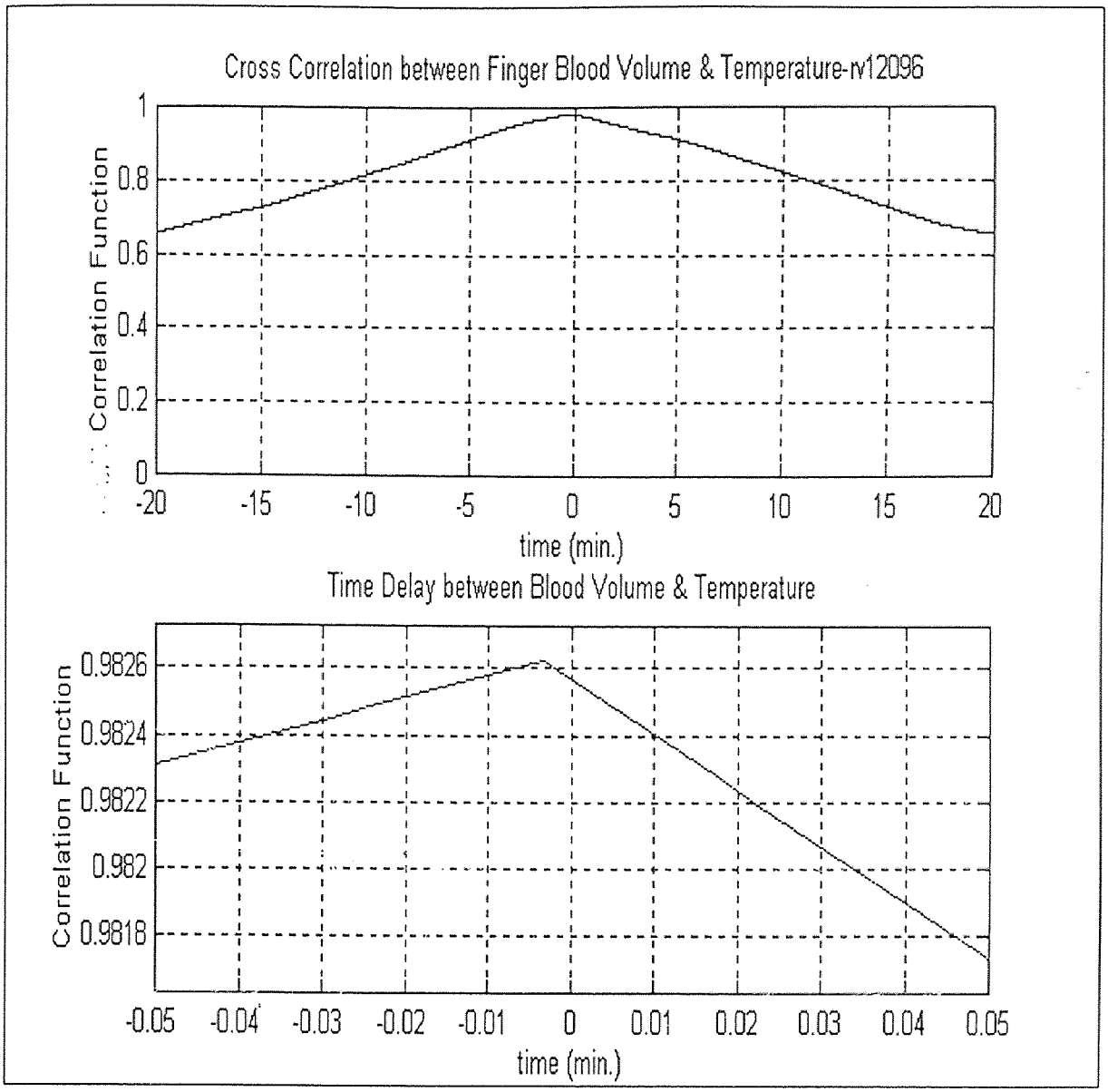

(c)

Figure 6.4 Blood Flow Experiment (3 mins-EO, 12 mins-Relaxation, 5 mins-Stress): Cross Correlation and Time Delay b/n Blood Volume & Finger Temperature

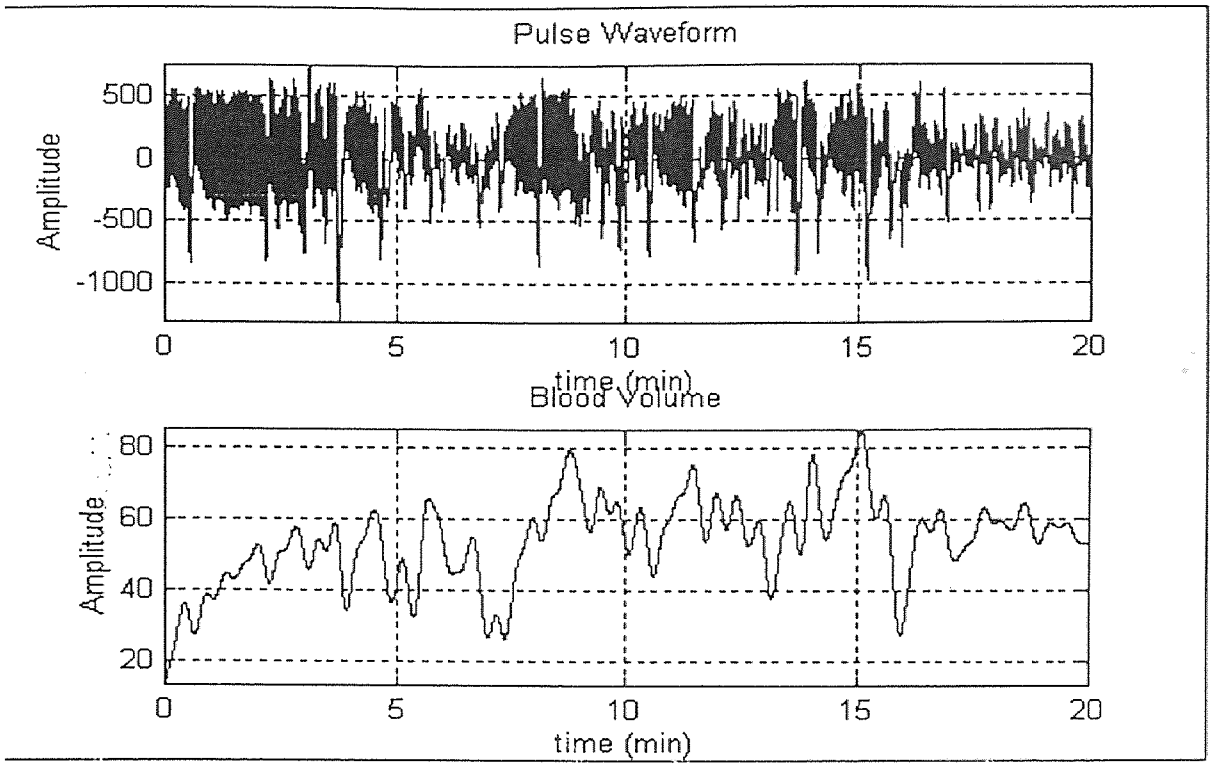

(a)

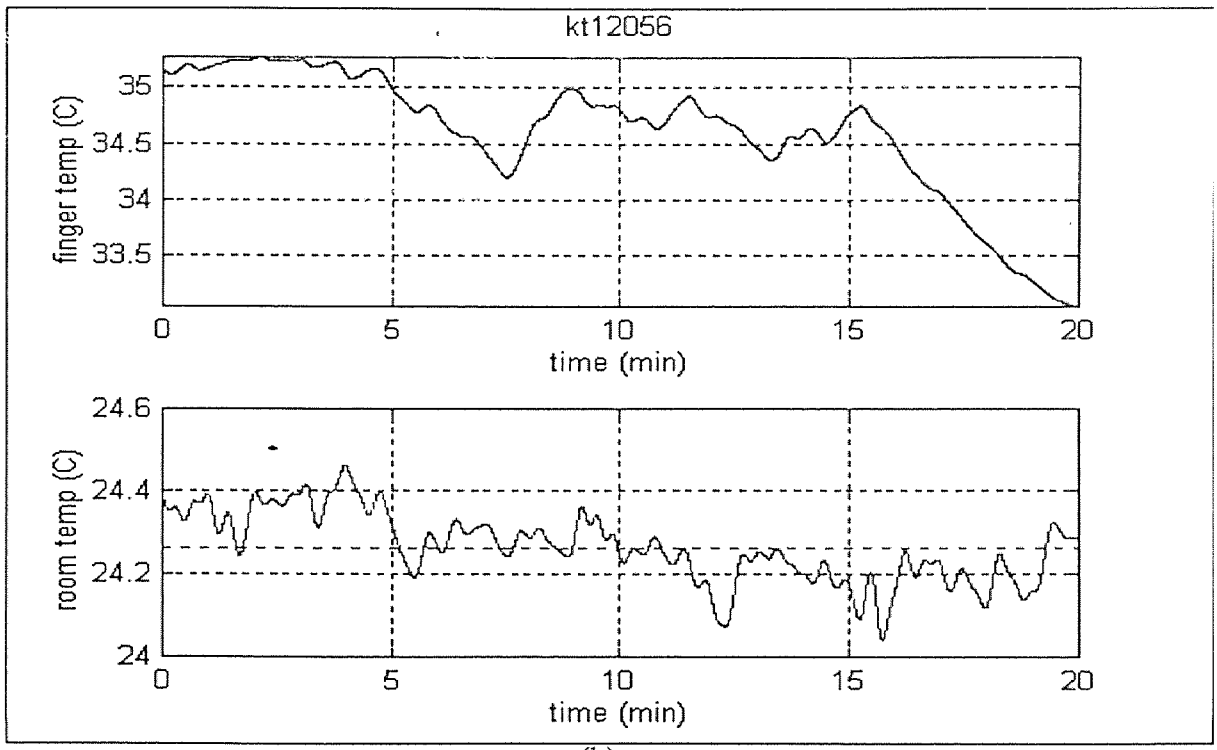

(b)

Figure 6.5 Blood Blood Flow Experiment(3 mins-EO, 12 mins-Relaxation, 5 mins-Stress): (a) Pulse Waveform, Finger Blood Volum
(b) Finger Temperature, Room Temperature

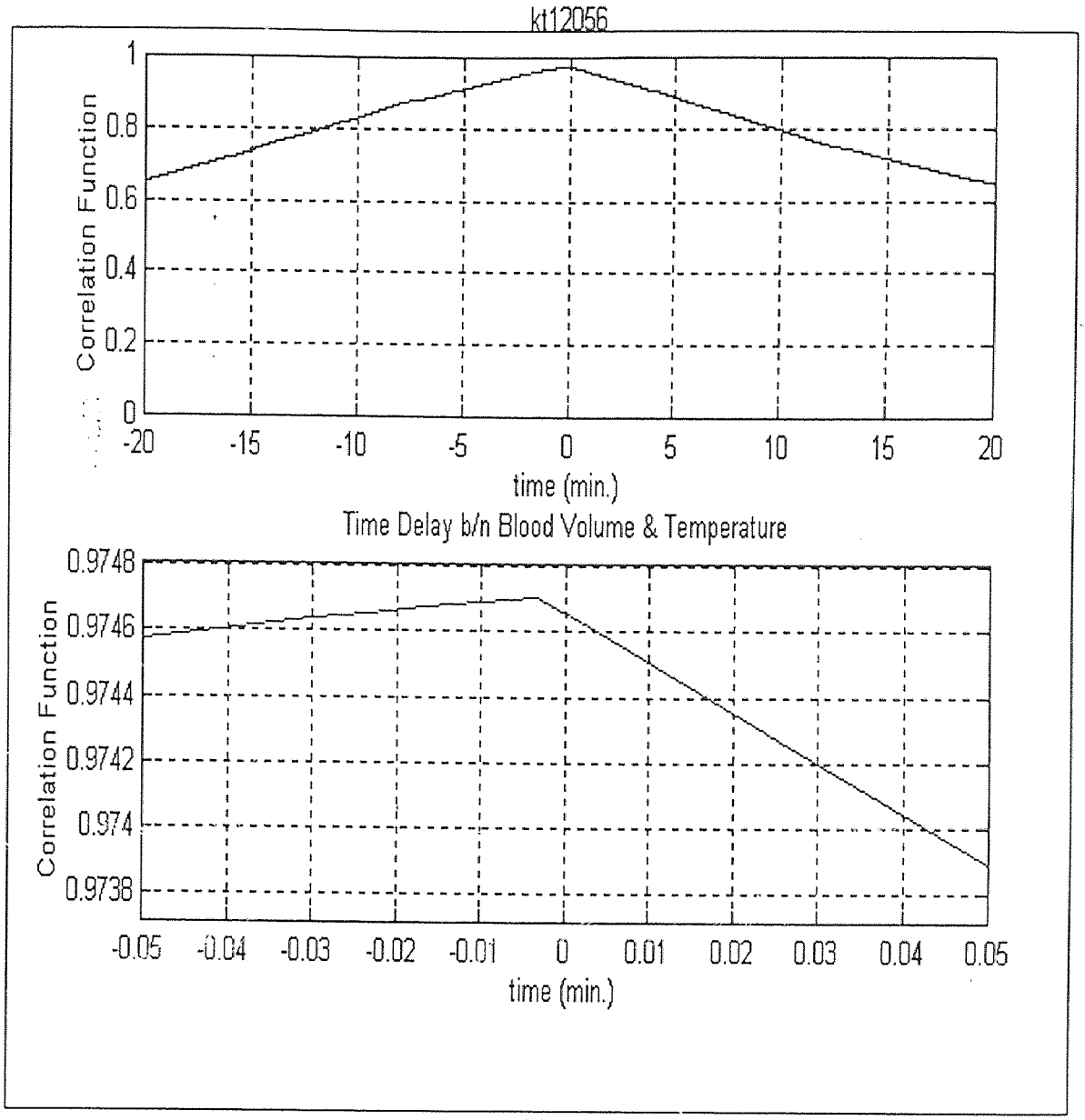

(c)

Figure 6.5 Blood Flow Experiment (3 mins-EO, 12 mins-Relaxation, 5 mins-Stress): Cross Correlation and Time Delay b/n Blood Volume & Finger Temperature

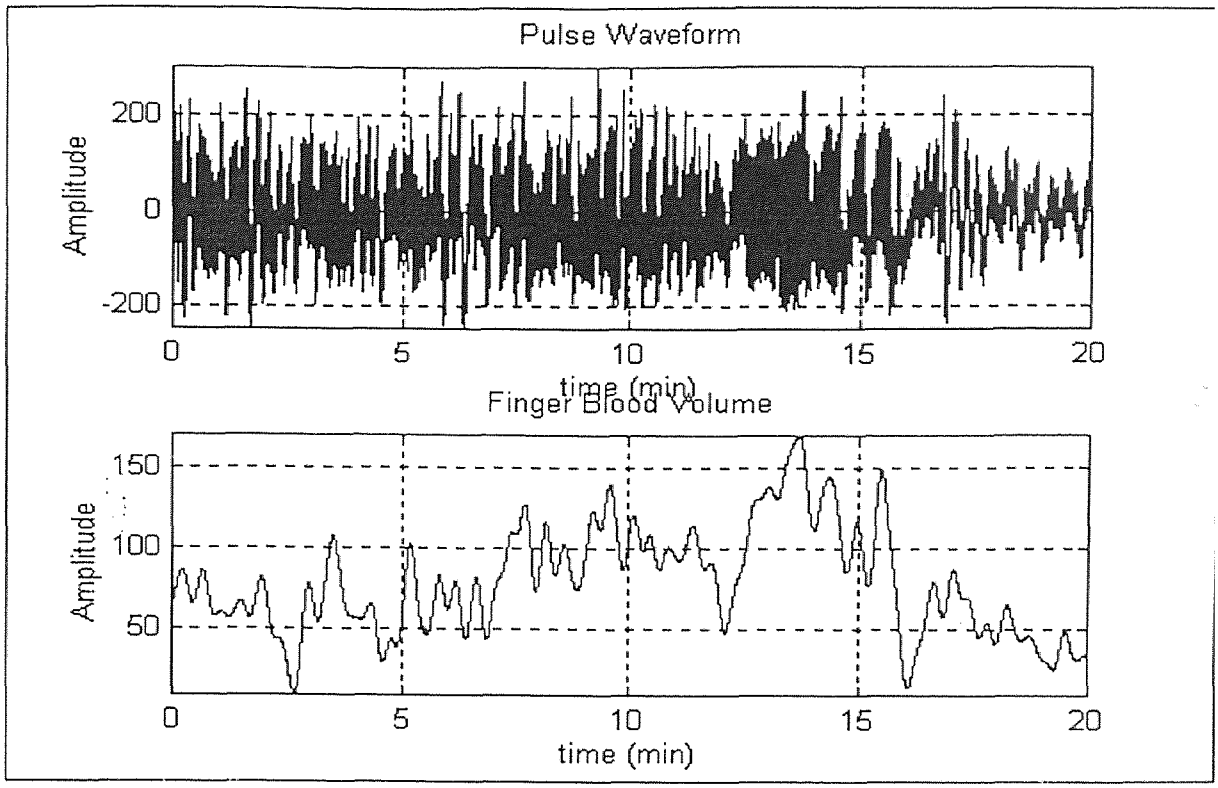

(a)

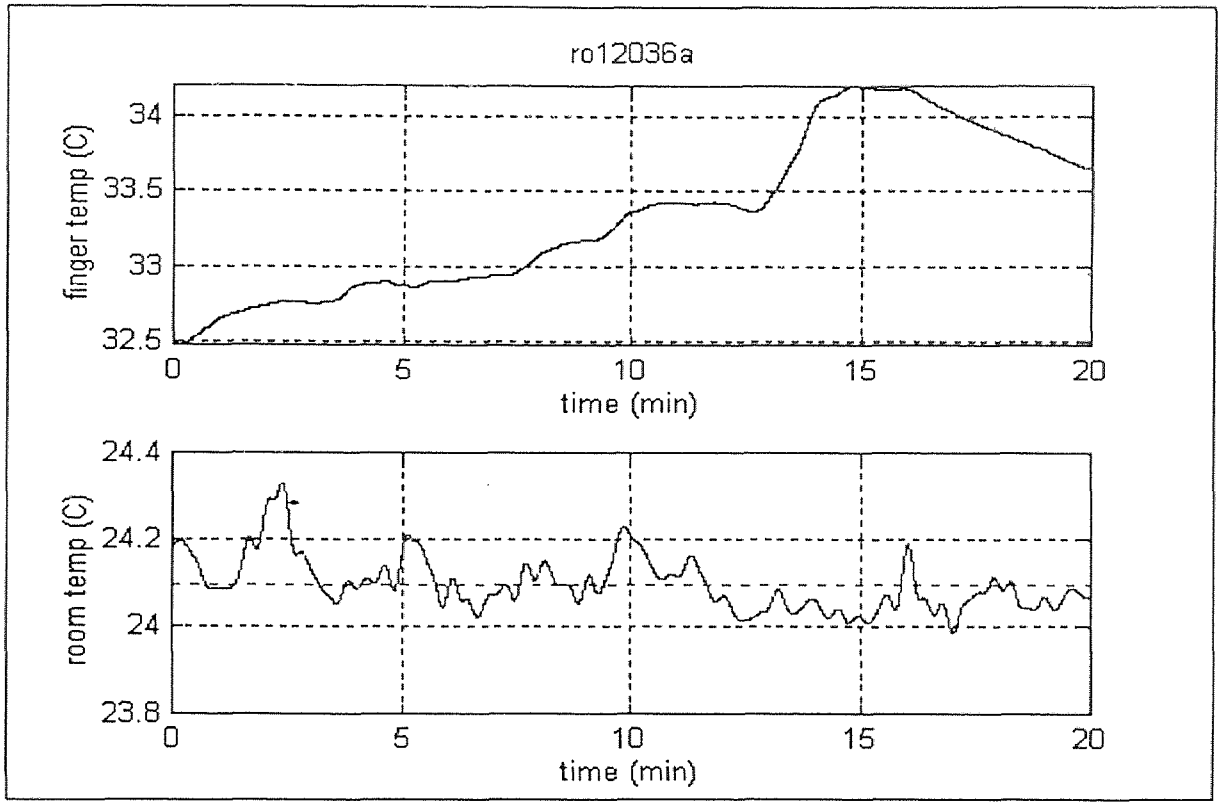

Figure 6.6 Blood Flow Experiment (3 mins-EO, 12 mins-Relaxation, 5 mins-Stress):
(a) Pulse Waveform, Finger Blood Volume
(b) Finger Temperature, Room Temperature

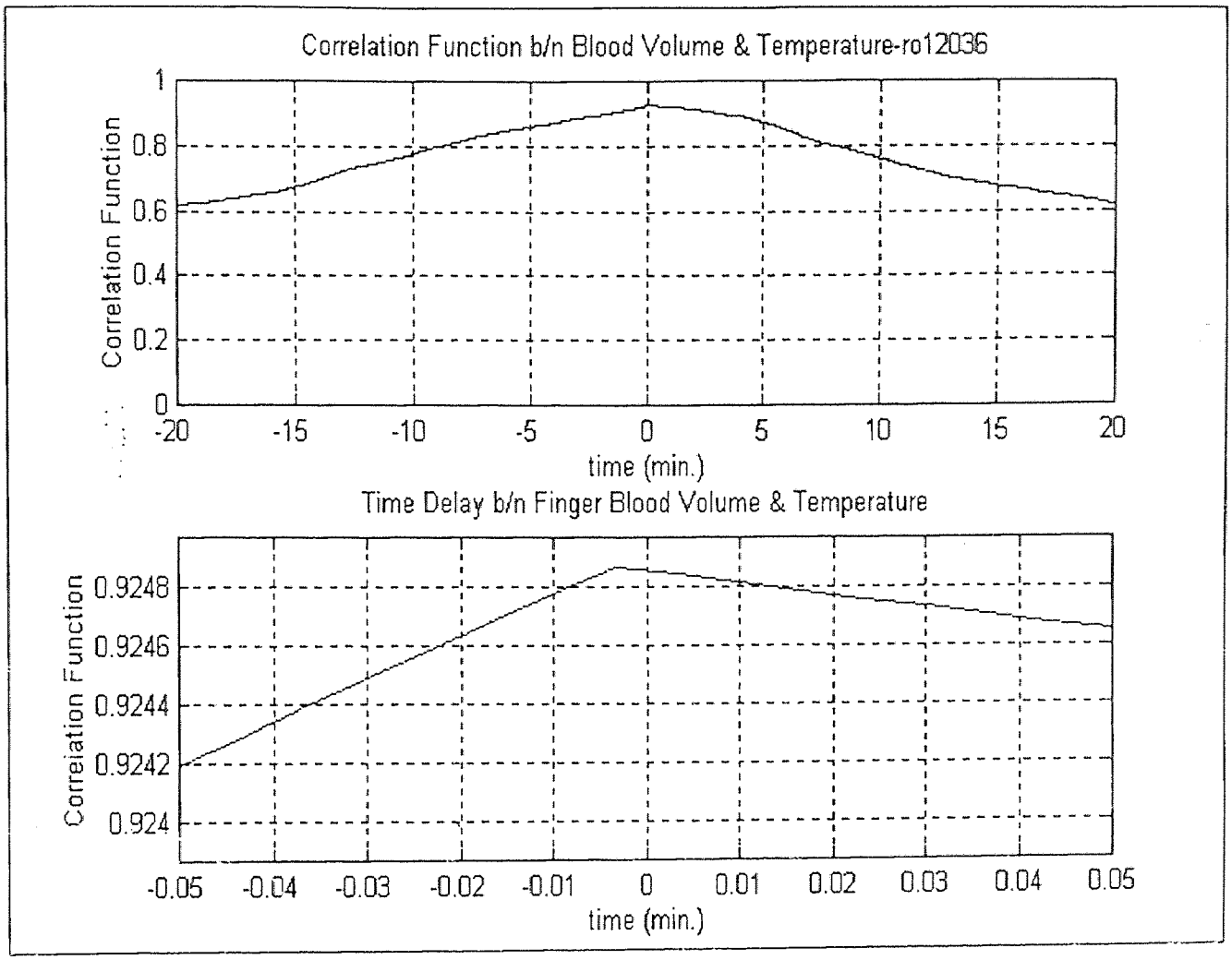

(c)

Figure 6.6 Blood Flow Experiment (3 mins-EO, 12 mins-Relaxation, 5 mins-Stress): Cross Correlation and Time Delay b/n Blood Volume & Finger Temperature

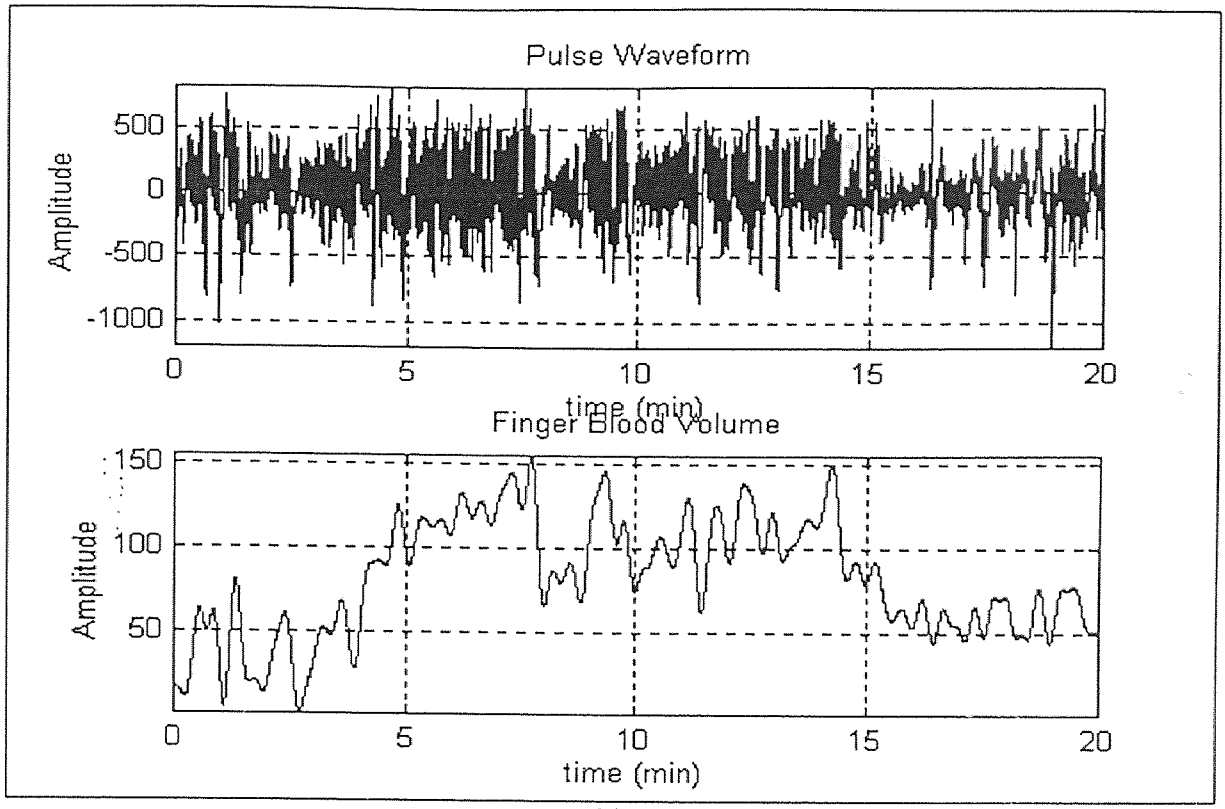

(a)

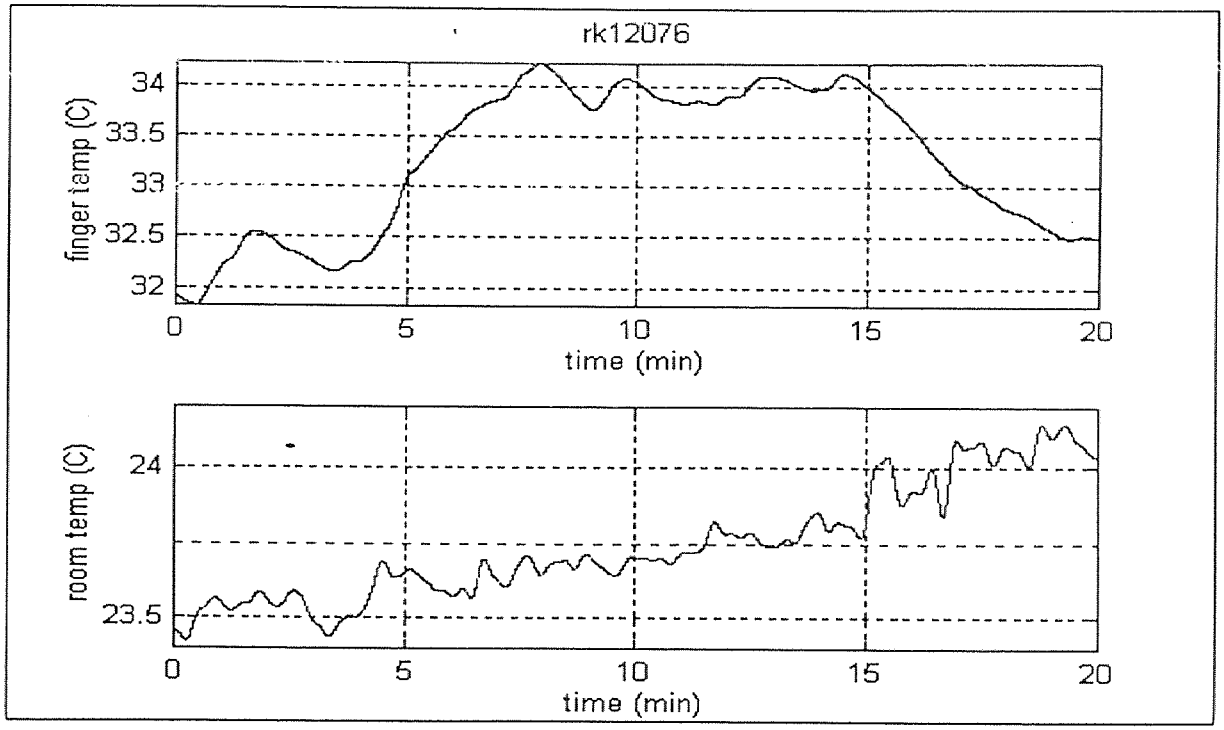

(b)

Figure 6.7 Blood Flow Experiment (3 mins-EO, 11 mins-Relaxation, 6 mins-Stress):
(a) Pulse Waveform, Finger Blood Volume
(b) Finger Temperature, Room Temperature

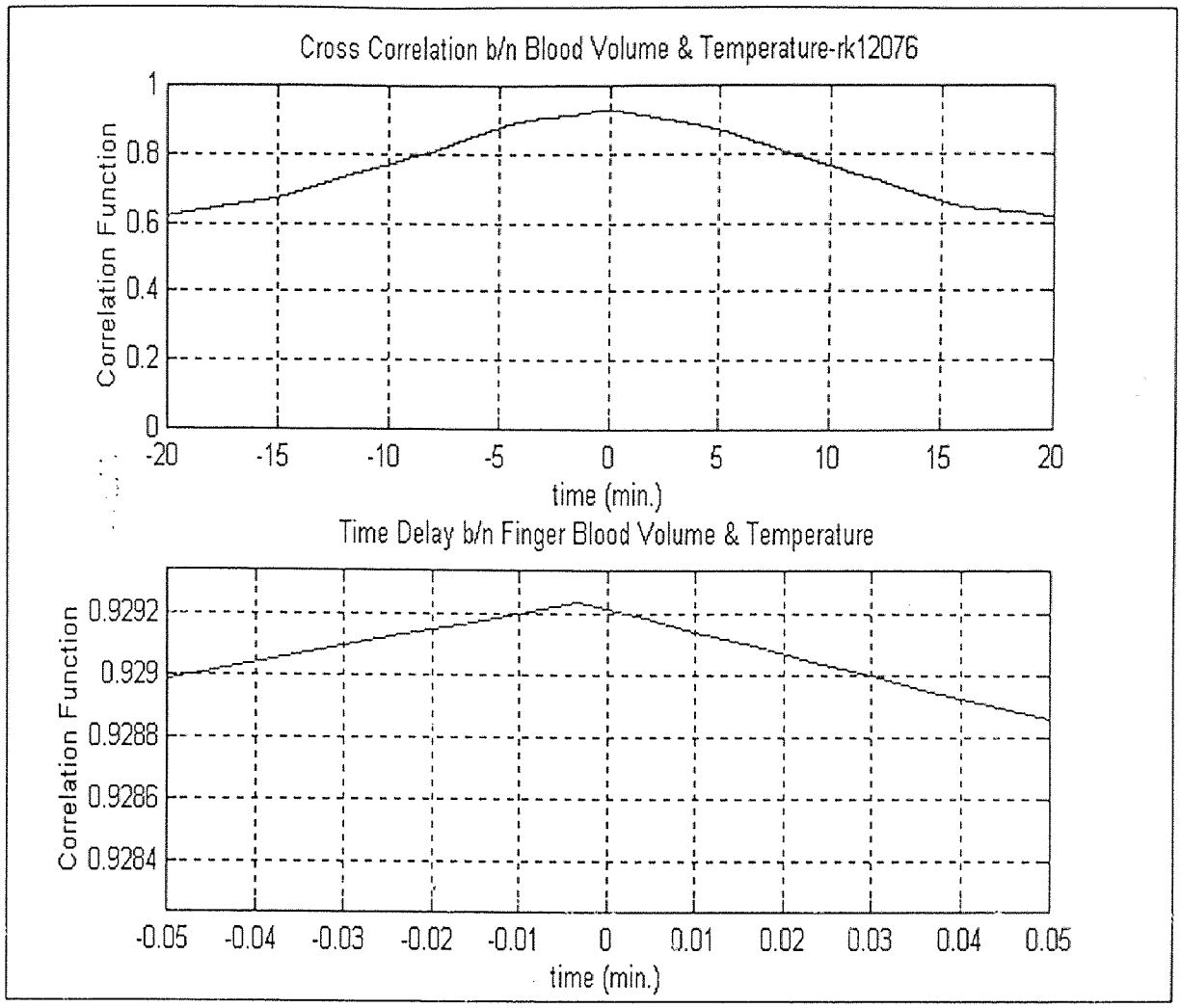

(c)

Figure 6.7 Blood Flow Experiment (3 mins-EO, 11 mins-Relaxation, 6 mins-Stress): Cross Correlation and Time Delay b/n Blood Volume & Finger Temperature

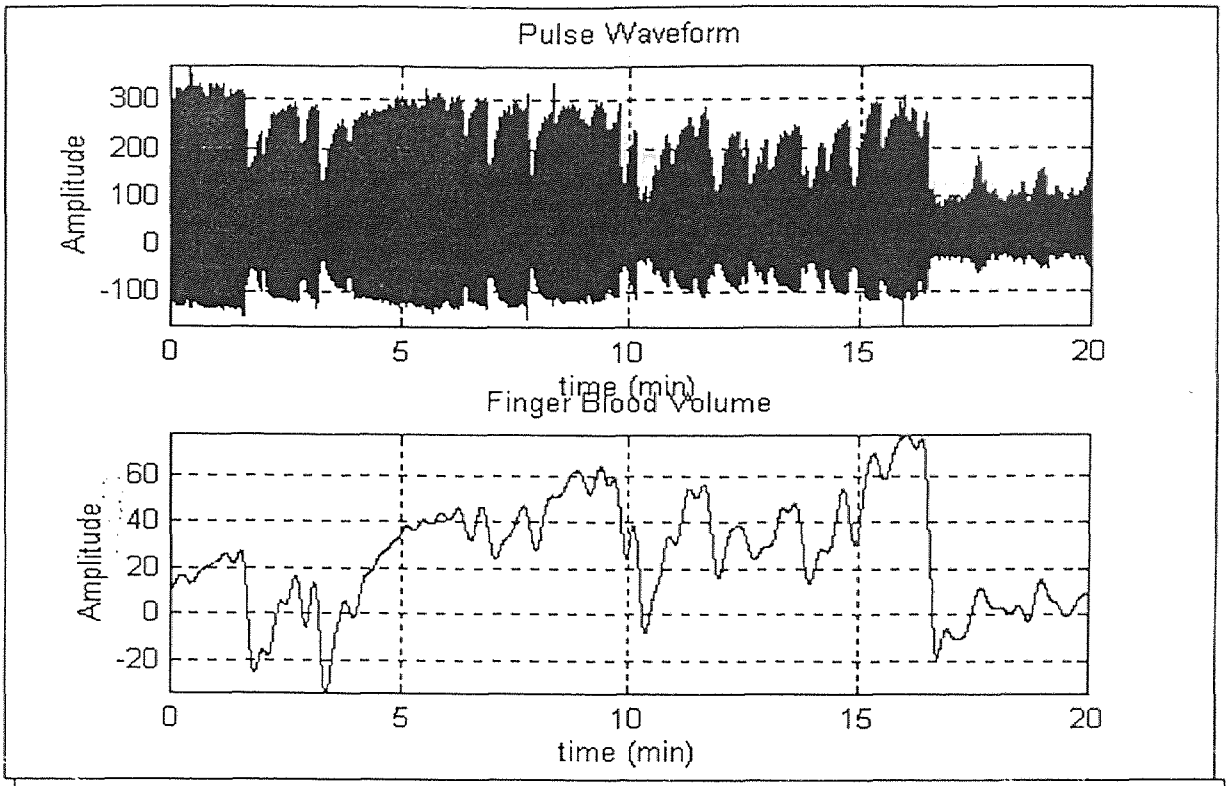

(a)

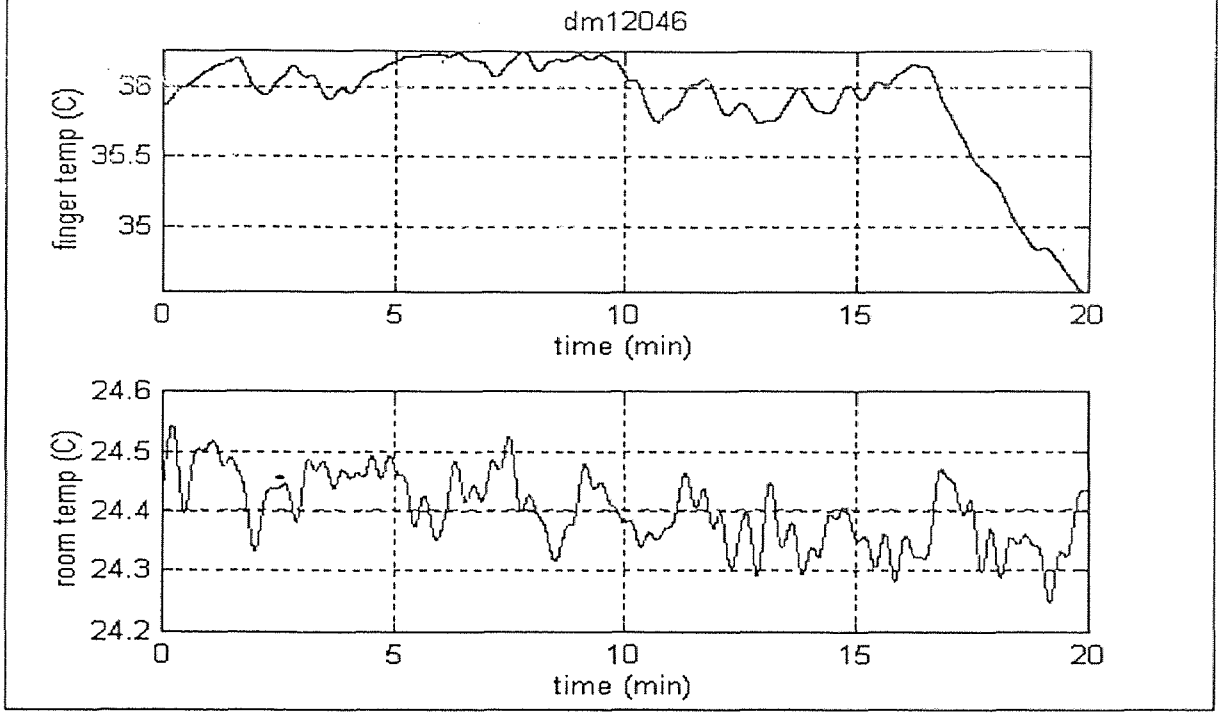

(b)

Figure 6.8 Blood Flow Experiment (3 mins-EO, 13.5 mins-Relaxation, 3.5 mins-Stress):
(a) Pulse Waveform, Finger Blood Volume
(b) Finger Temperature, Room Temperature

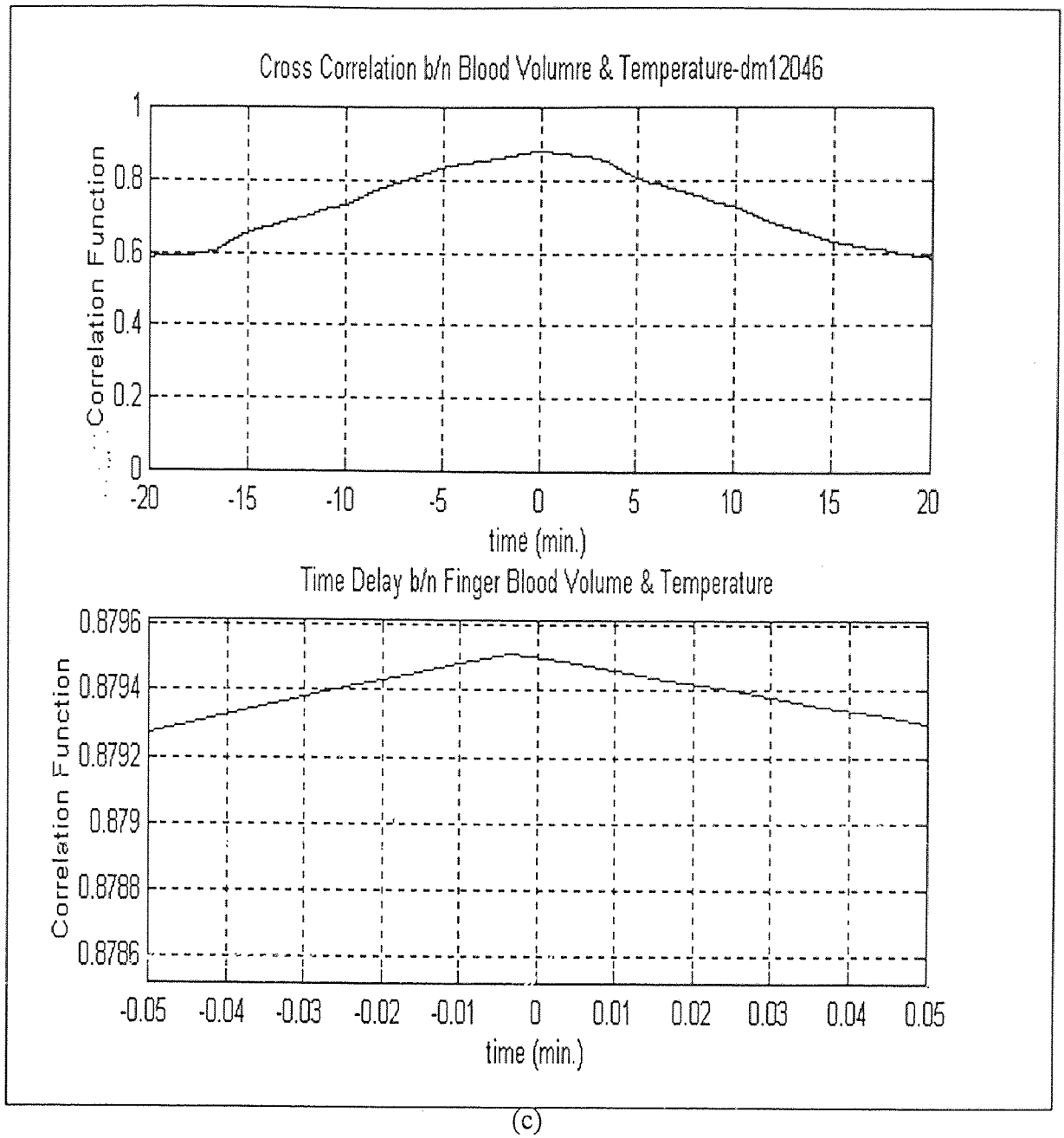

(c)

Figure 6.8 Blood Flow Experiment (3 mins-EO, 13.5 mins-Relaxation, 3.5 mins-Stress): Cross Correlation and Time Delay b/n Blood Volume & Finger Temperature

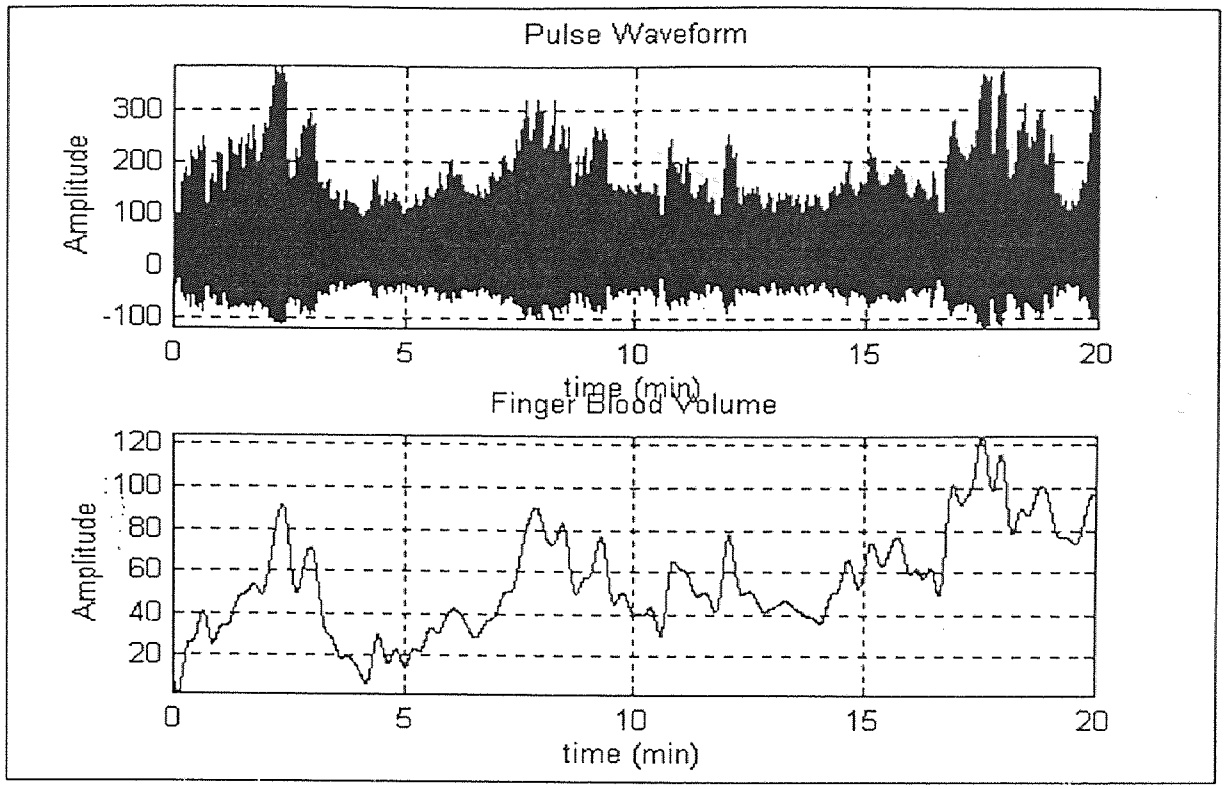

(a)

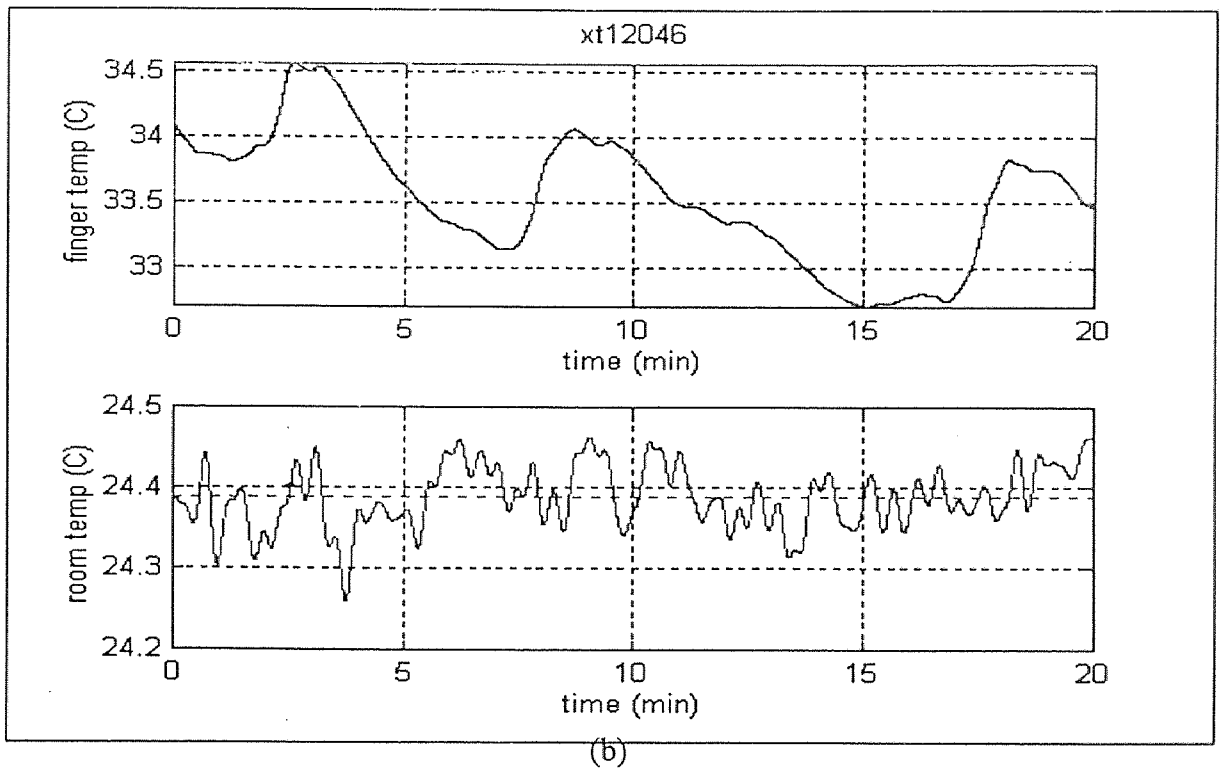

(b)

Figure 6.9 Blood Flow Experiment (3 mins-EO, 12 mins-Relaxation, 5 mins-Stress):
(a) Pulse Waveform, Finger Blood Volume
(b) Finger Temperature, Room Temperature

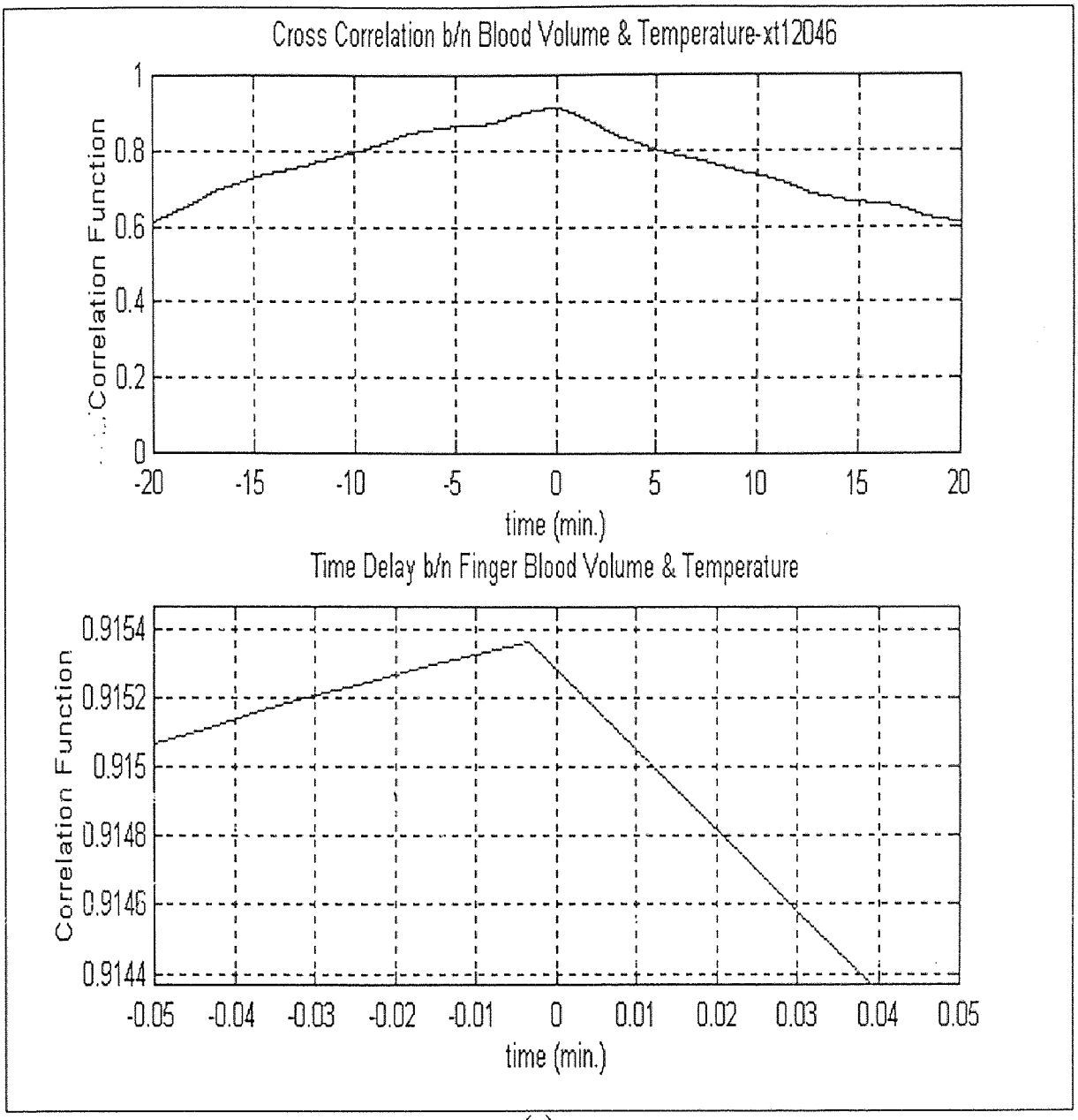

(c)

Figure 6.9 Blood-Flow Experiment (3 mins-EO, 12 mins-Relaxation, 5 mins-Stress): Cross Correlation and Time Delay b/n Blood Volume & Finger Temperature

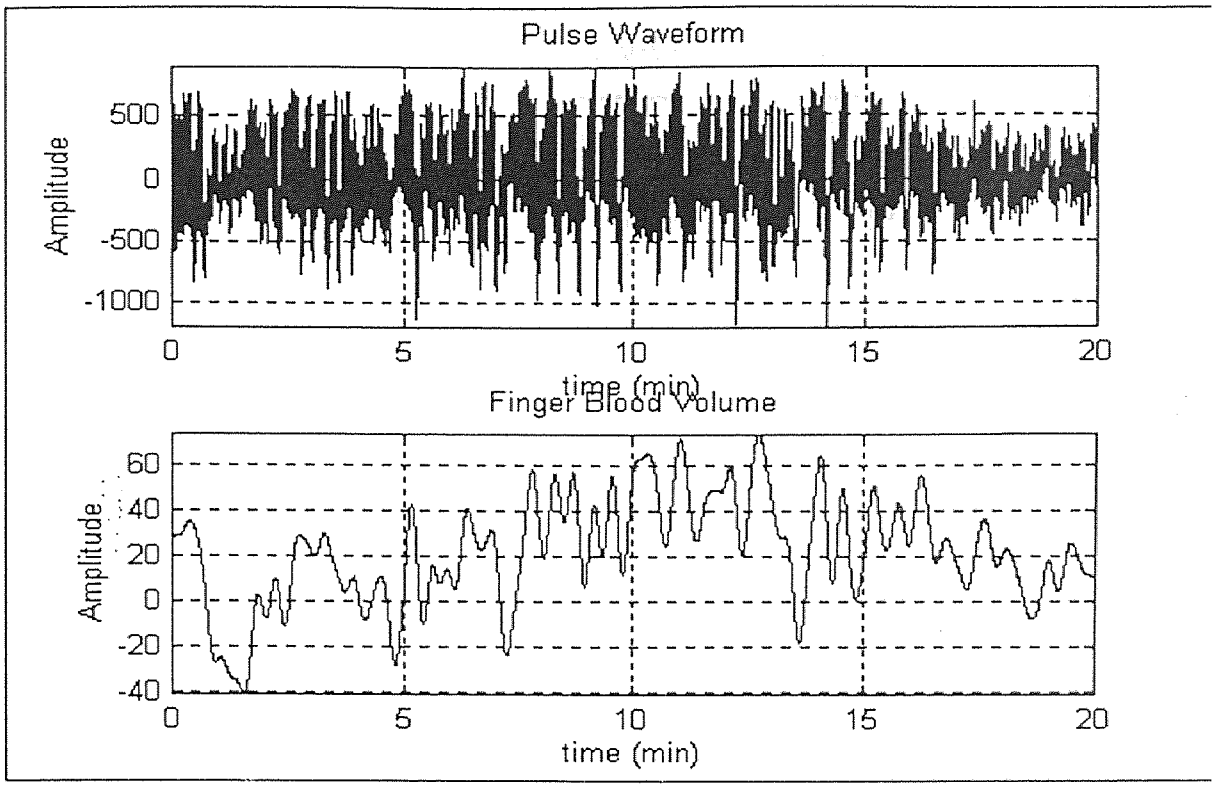

(a)

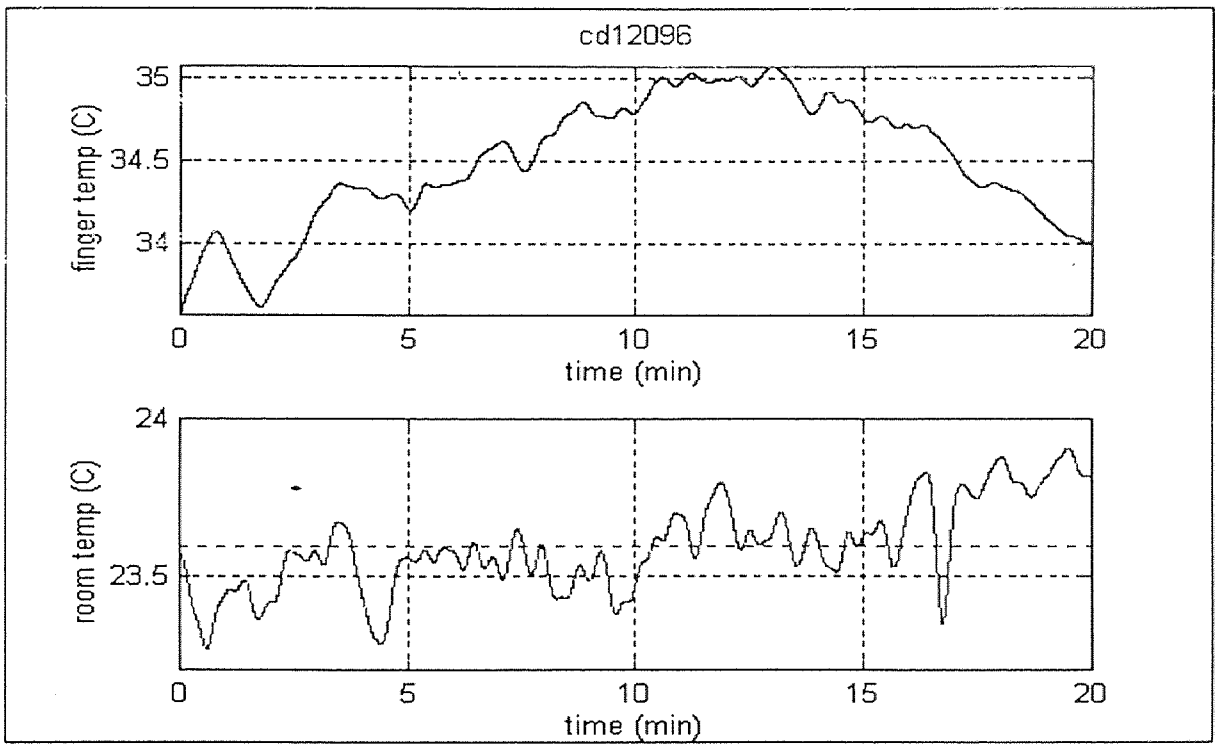

(b)

Figure 6.10 Blood Flow Experiment (3 mins-EO, 12 mins-Relaxation, 5 mins-Stress):
(a) Pulse Waveform, Finger Blood Volume
(b) Finger Temperature, Room Temperature

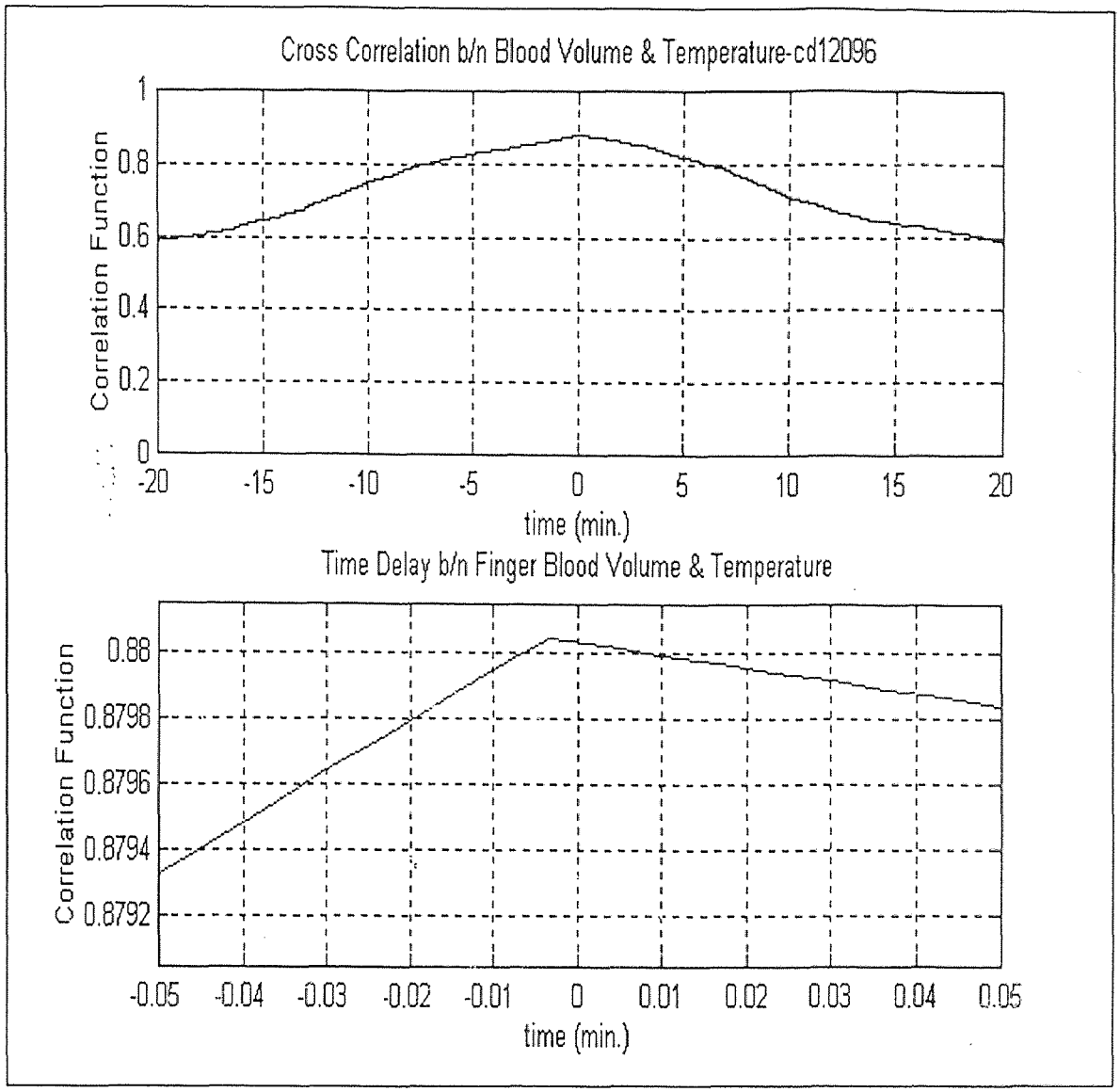

(c)

Figure 6.10 Blood Flow Experiment (3 mins-EO, 12 mins-Relaxation, 5 mins-Stress): Cross Correlation and Time Delay b/n Blood Volume & Finger Temperature

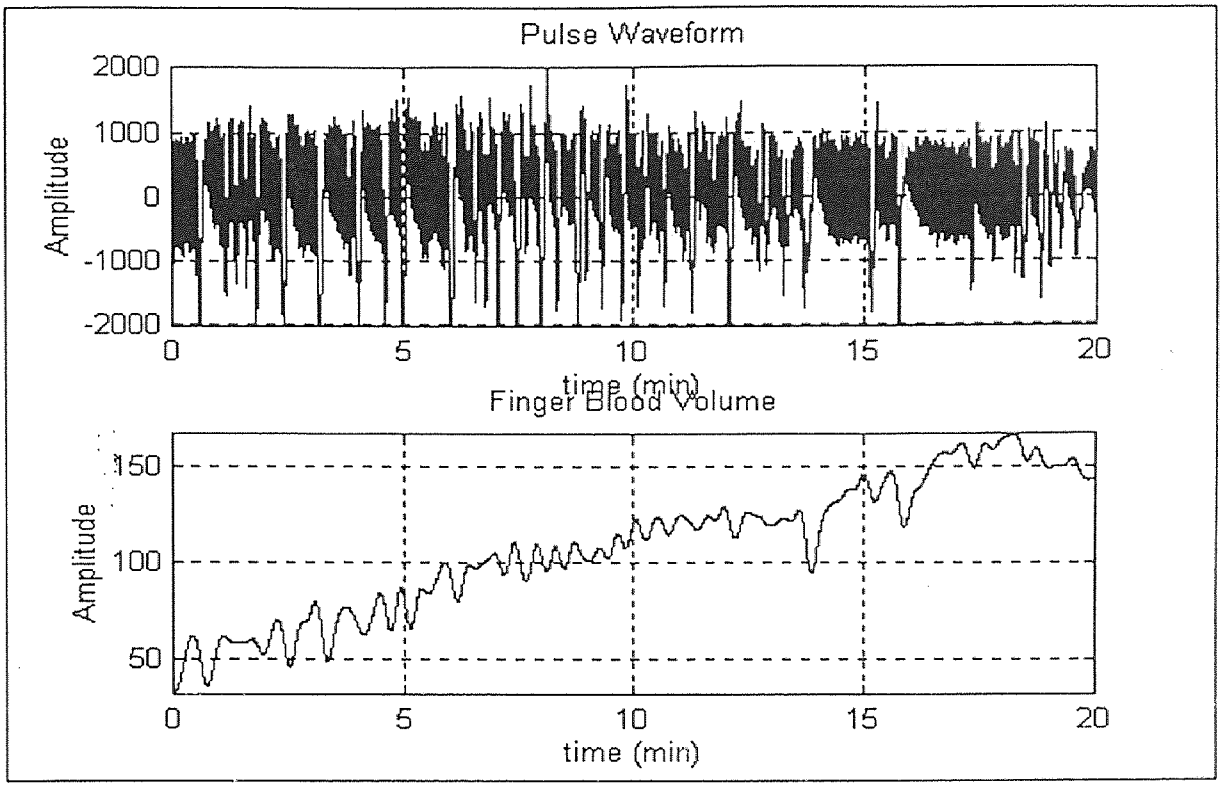

(a)

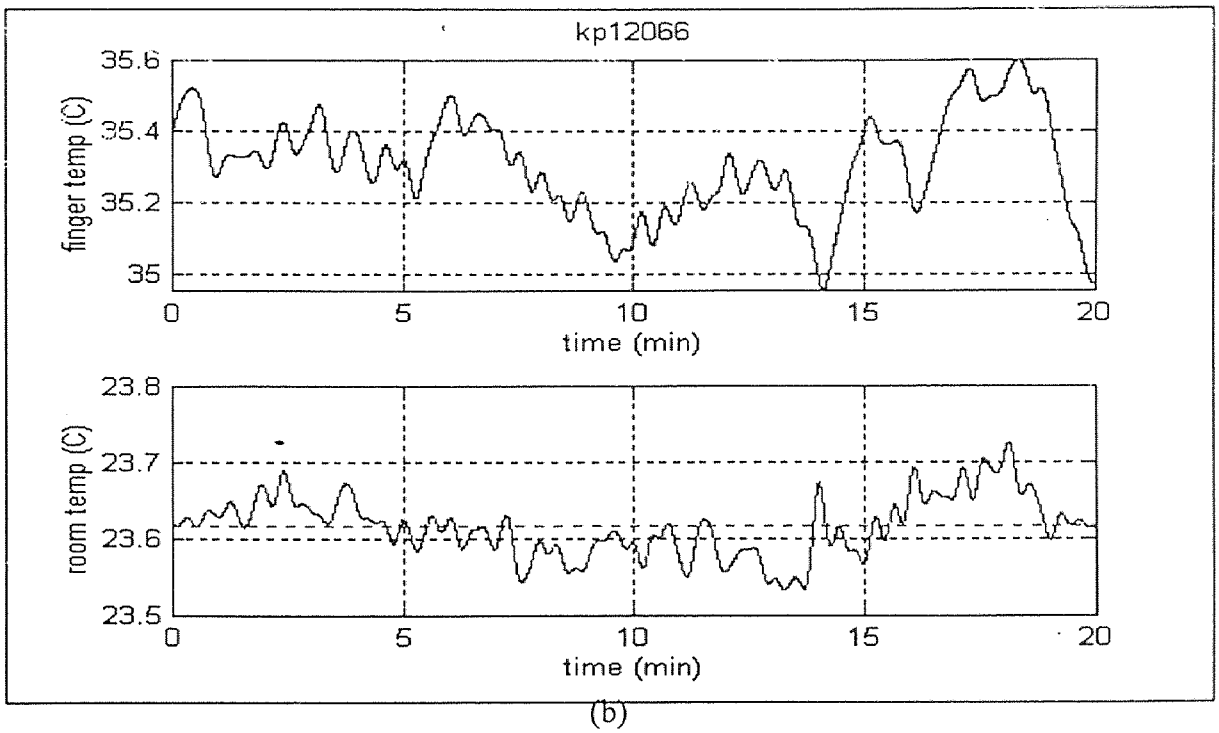

(b)

Figure 6.11 Blood Flow Experiment (3 mins-EO, 14 mins-Relaxation, 3 mins-Stress):
(a) Pulse Waveform, Finger Blood Volume
(b) Finger Temperature, Room Temperature

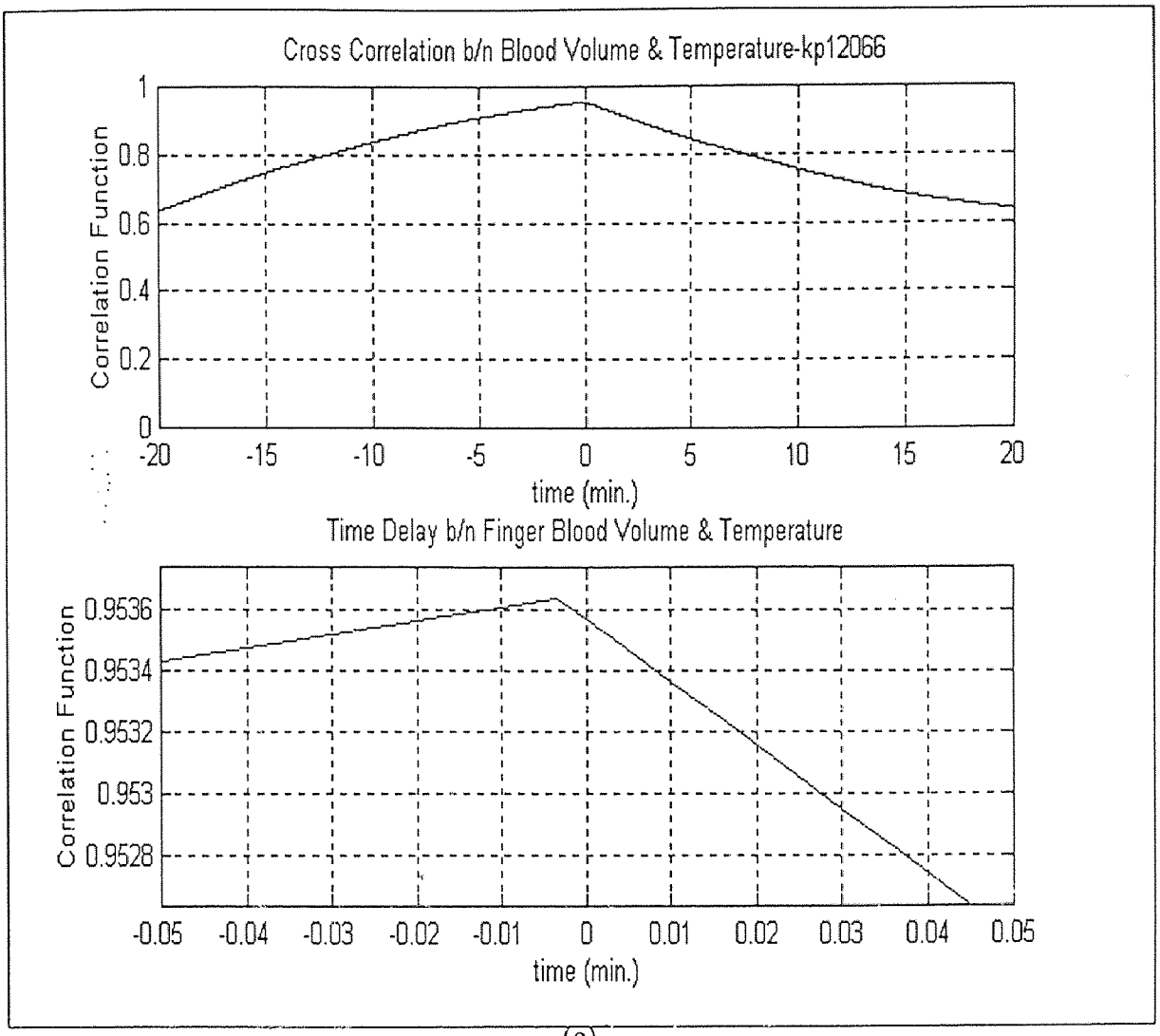

(c)

Figure 6.11 Blood Flow Experiment (3 mins-EO, 14 mins-Relaxation, 3 mins-Stress): Cross Correlation and Time Delay b/n Blood Volume & Finger Temperature

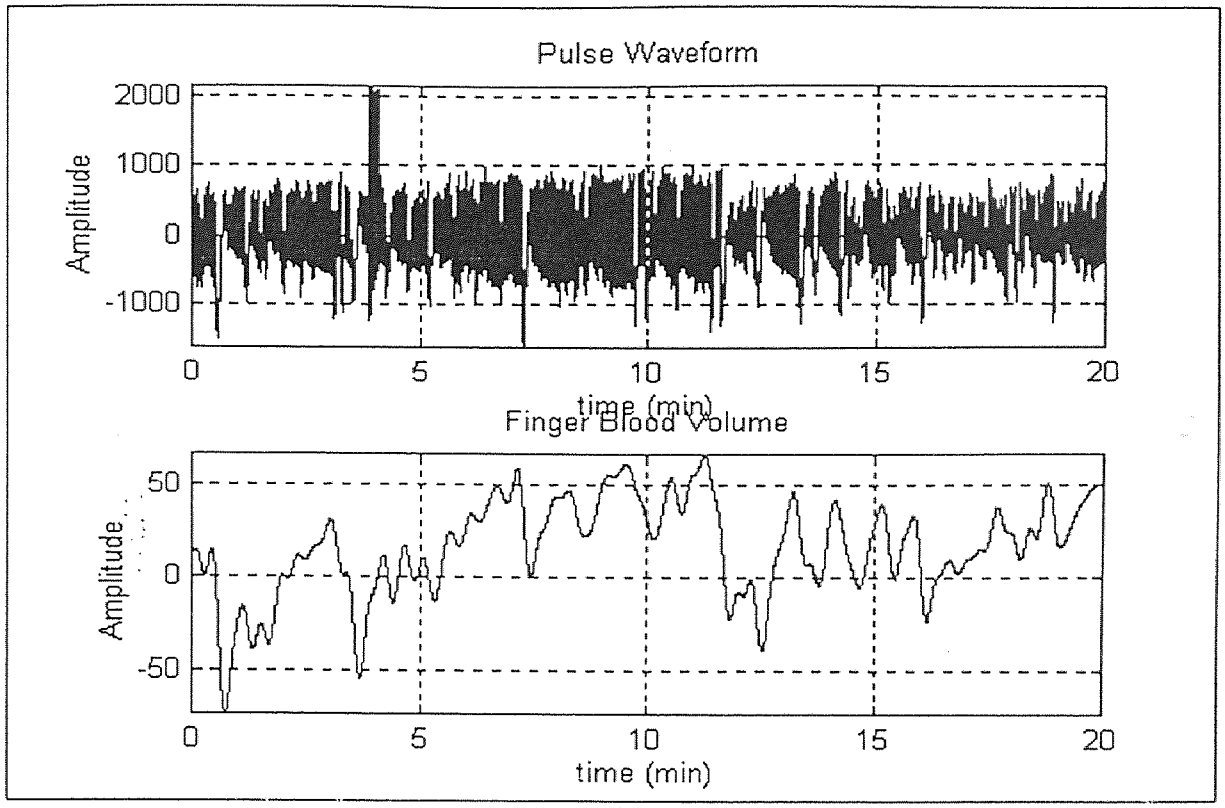

(a)

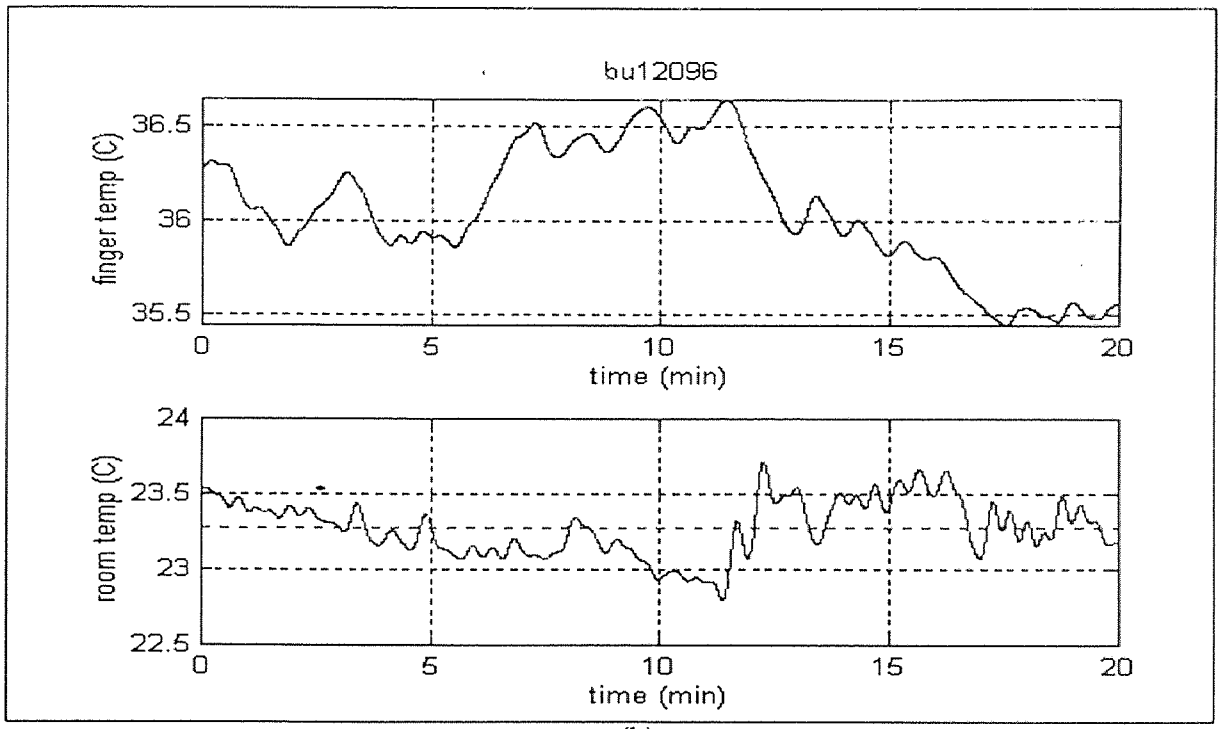

(b)

Figure 6.12 Blood Flow Experiment
(3 mins-EO, 8 mins-Relaxation, 6.5 mins-Stress, 2.5mins-EO):
(a) Pulse Waveform, Finger Blood Volume (b) Finger Temperature, Room Temperature

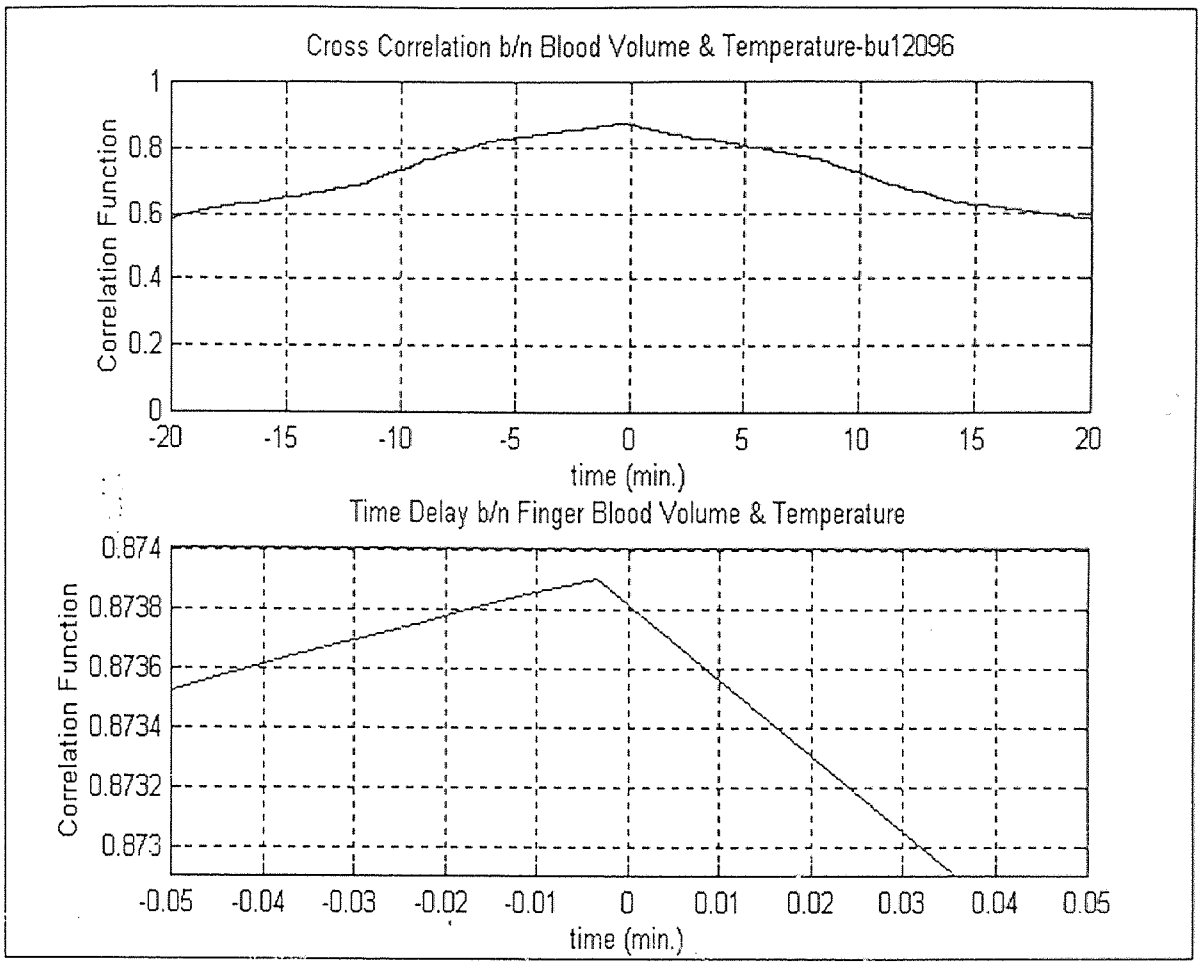

(c)

Figure 6.12 Blood Flow Experiment
(3 mins-EO, 8 mins-Relaxation, 6.5 mins-Stress, 2.5 mins-EO)
Cross Correlation and Time Delay b/n Blood Volume & Finger Temperature

CHAPTER 7

CONCLUSIONS

This project has attempted to measure noninvasively the responses of some physiological and psychological parameters to stress and relaxation (or meditation) such as the cutaneous blood volume, the cutaneous temperature and the EEG alpha coherence. The noninvasive measurement of stress and relaxation responses using physiological responses of . blood circulation and the nervous system can therefore, provide useful information about the state of health of an individual. For example, the cospar plots, and for that matter, the amount of alpha coherence provides valuable clues about the relative level reached in meditation. The reaction to stress and relaxation (meditation), involves a complex interplay between the mind, the body and the external environmentOne of the major conclusions of this project is the importance of conscious mind in inducing a stress or relaxation response. The act of meditation itself is a conscious control of the relaxation response, as the meditator initiaties a set of responses that cause the person to relax completely.

7.1 Meditation Study

It is been observed from the EEG data that during group meditation the EEG alpha wave band widens in both directions to the theta (sometimes extends to the delta) and the beta wave bands. It is also observed that the amplitude of the cospar plots increased, and therefore caused the changing of the threshold from 0.95 to 0.98. The area under the curve of the EEG alpha coherence above the threshold is higher for subject II during

group meditation than during eyes closed and single meditaton. The EEG alpha coherence for subject II during group meditation may imply that although the two subjects were in two separate rooms, and for that reason there was no physical and direct contact or verbal communication between the two subjects, there was some form of coupling between them. It could be hypothesized that the changes in the alpha and the delta coherence during group meditation for the two subjects (except for the case of subject I in experiment I in the group meditation study II), could have been propagated not on direct level of interaction, but may be via a "field". This supports the observations of Orme-Johnson that there is an increase in alpha coherence in group meditation. In general the existence of high alpha coherence is not unique to the meditators. However, the patterns of increased alpha coherence and its spread to other frequencies seems to be a characteristic of the group meditation. The zero value of the area of the EEG alpha coherence of subject I during group meditation in experiment I (table 6.3) might be that the subject's coherence was strongly "influenced" by subject II and that might have reduced subject I's EEG alpha coherence below the 0.98 threshold. Even if the changes in the EEG alpha coherence of the two subjects during group meditation were due to some field effects, we still have numerous unanswered questions (a few of them will be discussed later on).

7.2 Skin Blood Flow Study

It is observed in this study that the temperature of the skin closely follows the change of the skin blood volume but at a slower rate. Thus, the temperature reaponse to the changes

in the blood volume is delayed by some time constant. When the skin blood volume increases, the skin temperature increases as well but with a delayed time constant (at a slower rate), and again when the skin blood volume decreases, the skin temperature decreases with a delayed time constant (at a slower rate). The cross correlation plots show an average peak correlation at zero lag between these physiological parameters to be 0.9236 ± 0.0408. This means that the skin blood volume and the skin blood temperature are closely related.

The measurement of skin blood volume and skin temperature has shown that these physiological parameters decrease when a person is experiencing stress and they increase when a person is in a restful and relaxed state.

Another significant observation made in this research is that when the finger blood volume (finger temperature) increased or decreased there was a corresponding increase or decrease in the amplitude of the finger arterial pulse which is an indication of vasodilation or vasoconstriction of the finger arterioles respectively.

7.3 Future Research

It has been shown in this study that the presence of another person during a group meditation of two people caused some changes in their EEG alpha wave coherence. However, one can argue that increase in EEG coherence of the alpha band does not necessarily mean that the two different brains in the two different rooms were directly interacting. This result could be modeled as two independent generators outputting waves of somewhat similar spectral compositions. In this interpretation, increase in EEG

coherence between different brains may merely reflect the fact that everyone has more or less similar EEG, for example a strong, somewhat stationary 8 - 12 Hz alpha wave, with theta and beta frequency harmonics.

On the other hand, the observed increase in EEG alpha wave coherence could suggest a common influence operating on the two oscillators. Increased coherence indicates increased phase stability, that is, the brain waves of the two subjects had become more similar in frequency. Maybe the two oscillators were affected by a common influence, possibly due to a rise in the order in collective consciousness produced by a collective meditation. Does this mean that increasing the number of people in the group would increase the EEG alpha wave coherence ? And would the increment be linearly or nonlinearly dependent on the number of people in the group ? Future research could be focused on these issues plus finding out about how the distance between the groups as well as the orientation of the subjects affects the EEG alpha coherence. It is strongly suggested to use experienced meditators so that significant results could be obtained. Whatever the nature of the field may be, it is possible that its intensity may strongly depend on the extent of the experience of the subjects. It is also recommended to conduct this study in a sound–, electrical–, and electromagnetic–attenuated room.

Future blood flow studies could include estimation of the delayed time constant of the temperature to provide a transfer function for analytical investigations.

The physiological response of the finger arterioles to different psychological states by either vasodilating or vasoconstricting suggest either local humoral control or central autonomic control of the finger blood flow and temperature (see sections 2.3.2

and 2.3.4). Since the action of humoral and autonomic controls are dependent on each other, it is unclear which of these controls is responsible for the regulation of finger blood flow and temperature. However, results obtained from the group meditation studies show significant correlation between alpha EEG coherence and finger temperature during meditation. This suggests autonomic nervous regulation of finger temperature. Future research could be directed to investigate which of the autonomic nervous system (sympathetic or parasympathetic nervous system) is responsible for changes in these physiological processes. Further skin blood flow studies could also be directed to include whether meditation or relaxation could be used for the treatment of Raynaud's or Chronic Venous Insufficiency deseases.

APPENDIX A

COMPUTER PROGRAMS

```
function cosparea(x,y)
% COSPAREA(x,y,Fs) - Is a modification of Cospar. This routine
% calculates coherence for two signals and creates a cospar matrix
% using the methods of Levine (1976). The matrix is displayed
% in a mesh and contour plot with COHMESH. It calls the function
% COHAREA which computes the area above the threshhold for the
% alpha wave band

x=x(:);
y=y(:); %column vectors
n=max(size(x));
Fs=200;

% parameters for SPECTRUM
% 256 point windows shifted by 19 points
m=256;
noverlap=237;
threshhold=0.98;  % Coherence threshhold

 %filter data to remove low frequency components
[b,a]=ellip(7,0.05,50,1.5/(Fs/2),'high');
x=filtfilt(b,a,x);
y=filtfilt(b,a,y);

 %filter 60 Hz interference from the signal
[b,a]=butter(9,45/(Fs/2));
 x=filtfilt(b,a,x);
y=filtfilt(b,a,y);

% calculate coherence for 5 second intervals and compile in a matrix
k=fix(n/(5*Fs));
index=1:(5*Fs);
Coh=zeros(m/2,k);

for i=1:k
  P=spectr2(x(index),y(index),m,noverlap);
  Coh(:,i)=P(:,5);

index=index+(5*Fs);
  %disp(i)
end
```

```
Cohe=Coh(1:m/2,1:k);

% leave only coherence peaks above threshhold
for j=1:m/2;
for l=1:k;

   if Coh(j,l)<threshhold
     Coh(j,l)=threshhold;
   end
 end
end

% Calculate the area above the threshhold for the alpha wave band
coharea(Coh,Fs,threshhold)

 % plot the results
cohmesh(Coh,Fs);
Title=input('enter graph title: ','s');
subplot(211),title(Title);

function P = spectr2(x,y,m,noverlap)
%SPECTR2 Slightly modified SPECTRUM for use with COSPAR
%
%SPECTRUM Power spectrum estimate of one or two data sequences.
%       P = SPECTRUM(X,Y,M) performs FFT analysis of the two sequences
%       X and Y using the Welch method of power spectrum estimation.
%       The X and Y sequences of N points are divided into K sections of
%       M points each (M must be a power of two). Using an M-point FFT,
%       successive sections = are Hanning windowed, FFT'd and accumulated.
%       SPECTRUM returns the M/2 by 8 array
%         P = [Pxx Pyy Pxy Txy Cxy Pxxc Pyyc Pxyc]
%       where
%         Pxx  = X-vector power spectral density
%         Pyy  = Y-vector power spectral density
%         Pxy  = Cross spectral density
%         Txy  = Complex transfer function from X to Y
%              (Use ABS and ANGLE for magnitude and phase)
%         Cxy  = Coherence function between X and Y
%         Pxxc,Pyyc,Pxyc = Confidence range (95 percent).
%
%       See SPECPLOT to plot these results.
%       P = SPECTRUM(X,Y,M,NOVERLAP) specifies that the M-point sections
%       should overlap NOVERLAP points.
%       Pxx = SPECTRUM(X,M) and SPECTRUM(X,M,NOVERLAP) return the single
%       sequence power spectrum and confidence range.
```

```
%
%       See also ETFE, SPA, and ARX in the Identification Toolbox.

%       J.N. Little 7-9-86
%       Revised 4-25-88 CRD, 12-20-88 LS, 8-31-89 JNL, 8-11-92 LS
%       Copyright (c) 1986-92 by the MathWorks, Inc.

%       The units on the power spectra Pxx and Pyy are such that, using
%       Parseval's theorem:
%
%           SUM(Pxx)/LENGTH(Pxx) = SUM(X.^2)/LENGTH(X) COV(X)
%
%       The RMS value of the signal is the square root of this.
%       If the input signal is in Volts as a function of time, then
%       the units on Pxx are Volts^2*seconds = Volt^2/Hz.
%       To normalize Pxx so that a unit sine wave corresponds to
%       one unit of Pxx, use Pn = 2*SQRT(Pxx/LENGTH(Pxx))
%
%       Here are the covariance, RMS, and spectral amplitude values of
%       some common functions:
%       Function  Cov=SUM(Pxx)/LENGTH(Pxx)  RMS      Pxx
%       a*sin(w*t)      a^2/2          a/sqrt(2)  a^2*LENGTH(Pxx)/4
%Normal: a*rand(t)      a^2            a          a^2
%Uniform: a*rand(t)     a^2/12         a/sqrt(12) a^2/12
%
%       For example, a pure sine wave with amplitude A has an RMS value
%       of A/sqrt(2), so A = SQRT(*SUM(Pxx)/LENGTH(Pxx)).
%
%       See Page 556, A.V. Oppenheim and R.W. Schafer, Digital Signal
%       Processing, Prentice-Hall, 1975.

if (nargin == 2), m = y; noverlap = 0; end
if (nargin == 3)
        if (max(size(y)) == 1)
                noverlap = m;
                m = y;
                nargin = 2;
        else
                noverlap = 0;
        end
end

x = x(:);               % Make sure x and y are column vectors
y = y(:);
n = max(size(x));       % Number of data points
```

```
k = fix((n-noverlap)/(m-noverlap));   % Number of windows
                                      % (k = fix(n/m) for noverlap=0)
index = 1:m;
w = kaiser(m,9);        % Window specification; change this if you want:
                        % (Try HAMMING, BLACKMAN, BARTLETT, or your own)
                        %
                        % Kaiser was chosen here based on Harris (1978)
                        % for discriminating closely spaced frequency
                        % components.  -CK
                        %
KMU = k*norm(w)^2;              % Normalizing scale factor

if (nargin == 2)        % Single sequence case.
        Pxx = zeros(m,1); Pxx2 = zeros(m,1);
        for i=1:k
                xw = w.*detrend(x(index));
                index = index + (m - noverlap);
                Xx = abs(fft(xw)).^2;
                Pxx = Pxx + Xx;
                Pxx2 = Pxx2 + abs(Xx).^2;
        end
        % Select first half
        select = [1:m/2];
        Pxx = Pxx(select);
        Pxx2 = Pxx2(select);
        cPxx = zeros(m/2,1);
        if k > 1
                c = (k.*Pxx2-abs(Pxx).^2)./(k-1);
                c = max(c,zeros(m/2,1));
                cPxx = sqrt(c);
        end
        pp = 0.95; % 95 percent confidence.
        f = sqrt(2)*erfinv(pp);  % Equal-tails.
        P = [Pxx f.*cPxx]/KMU;
        return
end

Pxx = zeros(m,1); % Dual sequence case.
Pyy = Pxx; Pxy = Pxx; Pxx2 = Pxx; Pyy2 = Pxx; Pxy2 = Pxx;

for i=1:k
        xw = w.*detrend(x(index));
        yw = w.*detrend(y(index));
        index = index + (m - noverlap);
        Xx = fft(xw);
```

```
        Yy = fft(yw);
        Yy2 = abs(Yy).^2;
        Xx2 = abs(Xx).^2;
        Xy  = Yy .* conj(Xx);
        Pxx = Pxx + Xx2;
        Pyy = Pyy + Yy2;
        Pxy = Pxy + Xy;
        Pxx2 = Pxx2 + abs(Xx2).^2;
        Pyy2 = Pyy2 + abs(Yy2).^2;
        Pxy2 = Pxy2 + Xy .* conj(Xy);
end

% Select first half
select = [1:m/2];

Pxx = Pxx(select);
Pyy = Pyy(select);
Pxy = Pxy(select);
Pxx2 = Pxx2(select);
Pyy2 = Pyy2(select);
Pxy2 = Pxy2(select);

cPxx = zeros(m/2,1);
cPyy = cPxx;
cPxy = cPxx;
if k > 1
  c = max((k.*Pxx2-abs(Pxx).^2)./(k-1),zeros(m/2,1));
  cPxx = sqrt(c);
  c = max((k.*Pyy2-abs(Pyy).^2)./(k-1),zeros(m/2,1));
  cPyy = sqrt(c);
  c = max((k.*Pxy2-abs2 (Pxy).^2)./(k-1),zeros(m/2,1));
  cPxy = sqrt(c);
end

Txy = Pxy./Pxx;
Cxy = (abs(Pxy).^2)./(Pxx.*Pyy);

pp = 0.95; % 95 percent confidence.
f = sqrt(2)*erfinv(pp);  % Equal-tails.

P = [ [Pxx Pyy Pxy]./KMU ...
    Txy Cxy ...
    f.*[cPxx cPyy cPxy]./KMU ];
```

```
function cohmesh(C,Fs)
%  COHMESH Graph results of COSPAR.
%  COHMESH(C,Fs) generates a mesh plot and a contour plot of the
%  coherence spectral array calculated by COSPAR.

[m,n]=size(C);
t=((5*n)*(0:n-1)/n)/60;
f=(0:m-1)/m*Fs/2;
Co=C(1:m/2,:);

% mesh plot
subplot(211),mesh(f(1:m/2),t,Co');

view([15,55]);
ylabel('time (min)');
xlabel('frequency (Hz)');
zlabel('coherence');
colormap('gray');
brighten(-1);

%contour plot
subplot(212),contour(f(1:m/2),t,Co',5);
ylabel('time (min)');
xlabel('frequency (Hz)');

grid
end

% COHAREA calculates the area above the threshold in the
% EEG alpha band, and the maximum area

function coharea(C,Fs,threshhold)

[m,n]=size(C);
alpha=zeros(m/2,n);
malpha = zeros(m/2,1);
t=((5*n)*(0:n-1)/n)/60;

%%%%%%%%%%% Find the area above the threshhold for the alpha band
%%%%%%%%%

for r=1:m/2

   for s=1:5:n
```

```
f=r/m*Fs/2 ;
 Coh1=C(r,s);

     if Coh1 <= threshhold
       Coh1 = 0 ;
     else Coh1 = Coh1 - threshhold ;
    end

 if f >= 8 & f <= 12

    alpha = alpha + Coh1 ;
    malpha = malpha + 0.02 ;
   end
  end
end

alpha = mean(alpha(:))
malpha = mean(malpha)

function thm(therma,thermb,DVT)
therma=decimate(therma,DVT);
thermb=decimate(thermb,DVT);
% THM(therma,thermb)
% Thm is a calibration program that coverts das-1601 thermistor
% data into temperature in degrees Celcius. The contants used
% were calculated from logarithmic linearization
% obtained calibration data.
% Other thermistors and other acquisition computers may offer
% different calibrations.

Fs=100;

pPa=[-0.0356 0.5300];
%pPb=[-20.7 1217.6];

[b,a]=butter(9,2/(Fs/2));
therma=filtfilt(b,a,therma);
thermb=filtfilt(b,a,thermb);

time=DVT*(0:max(size(therma))-1)/(60*Fs);
T=DVT*(max(size(therma)))
Therma=0.0005114*therma;
Thermb=0.0005114*thermb;

clear therma thermb
```

```
thermA=(log(Therma)-pPa(2))/pPa(1);
thermB=(log(Thermb)-pPa(2))/pPa(1);
meanroomtemp=mean(thermA);
mrt=meanroomtemp*ones(size(thermA));

clear Therma Thermb


subplot(211)
plot(time,thermB,'b')
xlabel('time (min)');
ylabel('finger temp (C)');
Title=input('Enter graph title: ','s');
title(Title);
grid

clear thermB

subplot(212)
plot(time,thermA)
hold on;
plot(time,mrt,'m:')
hold off;

clear time T mrt thermA
xlabel('time (min)');
ylabel('room temp (C)');
grid


function stitch(A,B,DA,DVT)

%function data=stitch(A,B)
%
% data=STITCH(a,b) connects two matricies together sequentially,
% a then b. The output data is the rowa + rowb by col matrix
% containing a and b. The columns of a and b must be the same.
% The function also decimates the connected data by the
% coefficients:DA and DVT for arterial pulse and blood
% volume (temperature) respectively.

[r1,c]=size(A);
[r2,c]=size(B);
data=zeros([r1+r2,c]);
```

```
data(1:r1,:)=A;
data(r1+1:r1+r2,:)=B;

clear A B r1 r2 c
dataA=decimate(data(:,1),DA) ;
dataV=decimate(data(:,2),DVT) ;
dataT=decimate(data(:,4),DVT) ;
dataRT=decimate(data(:,3),DVT) ;
clear data
avt(dataA,dataV,dataRT,dataT,DA,DVT)
clear dataA
figure(2)
stavt(dataV,dataT,dataRT,DVT)
figure(3)
cor(dataV,dataT,DVT)
thm(dataRT,dataT,DVT)


function avt(art,ven,therma,thermb,DA,DVT)

Fs=100;
Ven=filtfilt(b,a,ven);

time=DVT*(0:max(size(Ven))-1)/(60*Fs);
timeA=DA*(0:max(size(Art))-1)/(60*Fs);
Time=DVT*max(size(Ven))/(Fs*60);
TimeA=DA*max(size(Art))/(Fs*60);

MinA=min(Art);
MaxA=max(Art);
%MaxA=1000;
%MinA=-100

subplot(211)
plot(timeA,Art,'b')
axis([0 TimeA MinA MaxA])
xlabel('time (min)');
ylabel('Amplitude')
%Title1=input('Enter graph title for Pulse : ','s');
title('Pulse Waveform');
grid

clear ART Fs pPa Thermb a b Art art MaxA MinA

MinV=min(Ven);
```

```
MaxV=max(Ven);
subplot(212)
plot(time,Ven,'b')
axis([0 Time MinV MaxV])
xlabel('time (min)');
ylabel('Amplitude');
%Title2=input('Enter graph title for Blood Vol. : ','s');
title('Finger Blood Volume');
grid

clear VEN ven Ven MinV MaxV

MinT=min(thermB);
MaxT=max(thermB);

figure(2)

subplot(211)
plot(time,thermB,'b')
axis([0 Time MinT MaxT])
ylabel('finger temp (C)');
xlabel('time (min)');
Title=input('Enter graph title for Finger Temp. : ','s');
title(Title);
grid

clear thermB thermb Thermb MaxT MinT

MinR=min(thermA) ;
MaxR=max(thermA) ;

subplot(212)
plot(time,therma,'b')
axis([0 Time MinR MaxR])
plot(time,thermA)
hold on;
plot(time,mrt,'m:')
hold off;
xlabel('time (min)');
ylabel('room temp (C)');
grid

clear time timeA

function stavt(ven,thermb,therma,DV)
```

```
subplot(311)
plot(time,Ven,'b')
axis([0 Time MinV MaxV])
xlabel('time (min)');
ylabel('Amplitude');
Title2=input('Enter graph title for Blood Vol. : ','s');
title(Title2);
grid

MinT=min(thermB);
MaxT=max(thermB);

subplot(312)
plot(time,thermB,'b')
axis([0 Time MinT MaxT])
ylabel('finger temp (C)');
xlabel('time (min)');

grid

 MinR=min(thermA) ;
MaxR=max(thermA) ;

subplot(313)
plot(time,therma,'b')
axis([0 Time MinR MaxR])
plot(time,thermA)
hold on;
plot(time,mrt,'m:')
hold off;
xlabel('time (min)');
ylabel('room temp (C)');
grid

clear MinV MinT MaxV MaxT Th Ven thermB time Time pPa MinR MaxR thermA
clear Fs thermb time Thermb therma Therma thermA meanroomtemp mrt


% Cor.m calculates the cross correlation function between the blood
% volume and the temperature of the finger

function cor(ven,thermb,DVT)
for i=1:max(size(ven))
 if ven(i) < 0
   ven(i)=mean(ven) ;
```

```
 end
 end
F%%%%%%%%% Correlation Coefficient b/n Blood Vol. & Finger Temp. %%%%%%%

  [rv,c]=size(Ven);

 datV=zeros([3*rv,c]);
  datV(1:rv,:)=Ven;
  datV(rv+1:2*rv,:)=Ven;
  datV(2*rv+1:3*rv,:)=Ven;

   [rt,c]=size(thermB);

   datT=zeros([3*rt,c]);
   datT(1:rt,:)=thermB;
   datT(rt+1:2*rt,:)=thermB;
  datT(2*rt+1:3*rt,:)=thermB;

    clear Ven thermB ven c

    datV=datV(:) ;
    datT=datT(:) ;



A=xcorr(datV,datT,'coeff') ;
 time=DVT*(0:max(size(A))-1)/(60*Fs);
  %time=DVT*(0:max(size(A))-1)/(Fs);
 Amax=max(A)

Time=max(size(A))/2 ;
 t1=Time-rv ; %fix(rv/40) ;
  t2=Time+rv ; %fix(rv/40) ;
TIME=(DVT*max(size(A))/2)/(60*Fs) ;


clear datV datT

   subplot(2,1,1)
  plot((time(t1:t2)-TIME),A(t1:t2,:))
  axis([-20 20 0 1])
  xlabel('time (min.)')
  grid
    ylabel('Correlation Function')
  Title=input('Enter title for Correlation Function of Blood Vol. & Temp : ','s')
```

```
  title(Title);

  subplot(2,1,2)
  plot((time(t1:t2)-TIME),A(t1:t2,:))
  axis([-.05 .05 Amax-0.001 Amax+.0001])
  xlabel('time (min.)')
  grid

   clear time A Fs rv t1 t2 TIME

  ylabel('Correlation Function')
  %Title=input('Enter title for Correlation Function of Blood Vol. & Temp : ','s')
  title('Time Delay b/n Finger Blood Volume & Temperature');

% Cor.m calculates the cross correlation function between the blood
% volume and the temperature of the finger

function cor(ven,thermb,DVT)
for i=1:max(size(ven))
 if ven(i) < 0
  ven(i)=mean(ven) ;
 end
end

clear b a pPa Thermb thermb

%%%%%%%%%% Correlation Coefficient b/n Blood Vol. & Finger Temp. %%%%%%%

  [rv,c]=size(Ven);

 datV=zeros([3*rv,c]);
  datV(1:rv,:)=Ven;
  datV(rv+1:2*rv,:)=Ven;
  datV(2*rv+1:3*rv,:)=Ven;

   [rt,c]=size(thermB);

   datT=zeros([3*rt,c]);
   datT(1:rt,:)=thermB;
   datT(rt+1:2*rt,:)=thermB;
  datT(2*rt+1:3*rt,:)=thermB;

    clear Ven thermB ven c

    datV=datV(:) ;
```

```
    datT=datT(:) ;

A=xcorr(datV,datT,'coeff') ;
 time=DVT*(0:max(size(A))-1)/(60*Fs);
  %time=DVT*(0:max(size(A))-1)/(Fs);
 Amax=max(A)

Time=max(size(A))/2 ;
 t1=Time-rv ; %fix(rv/40) ;
  t2=Time+rv ; %fix(rv/40) ;
TIME=(DVT*max(size(A))/2)/(60*Fs) ;

clear datV datT

   subplot(2,1,1)
  plot((time(t1:t2)-TIME),A(t1:t2,:))
  axis([-20 20 0 1])
  xlabel('time (min.)')
  grid
    ylabel('Correlation Function')
  Title=input('Enter title for Correlation Function of Blood Vol. & Temp : ','s')
  title(Title);

function c = xcorr(a, b, option)
%XCORR      Cross-correlation function estimates.
%       XCORR(A,B), where A and B are length M vectors, returns the
%       length 2*M-1 cross-correlation sequence in a column vector.
%       XCORR(A), when A is a vector, is the auto-correlation sequence.
%       XCORR(A), when A is an M-by-N matrix, is a large matrix with
%       2*M-1 rows whose N^2 columns contain the cross-correlation
%       sequences for all combinations of the columns of A.
%       The zeroth lag of the output correlation is in the middle of the
%       sequence, at element or row M.
%       By default, XCORR computes a raw correlation with no normalization.
%       XCORR(A,'biased') or XCORR(A,B,'biased') returns the "biased"
%       estimate of the cross-correlation function.  The biased estimate
%       scales the raw cross-correlation by 1/M.
%       XCORR(...,'unbiased') returns the "unbiased" estimate of the
%       cross-correlation function.  The unbiased estimate scales the raw
%       correlation by 1/(M-abs(k)), where k is the index into the result.
%       XCORR(...,'coeff') normalizes the sequence so that the
%       correlations at zero lag are identically 1.0.
%       See also XCOV, CORRCOEF, CONV and XCORR2.
```

```
%       Author(s): L. Shure, 1-9-88
%                  L. Shure, 4-13-92, revised
%       Copyright (c) 1984-94 by The MathWorks, Inc.
%       $Revision: 1.7 $  $Date: 1994/01/25 18:00:07 $

%       References:
%        [1] J.S. Bendat and A.G. Piersol, "Random Data:
%           Analysis and Measurement Procedures", John Wiley
%           and Sons, 1971, p.332.
%        [2] A.V. Oppenheim and R.W. Schafer, Digital Signal
%           Processing, Prentice-Hall, 1975, pg 539.

onearray = 1;
if nargin == 1
        option = 'none';
        if min(size(a)) == 1    % a is a vector
                a = [a(:) a(:)];
        else
                onearray = 0;
        end
elseif nargin == 2
        if isstr(b)
                option = b; clear b
                na = max(size(a));
                if min(size(a)) == 1    % a is a vector
                        a = [a(:) a(:)];
                else    % a is a matrix
                        onearray = 0;
                        [m,n] = size(a);
                end
   else % b is truly a second arg
                if min(size(a)) ~= 1 & min(size(b)) ~= 1
                        error('You may only specify 2 vector arrays.')
                end
                option = 'none';
                onearray = 2;
        end
else
        if max(size(a)) ~= max(size(b)) & ~strcmp(option,'none')
                error('OPTION must be "none" for different length vectors A and B')
        end
        onearray = 2;
end
% check validity of option
nopt = nan;
```

```
if strcmp(option, 'none')
        nopt = 0;
elseif strcmp(option, 'coeff')
        nopt = 1;
elseif strcmp(option, 'biased')
        nopt = 2;
elseif strcmp(option, 'unbiased')
        nopt = 3;
end
if isnan(nopt)
        error('Unknown OPTION')
end
if onearray == 2
        [ar,ac] = size(a);
        na = max([ar ac]);
        nb = max(size(b));
        if na > nb
                b(na) = 0;
        elseif na < nb
                a(nb) = 0;
        end
        a = [a(:) b(:)];
end
[nr, nc] = size(a);
nsq  = nc^2;
mr = 2 * nr - 1;
c = zeros(mr,nsq);
ci = zeros(1,nsq);
cj = ci;
nfft = 2^nextpow2(2*nr);
for i = 1:nc
        atmpi = a(:,i);
        if ~any(any(atmpi))
                real1-= 1;
        else
                real1 = 0;
        end
        atmpi = fft([atmpi(:); zeros(nfft-nr,1)]);
        for j = 1:i
                col = (i-1)*nc+j;
                colaux = (j-1)*nc+i;
                tmp = fft([a(:,j); zeros(nfft-nr,1)]); % pad with zeros for fft
                tmp = fftshift(ifft(atmpi.*conj(tmp)));
                c(:,colaux) = tmp((1:mr)+nfft/2-nr+1);
                ci(col) = i;
```

```
                cj(col) = j;
                ci(colaux) = j;
                cj(colaux) = i;
                if ~any(any(imag(a(:,j)))) & real1
                        c(:,colaux) = real(c(:,colaux));
                end
                if i~= j
                        c(:,col) = conj(c(mr:-1:1,colaux));
                end
        end
end
if nopt == 1    % return normalized by sqrt of each autocorrelation at 0 lag
% do column arithmetic to get correct autocorrelations
        cdiv = ones(mr,1)*sqrt(c(nr,1+(ci-1)*(nc+1)).*c(nr,1+(cj-1)*(nc+1)));
        c = c ./ cdiv;
elseif nopt == 2        % biased result, i.e. divide by nr for each element
        c = c / nr;
elseif nopt == 3        % unbiased result, i.e. divide by nr-abs(lag)
        c = c ./ ([1:nr (nr-1):-1:1]' * ones(1,nsq));
end
if onearray == 1
        c = c(:,1);     % just want the autocorrelation
        [am, an] = size(a);
        if am == 1
                c = c.';
        end
elseif onearray == 2    % produce only cross-correlation
        c = c(:,2);
        if ar == 1
                c = c.';
        end
end
if ~any(any(imag(a)))
        c = real(c);
end

  subplot(2,1,2)
  plot((time(t1:t2)-TIME),A(t1:t2,:))
  axis([-.05 .05 Amax-0.001 Amax+.0001])
  xlabel('time (min.)')
  grid

   clear time A Fs rv t1 t2 TIME

  ylabel('Correlation Function')
```

```
%Title=input('Enter title for Correlation Function of Blood Vol. & Temp : ','s')
title('Time Delay b/n Finger Blood Volume & Temperature');

function c = xcorr(a, b, option)
%XCORR    Cross-correlation function estimates.
%    XCORR(A,B), where A and B are length M vectors, returns the
%    length 2*M-1 cross-correlation sequence in a column vector.
%    XCORR(A), when A is a vector, is the auto-correlation sequence.
%    XCORR(A), when A is an M-by-N matrix, is a large matrix with
%    2*M-1 rows whose N^2 columns contain the cross-correlation
%    sequences for all combinations of the columns of A.
%    The zeroth lag of the output correlation is in the middle of the
%    sequence, at element or row M.
%    By default, XCORR computes a raw correlation with no normalization.
%    XCORR(A,'biased') or XCORR(A,B,'biased') returns the "biased"
%    estimate of the cross-correlation function.  The biased estimate
%    scales the raw cross-correlation by 1/M.
%    XCORR(...,'unbiased') returns the "unbiased" estimate of the
%    cross-correlation function.  The unbiased estimate scales the raw
%    correlation by 1/(M-abs(k)), where k is the index into the result.
%    XCORR(...,'coeff') normalizes the sequence so that the
%    correlations at zero lag are identically 1.0.
%    See also XCOV, CORRCOEF, CONV and XCORR2.

%    Author(s): L. Shure, 1-9-88
%               L. Shure, 4-13-92, revised
%    Copyright (c) 1984-94 by The MathWorks, Inc.
%    $Revision: 1.7 $  $Date: 1994/01/25 18:00:07 $

%    References:
%      [1] J.S. Bendat and A.G. Piersol, "Random Data:
%          Analysis and Measurement Procedures", John Wiley
%          and Sons, 1971, p.332.
%      [2] A.V. Oppenheim and R.W. Schafer, Digital Signal
%          Processing, Prentice-Hall, 1975, pg 539.

onearray = 1;
if nargin == 1
    option = 'none';
    if min(size(a)) == 1    % a is a vector
        a = [a(:) a(:)];
    else
        onearray = 0;
    end
elseif nargin == 2
```

```
        if isstr(b)
                option = b; clear b
                na = max(size(a));
                if min(size(a)) == 1    % a is a vector
                        a = [a(:) a(:)];
                else    % a is a matrix
                        onearray = 0;
                        [m,n] = size(a);
                end
   else % b is truly a second arg
                if min(size(a)) ~= 1 & min(size(b)) ~= 1
                        error('You may only specify 2 vector arrays.')
                end
                option = 'none';
                onearray = 2;
        end
else
        if max(size(a)) ~= max(size(b)) & ~strcmp(option,'none')
                error('OPTION must be "none" for different length vectors A and B')
        end
        onearray = 2;
end
% check validity of option
nopt = nan;
if strcmp(option, 'none')
        nopt = 0;
elseif strcmp(option, 'coeff')
        nopt = 1;
elseif strcmp(option, 'biased')
        nopt = 2;
elseif strcmp(option, 'unbiased')
        nopt = 3;
end
if isnan(nopt)
        error('Unknown OPTION')
end
if onearray == 2
        [ar,ac] = size(a);
        na = max([ar ac]);
        nb = max(size(b));
        if na > nb
                b(na) = 0;
        elseif na < nb
                a(nb) = 0;
        end
```

```
        a = [a(:) b(:)];
end
[nr, nc] = size(a);
nsq  = nc^2;
mr = 2 * nr - 1;
c = zeros(mr,nsq);
ci = zeros(1,nsq);
cj = ci;
nfft = 2^nextpow2(2*nr);
for i = 1:nc
        atmpi = a(:,i);
        if ~any(any(atmpi))
                real1 = 1;
        else
                real1 = 0;
        end
        atmpi = fft([atmpi(:); zeros(nfft-nr,1)]);
        for j = 1:i
                col = (i-1)*nc+j;
                colaux = (j-1)*nc+i;
                tmp = fft([a(:,j); zeros(nfft-nr,1)]); % pad with zeros for fft
                tmp = fftshift(ifft(atmpi.*conj(tmp)));
                c(:,colaux) = tmp((1:mr)+nfft/2-nr+1);
                ci(col) = i;
                cj(col) = j;
                ci(colaux) = j;
                cj(colaux) = i;
                if ~any(any(imag(a(:,j)))) & real1
                        c(:,colaux) = real(c(:,colaux));
                end
                if i~= j
                        c(:,col) = conj(c(mr:-1:1,colaux));
                end
        end
end
if nopt == 1    % return normalized by sqrt of each autocorrelation at 0 lag
% do column arithmetic to get correct autocorrelations
        cdiv = ones(mr,1)*sqrt(c(nr,1+(ci-1)*(nc+1)).*c(nr,1+(cj-1)*(nc+1)));
        c = c ./ cdiv;
elseif nopt == 2        % biased result, i.e. divide by nr for each element
        c = c / nr;
elseif nopt == 3        % unbiased result, i.e. divide by nr-abs(lag)
        c = c ./ ([1:nr (nr-1):-1:1]' * ones(1,nsq));
end
if onearray == 1
```

```
        c = c(:,1);        % just want the autocorrelation
        [am, an] = size(a);
        if am == 1
                c = c.';
        end
elseif onearray == 2    % produce only cross-correlation
        c = c(:,2);
        if ar == 1
                c = c.';
        end
end
if ~any(any(imag(a)))
        c = real(c);
end
```

APPENDIX B

INSTRUMENTATION FOR THE RESEARCH

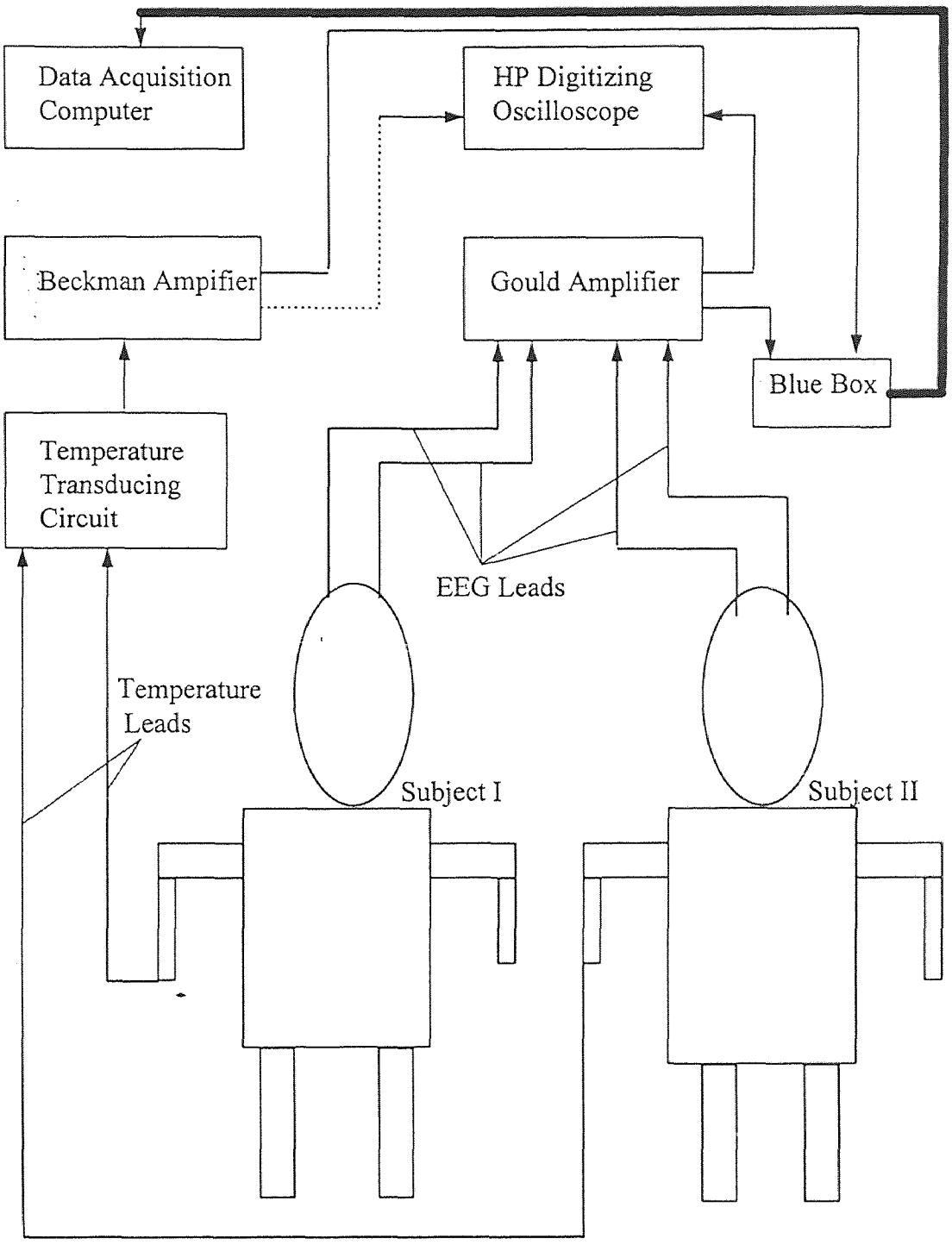

Figure B.1 Instrumentation for group meditation studies

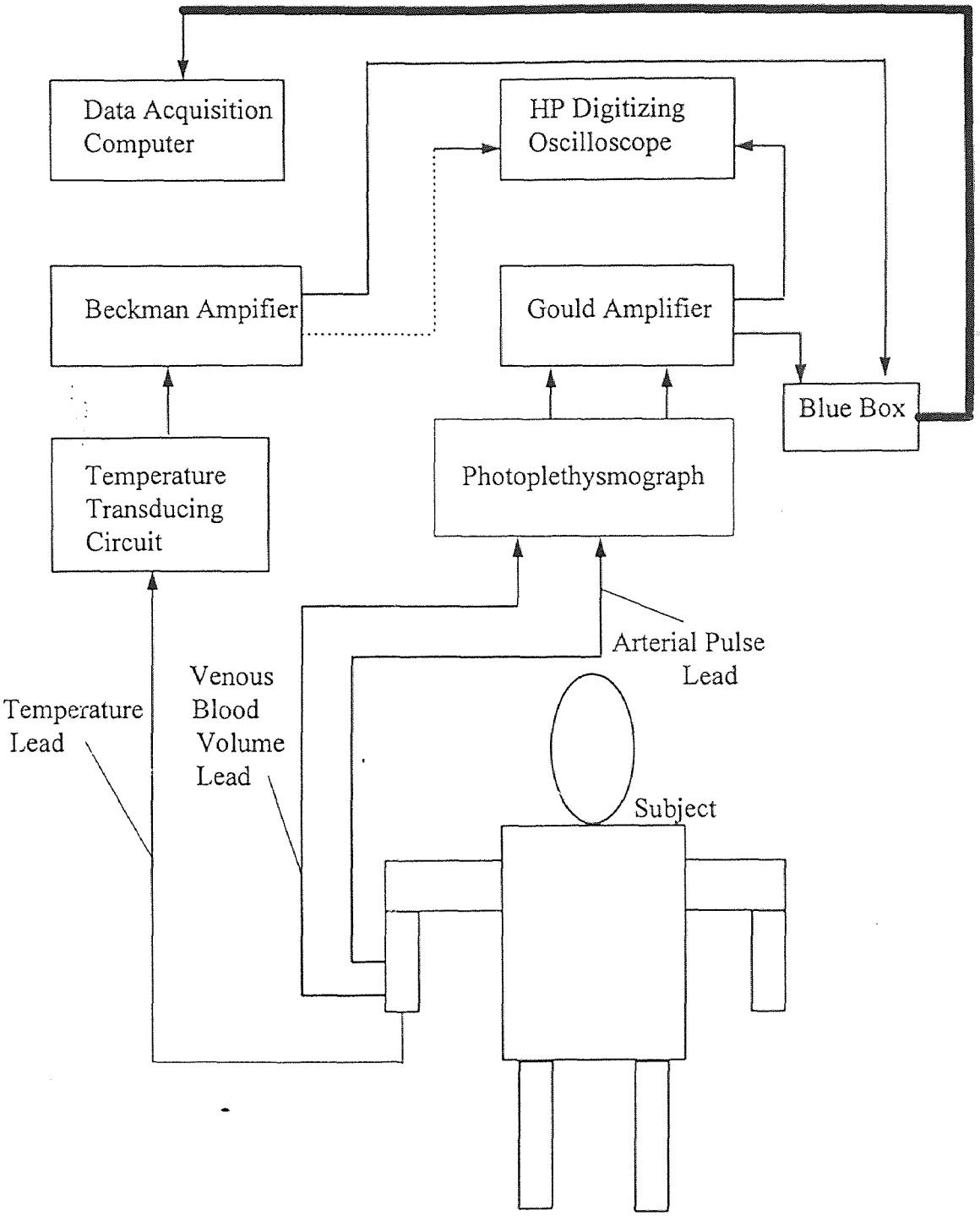

Figure B.2 Instrumentation for blood flow study

REFERENCES

[1] J. L. Halperin, R. A. Cohen, and J. D. Coffman."Digital vasodilation during stress in patients with Raynaud's disease," *Cardiovascular Research*, 17:671-77, 1983.

[2] J. W. Hofman, H. Benson, P. A. Arns, *et al.*, "Reduced sympathetic system Responsivity associated with the relaxation response," *Science*, 215:190-2, Jan. 1982.

[3] J. Oberle, M. Elam, T. Karlsson, and B. G. Wallin. "Temperature-dependent interation between vasoconstrictor and vasodilator mechanisms in human skin," *Acta Physiol Scand*, 132:459-464, 1988.

[4] J. P. Cooke, M. A. Creaker, P. H. Osmundson, and J. T. Shepherd. "Sex differences in control of cutaneous blood flow," *Circulation*, 82(5):1607-15, Nov. 1990.

[5] H. Blumberg, and B. G. Wallin. "Direct evidence of neurally mediated vasodilation in hairy skin of the human foot," *J. Physiol*, 382:105-21, 1987.

[6] A. C. Guyton. *Human Physiology and Mechanisms of Disease*, Fifth Edition, Philadelphia, PA, Harcourt Brace Jovanovich, 1992.

[7] G. Bini, K. E. Hynninen, et al. "Thermoregulatory and Rhythm-generating mechanisms governing the sudomotor and vasoconstrictor outflow in human cutaneous nerves," *J. Physiol (London)*, 306:537-52, 1980.

[8] M. Elam, B. G. Wallin. "Skin blood flow responses to mental stress in man depend on body temperature," *Acta Physiol Scand*, 129:429-31.

[9] J. D. Coffman. *Raynaud's Phenomenon*, Oxford, Oxford University Press, UK, 1989.

[10] C. T. Araki. "Chronic Venous Insufficiency," *A review paper on Vascular Lab.*, University Hospital, Newark.

[11] T. Lewis. "Experiments relating to the peripheral mechanisms involved in spasmodic arrest of the circulation in the fingers," *Heart* 15:7-101, 1929.

[12] A. J. Vander, and J. H. Sherman. *Human Physiology*, Sixth Edition. McGraw Hill,1994.

[13] Photoplethysmograph Model PPG 13, *Service Manual*. MedaSonics, Kendall Hospital Company, 1984.

[14] R. K. Wallace, and H. Benson. "The Physiology of Meditation," *Scientific American,* 226:74, 84-90, 1972.

[15] H. H. Boomfield, M. P. Cain, and D. T. Jaffe. TM: *Discovering Inner Energy and Overcoming Stress*. New York, Delacorte Press, 1975.

[16] W. R. Adey, and S. M. Bawin. "Brain interactions with electric and magnetic fields," *Neurosciences Research Program Bulletin*,15:1-129, the 1974.

[17] L. H. Domash. "The Transcendental Meditation Technique and Quantum Physics: Is conciousness a macroscopic quantum state in the brain?,"*Scientific Research on the Transcendental Meditation Program: Collected Papers*, Vol. 1, Weat Germany, MERU Press, 1976.

[18] D. Orme-Johnson, M. C. Dillbeck, R. Wallace. "Intersubject EEG Coherence: Is conciousness a field?," *InternJ. Neuroscience*, 16:203-9, 1982.

[19] D. Orme-Johnson, C. T. Haynes. "EEG Phase Coherence, Pure Conciousness, Creativity, and TM-Sidhi Experiences," *Intern. J. Neuroscience*, 13:211-17, 1981.

[20] Maharishi Mahesh Yogi. *Enlightenment and Invicibility*, West Germany, MERU Press, 26-37, 43-50, 228-262, 406-410, 419-449, 1978.

[21] D. Orme-Johnson, M. C. Dillbeck, and R. Wallace. "Physiological Differences between Meditation and Rest," *American Psychologist*. 879-81, Sept. 1987.

[22] P. Levine. "The Coherence Spectral Array (COSPAR) and its application to the study of spatial ordering in the EEG," *Proceedings of San Diego Biomedical Symposium*. San Francisco, CA, Academic Press. 15:237-47, 1976.

[23] M. A. West. "Meditation and EEG," *Psychological Medicine*. 10:369-75, 1980.

[24] P. D. Welch. "The use of Fast Fourier Transform for the estimation of power spectra: A method based on time averaging over short periodograms," *IEEE Transactions on Audio and Electronics*. AU-15(. 2):70-3, 1967.

[25] M. C. Dillbeck, and E. C. Bronson. "Shortwazzu -term longitudinal effects of the Transcendental Meditation Technique on EEG Coherence," *Intern J. Neuroscience.* 14:147-51, 1981.

[26] D. Orme-Johnson, M. C. Dillbeck, and R. Wallace. "Frontal EEG coherence, H-reflex recovery, concept learning, and the TM-Sidhi Program," *Intern J. Neuroscience*. 15:151-57, 1981.

[27] C. J. Tourenne. "A model of the Electric Field of the Brain at EEG and Microwave Frequencies," *J. Theor. Biol.* 116:495-507, 1985.

[28] F. T. Travis, D. W. Orme-Johnson. "Field model of conciousness: EEG coherence as indicators of field effect," *Intern. J. Neuroscience*. 49:203-11, 1989.

[29] R. K. Wallace, P. J. Mills, D. W. Orme-Johnson, M. C. Dillbeck, and E. Jacobe. Modification of the paired H-reflex through the TM and TM-Sidhi Program," *Experimental Neurology*. 79:77-86, 1983.

[30] C. B. King "Measurement of the Reaction to Stress and Meditation Using Brain Wave Coherence and Heart Rate Variability," Master's Thesis, Department of Biomedical Engineering, New Jersey Institute of Technology, Newark, NJ.,1994.

[31] D. A. Newandee. "Measurement of the EEG Coherence, Atmospheric Noise, and Schumann Resonances in Group Meditation,". Master's Thesis, Department of Biomedical Engineering, New Jersey Institute of Technology, Newark, NJ., Jan. 1996.

[32] F. H. Duffy, V. G. Iyer, and W. W. Surwillo."*Clinical electroencephalography and topographic brain mapping,"* Springerverlag, New York, 1989.

[33] R. K. Wallace. "Physiological effects of Transcendental Meditation," *Science*. 167:1751-54,1970.

[34] R. K. Wallace, H. Benson, and A. F. Wilson. "A wakeful hypometabolic physiologic state," *American J. Physiol.* 221:795-9, 1971.

[35] R. Jeving, R. K. Wallace, and M. Beidebach. "The Physiology of meditation: A review . A wakeful hypometabolic integrated respon," *Neuroscience and Behavioral Reviews*. 16:415-24, 1992.

[36] J. W. Clark, *Medical Instrumentation and Design*, J. G. Webster, ed. Boston, MA, Houghton Mifflin Company, 1992.

[37] J. S. Bendat. *"Engineering Applications of Correlation and Spectral Analysis,"* John Wiley & Sons, New York, 1980.